Oxepinobenzofurans: Controlled-Copper Catalyzed Aerobic Synthesis and Reactivity as Oxidants

Laurène Petitjean

A thesis submitted to McGill University in partial fulfillment
of the requirements of the degree of Master of Science

Department of Chemistry
McGill University, Montreal
March 2014

Abstract

Copper catalyzed phenolic oxidations have historically shown a lack of selectivity due to the ease of autoxidation of phenols. The resulting phenoxyl radicals provide complex mixtures of oxygenation and oxidation products, such as quinones, biphenols, oxepinobenzofurans and polymeric materials. Despite this lack of selectivity, phenolic aerobic oxidations show promise as environmentally benign, efficient and versatile means to access a wide variety of structurally different products from a single starting compound. In Chapter One, an overview of previous efforts towards the selective oxygenation of phenols *via* copper-catalyzed aerobic oxidation is provided, along with a detailed summary of previous syntheses of oxepinobenzofurans and a review of their reactivity.

Chapter Two describes the successful development and optimization of a copper-catalyzed aerobic synthesis of both oxepinobenzofurans and biphenols. Subtle changes to the catalytic system enabled the identification of factors that govern selectivity between each product class. The scope of each of these reactions was demonstrated, and showed that subtle steric and electronic factors influence efficacy and selectivity.

Chapter Three relates efforts towards the development of a catalytic aerobic dehydrogenation through the use of oxepinobenzofurans as hydrogen transfer agents. The dehydrogenation of dihydroanthracene by several oxepinobenzofurans is demonstrated, furnishing anthracene and biphenols. Proof of a potential catalytic aerobic dehydrogenation method is given by the fruitful development and optimization of copper-catalyzed aerobic oxidation of biphenols to oxepinobenzofurans. Electron spin resonance measurements of oxepinobenzofurans demonstrate an equilibrium with radical species, observed at high temperatures. Initial results thus indicate a biphenoxyl species as the reactive intermediate mediating dehydrogenation.

Resumé

Historiquement, les oxydations phénoliques aérobiques catalysées par le cuivre ont démontrées un manque de sélectivité, due à la facilité d'auto-oxydation des phénols, donnant des mélanges complexes de produits d'oxydation et d'oxygénation, comme les quinones, les biphénols, les oxepinobenzofuranes ainsi que certains polymères. Néanmoins, les oxydations aérobiques de phénols possèdent un énorme potentiel en tant que méthodes versatiles et efficaces permettant l'accès à de nombreux produits structurellement différents à partir d'un seul phénol. Le Chapitre Un propose un aperçu des efforts préalables en ce qui trait au développement d'oxygénations sélectives de phénols *via* des oxydations aérobiques catalysées par le cuivre. Un sommaire détaillé des synthèses et de la réactivité établie des oxepinobenzofuranes est aussi donné.

Le Chapitre Deux décrit le développement et l'optimisation réussis des synthèses d'oxepinobenzofuranes et de biphénols par oxydations catalytiques et sélectives de phénols. Des changements subtiles au système catalytique ont permis l'identification des besoins du complexe de cuivre afin d'être sélectif. L'essai des deux réactions avec plusieurs phénols ont démontrés les facteurs électroniques et stériques subtiles qui influencent l'efficacité et la sélectivité du système.

Le Chapitre Trois relate les efforts vers le développement de déshydrogénations aérobiques et catalytiques en cuivre, possible grâce à l'habilitée des oxepinobenzofuranes à agir comme agents de transfert d'atomes d'hydrogène. La déshydrogénation de dihydroanthracene par plusieurs oxepines est décrite, donnant le produit oxydé anthracène et des biphénols comme produits réduits des oxepines. Le potentiel d'une méthode catalytique aérobique de déshydrogénation est prouvé grâce au développement et à l'optimisation avec succès de l'oxydation des biphénols donnant des oxepinobenzofuranes sous l'action de l'oxygène et du cuivre. Des mesures d'oxepines par résonance paramagnétique électronique ont démontrées l'existence d'un équilibre entre les oxepines et des espèces radicalaires observées à hautes températures. Les résultats préliminaires indiquent qu'un biphénoxyl serait l'intermédiaire réactif dans les déshydrogénations par les oxepines.

Acknowledgments

Over the past two years I have received support, encouragement and advice from a great number of individuals. I would like to thank Chantal Marotte, Claude Perryman and Dr. Alex Wahba for helpful discussions. Dr. Frederick Morin and Dr. Mark Andrews provided invaluable spectroscopic advice. Special thanks to my supervisor, Dr. Jean-Philip Lumb, for his constant guidance, and without whom this thesis would not have been possible.

Thanks to Zoe and Michael for reminding me that my life extends beyond the laboratory boundaries and for their overall inestimable support. My parents' love and encouragements have made it possible for me to be writing these lines. Merci to Theo Petitjean who always saw the best in me and to Hugo Petitjean, who allowed me to indulge in culinary Epicureanism while pursuing this degree. Thank you JFL for your patience.

Table of Contents

List of Schemes

List of Figures

List of Tables

List of Abbreviations

^{o}C – Degrees Celsius
2,4-DTBP – 2,4-di-*tert*-butyl phenol
3,5-DTBQ – 3,5-di-*tert*-butyl quinone
Ac – Acetate
Ar – Aryl
BINAP – 2,2'-bis(diphenylphosphino)-1,1'-binaphthyl
BINOL – 1,1'-bi-2-naphthol
Bn - benzyl
d – doublet
dB - decibel
DBED – *N,N'*-di-*tert*-butylethylenediamine
DCM – dichloromethane
DPPH - 2,2-diphenyl-1-picrylhydrazyl
EDG – Electron donating group
Et – Ethyl
EPR – electron paramagnetic resonance
EWG – Electron withdrawing group
G - Gauss
h – hour(s)
Hc – Hemocyanin
HRMS – High resolution mass spectroscopy
Hz – Hertz
*i*Bu - isobutyl
*i*Pr – isopropyl
IR – infrared
J – Coupling constant
LAH – lithium aluminum hydride
m – multiplet
Me - methyl
min – minute(s)
MTBP – 4-methoxy-2-*tert*-butyl phenol
NMR – nuclear magnetic resonance
PCET – proton coupled electron transfer
Ph - phenyl
phen – 1,10-phenanthroline
PPE – polyphenylether
Py - pyridyl
q - quartet
s – singlet
t – triplet
*t*Amyl – *tert* amyl
*t*Bu – *tert*- butyl
TEMPO - 2,2,6,6-Tetramethylpiperidin-1-yl)oxy
TMEDA – *N,N',N'',N'''*-tetra-methylethylene diamine
Ty-Tyrosinase

CHAPTER ONE

INTRODUCTION: TYROSINASE MIMICS & OXEPINOBENZOFURAN CHEMISTRY

1.1 Perspective

Dioxygen (O_2) is an attractive terminal oxidant for the development of synthetic chemical methods, because it is readily available, cheap, and does not form toxic byproducts upon reduction[1]. Safety concerns hinder large-scale developments of aerobic process reactions, but these constraints are being addressed[2]. O_2 requires to be activated to become a useful oxidant, as the reaction of its triplet ground state with singlet state molecules is a spin forbidden process[3]. Metalloenzymes are capable of activating O_2, mostly through the use of transition metals, for further oxidation or oxygenation of organic substrates[4].

Significant effort has been invested into the development of transition-metal catalyzed aerobic oxidations of organic substrates[1]. Although success has been reached in certain areas, such as alcohol oxidation[5-6], phenolic oxidations remain unviable as synthetic methodologies, being limited to substrates capable of undergoing selective radical chemistry[1]. This is due to the ease of autoxidation of phenols[7], which generates reactive phenoxyl radicals. Phenoxyl radicals recombine without catalyst control, leading to mixtures of products where chemo- and regioselectivity is determined by the substitution pattern of the starting material. This is in opposition to catalyst-controlled oxidations, which are significantly more versatile for chemical synthesis.

Oxidations of readily available phenols could provide access to a variety of diversely functionalized products that are very attractive as intermediates in complex molecule synthesis. Catalytic aerobic oxidations are extensively utilized in biological systems to yield a wide array of useful natural products and materials[8-9]. For example, the bioactive lignans, including (+)-pinoresinol, a strong anti-inflammatory[10] and anti-fungal[11] agent, are synthesized *in vivo* through one-electron phenolic oxidation of monolignols (Figure 1.1)[12-13]. Further oxidation and

rearrangement yield the wide range of lignan molecular frameworks and lignin polymer[13]. In mushrooms, the rate-limiting step in the synthesis of the melanin polymers consists of metalloenzyme mediated aerobic oxidation of L-Tyrosine to L-Dopaquinone[14]. Metalloenzymes are adept at activating O_2 for regio- and chemo- selective oxidation. In industrial settings, polyphenylene ether (PPE), a high performance plastic with extensive applications in electronics, structural parts and automobile items, is furnished by a copper catalyzed phenolic aerobic oxidation [15-16]. Metalloenzyme efficiency and General Electric's success with PPE evidence the large potential of catalytic aerobic oxidations as synthetic methodologies.

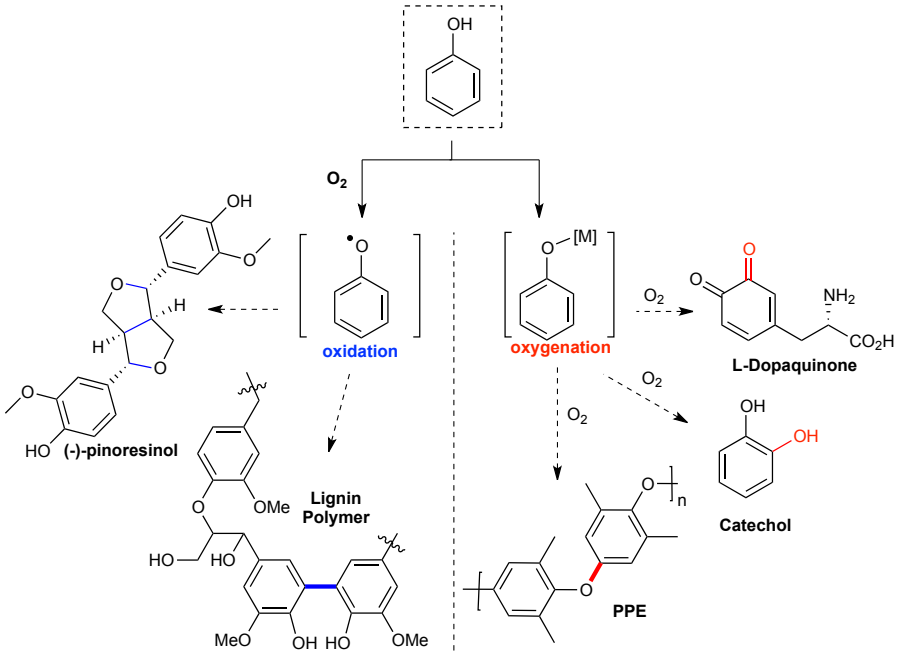

Figure 1.1 Potential Pathways of Phenolic Oxidations

One-electron oxidations of phenols yield phenoxyl radicals that are resonance stabilized, and possess radical character at both the *ortho*- and *para*-positions of the phenol. This can provide a means of forming carbon-carbon bonds (C-C coupling) without the requirement of substrate pre-functionalization. Phenolic oxygenation gives electron-rich catechols, which are widely distributed in natural products. Alternatively, *ortho*-oxygenation can also lead to *ortho*-quinones, which are electrophilic species that are activated at each of the carbon centers. Given this broad landscape of reactivity, a catalytic aerobic method for the oxidation of phenols that is selective has the potential to become a versatile method for organic synthesis, provided that issues of selectivity can be overcome. Currently, the majority of phenolic oxidations rely on the

use of stoichiometric amounts of an oxidant other than O_2, thus decreasing their atom and step efficiency.

In contrast to current synthetic systems, enzymes are able to activate O_2 for selective oxidations[8, 14]. The activation of O_2 by enzymes is a subject of historical importance in the chemical sciences[3, 8]. The elucidation of enzymatic methods for O_2 activation has been fundamentally important for the development of synthetic methods, and provides additional insight into the mechanisms of various biological systems. Given the reactive nature of transition-metal O_2 species, a strategy commonly utilized for the unraveling of biological O_2 activation is the use of model catalytic systems[17]. This has been particularly true in the case of Tyrosinase, a dinuclear type 3 copper enzyme capable of activating O_2 for the selective oxygenation and subsequent two-electron oxidation of L-Tyrosine to L-Dopaquinone (Figure 1.2)[18]. Mimicking Tyrosinase provides an important means for the development of a selective catalytic aerobic oxygenation of phenols to *ortho*-quinones, and provides insight into the subtle factors that govern selectivity during phenolic oxidation. Thus, we set out to develop selective catalytic aerobic phenol oxidations to *ortho*-quinones by mimicking Tyrosinase, with the ultimate goal of providing access to all different products of phenolic oxidations. Through rational changes to a catalytic system, factors that influence selectivity in aerobic phenolic metal-catalyzed oxidations will be evidenced.

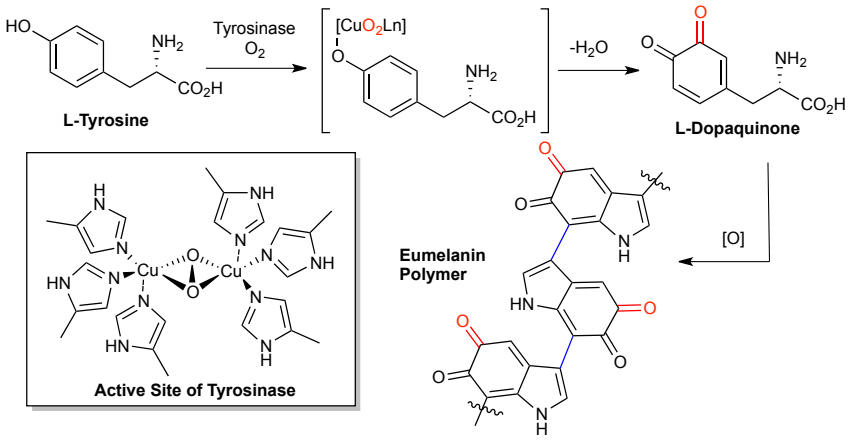

Figure 1.2 Tyrosinase active site and oxygenase reactivity

Section 1.2 comprises a review of synthetic Tyrosinase mimics and details the mechanistic factors that influence reactivity and selectivity during the catalytic aerobic oxidation of phenols. Section 1.3 will focus on the synthesis and reactivity of oxepinobenzofurans, because

these compounds are sometimes observed instead of *ortho*-quinones in catalytic aerobic oxidation of phenols, and thus they also constitute important targets by catalytic aerobic phenol oxidations.

1.2 Catalytic Aerobic *Ortho*-Quinone Synthesis – Tyrosinase Mimics

1.2.1 Introduction

Dinuclear copper centers play an important role in biological O_2 binding and activation, and are found in enzymes such as Hemocyanin (Hc)[19], Catechol Oxidase (CO)[20] and Tyrosinase (Ty)[21-22]. These three enzymes all possess type three copper active sites, which are composed of two copper atoms ligated by three histidine residues.

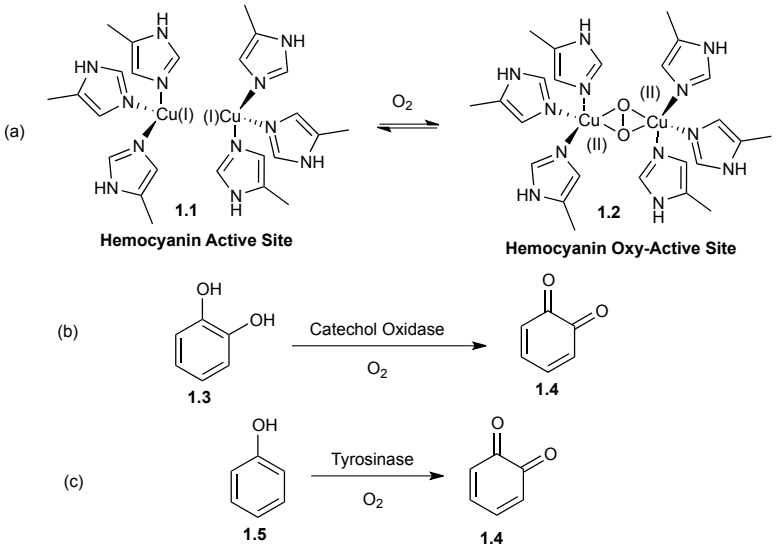

Figure 1.3 Reactivity of (a) Hemocyanin (b) Catechol Oxidase and (c) Tyrosinase enzymes

Although Tyrosinase, Catechol Oxidase, and Hemocyanin show very similar active sites, Hemocyanin serves solely as an O_2 carrier protein in molluscs and arthropods[23], Catechol Oxidase can catalyze catechol two-electron oxidation (oxidase activity)[24], and Tyrosinase can perform the latter reaction preceded by phenol hydroxylation (oxygenase activity)[25] (Figure 1.3a-c). Even before crystal structures of Tyrosinase were obtained, the reactivity differences of the three enzymes were attributed to varying accessibility to the Cu-active sites[17]. In Hemocyanin, the active site is isolated from potential substrates by the protein matrix, which blocks substrates

from reaching the active site. In fact, Hemocyanin shows phenol oxidase activity in environments where it is denatured (treatment with detergents or proteolytic cleavage)[26].

Tyrosinase, as well as Catechol oxidase and Hemocyanin, bind O_2 in a characteristic side-on bridging (μ-η^2:η^2) geometry in their *oxy* form[22], converting the dinuclear *deoxy* copper (I) atoms to two copper (II) atoms (Figure 1.4a). This was revealed by crystal structures, and by spectroscopic investigations of the dinuclear- $Cu(II)_2$, which possesses an absorbance in the ultraviolet at ~350 nm as well as an O-O stretching vibration at ~750 cm^{-1} in the Raman spectrum[17].

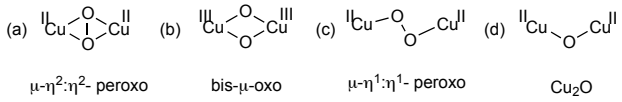

Figure 1.4 Different geometries of O_2 binding to dinuclear copper

Other known intermediates of the Tyrosinase enzyme include the *deoxy* ($Cu(I)_2$) and the *met* ($Cu(II)_2OH$) forms of the active site (Scheme 1.1)[14]. The *met* form of the enzyme is believed to be the resting state of Tyrosinase, and will readily bind catechols[14]. Subsequent dehydrogenation of the catechol yields the *ortho*-quinone, along with H_2O and the reduced bis-Cu(I)-*deoxy* active site. Tyrosinase, in its *deoxy* form, is capable of binding O_2 to generate the *oxy* state of the enzyme, which is subsequently attacked by phenolate. Oxygenation is thought to occur through electrophilic aromatic substitution[27-31], and generates the dinuclear copper catecholate, which undergoes redox exchange to afford *ortho*-quinone, H_2O and the *deoxy* form of tyrosinase (Scheme 1.1). Despite this blueprint, the mechanism of oxidation of Tyrosinase remains poorly understood. It is still unclear whether the side-on peroxo species is truly the one effecting hydroxylation[17], whether catechols are intermediates in *ortho*-quinone formation[32], and finally whether electrophilic aromatic substitution is the oxygenation mechanism[17].

In the absence of the protein scaffold, Cu(I) activates O_2 in a variety of geometries, including the *trans*-μ-1,2-peroxo ($Cu(III)_2$), the bis-μ-oxo ($Cu(II)_2$) and the μ-oxo-copper(II) geometries (Figure 1.4b-d)[3, 17, 33-34]. As can be expected, electronic and steric factors affect the activated O_2 species, and influence which of these species is favored[35-36]. The different binding geometries lead to reactivity differences[37], and the ligand environment is thus an important consideration for the development of rational reaction parameters for a given mode of reactivity. In 1996 Tolman and co-workers showed not only that an equilibrium between the side-on peroxo species and the *trans*-oxo species existed, but additionally that the energy difference between the

two states was very small[27]. In section 1.2.2, the different Cu-O_2 binding geometries will be discussed in the context of their reactivity towards external phenolic substrates, first in the stoichiometric reports, and subsequently in the few catalytic systems able to reproduce Tyrosinase oxygenase chemistry.

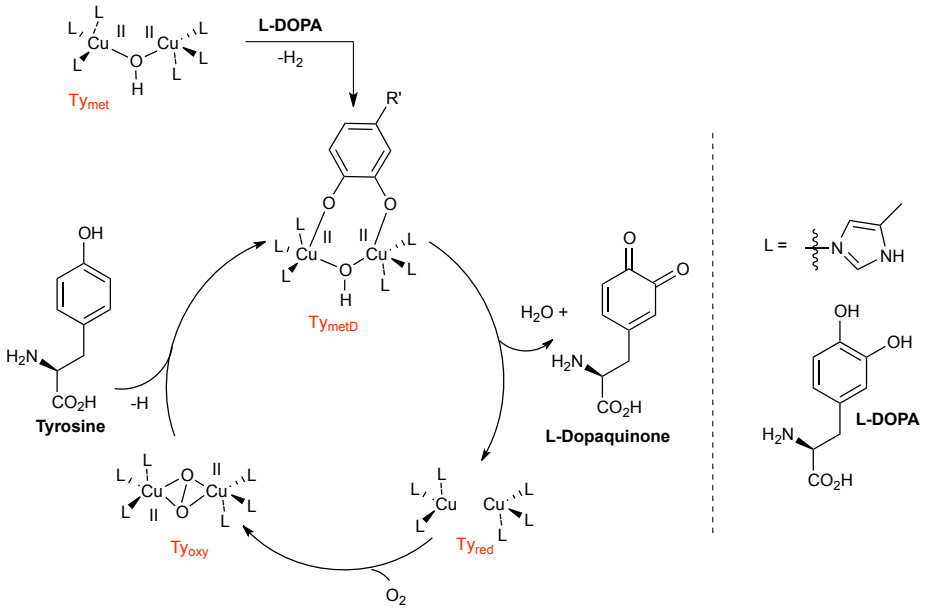

Scheme 1.1 Tyrosinase monophenolase and diphenolase activity

1.2.2 Stoechiometric synthetic models of Tyrosinase

A. Stoechiometric Models with unresolved Cu_2O_2 binding geometry

Evidence that simplified synthetic Cu-O_2 systems could mimick Tyrosinase reactivity by performing hydroxylations of external phenolic substrates was evidenced by the early work of Brackman and Havinga, in 1955. Phenolic oxygenations were mediated by copper nitrate in the presence of morpholine to afford the *ortho*-quinone product **1.6** (Scheme 1.2)[38-42]. Although other copper salts such as copper acetate, chloride, sulphate, formate or stereate can be utilized in this reaction, the authors report the inefficacy of any other metallic ions (Pt powder, MnO_2, Ag powder, Ag_2O, PbO_2, $K_3Fe(CN)_6$, $K_4Fe(CN)_6$, Mn^{2+}, Fe^{2+}, Fe^{3+}, Co^{2+}, Ni^{2+}, Zn^{2+}, UO_2^{2-}, and NH_4VO_3)[38]. Both primary and secondary amine bases can catalyze phenolic oxygenation, however tertiary amines remain inactive except in the case of naphthols.

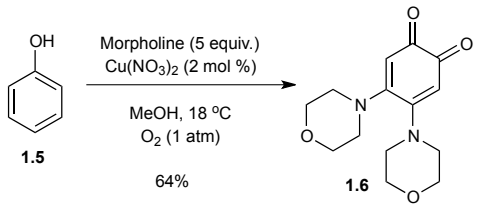

Scheme 1.2 Copper nitrate and morpholine aerobic phenol oxidation

In 1982, Maumy and co-workers reported hydroxylation and subsequent oxidation to the *ortho*-quinone upon exposing to O_2 the copper bound 2,4-di-*tert*-butyl phenolate **1.7**, generated by reacting the phenol with sodium hydride and CuCl (Scheme 1.3)[43-44]. By time-dependent aliquot analyses, they revealed the primary formation of the catechol (2,4-DTBC), followed by the *ortho*-quinone (3,5-DTBQ) and finally formation of 3,3',5,5'-tetra-*tert*-butyl biphenol (D1). The biphenol is thought to arise from autoxidation of 2,4-DTBP to the corresponding phenoxyl radical, after water generated *in situ* during reaction has poisoned the catalytic system. Maumy and Capdevielle subsequently reported the synthetically useful copper-mediated aerobic oxidation of phenols to their corresponding catechols in 70-90% yield, using catalytic amounts of Cu_2Cl_2, excess Cu (0) and sodium hydride (~1 equivalent). These conditions provided a versatile method for the Cu-mediated aerobic oxidation of phenols into catechol.

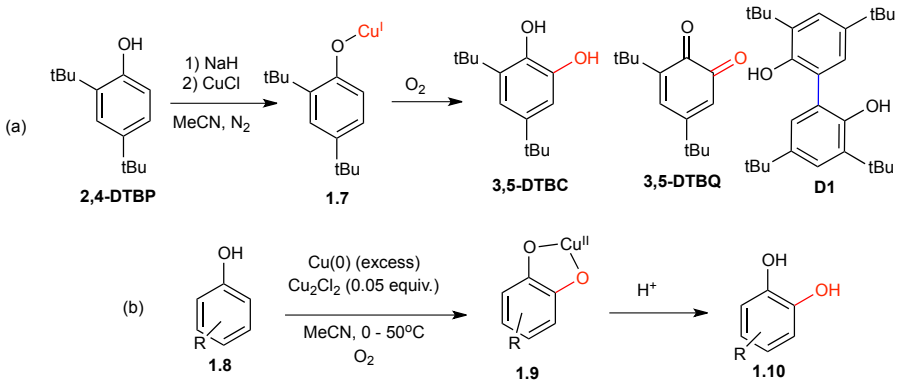

Scheme 1.3 Maumy and Capdevielle's (a) ortho-quinone and (b) selective catechol syntheses

These results started many efforts towards optimization of oxygenation reactions of phenols using catalytic quantities of Cu. In 2004, Cheng reported mononuclear, tridentate 1,3-bis(pyrid-2-yl)-2-oxapropane (bpmo) and 1,3-bis(N-*n*-propylbenzimidazol-2-yl)-2-oxapropane (bb^{Pr}mo) N-O-N type ligands (Scheme 1.4) for reaction of 1 molar equivalent of 2,4-DTBP or its corresponding triethylammonium phenolate, in the presence of copper (I) and O_2 in dichloromethane at room temperature over 24 hours[45]. These reactions were not selective as

determined with isolated yields, and generated the C-C coupled biphenol as the major product along with trace quantities of the corresponding *ortho*-quinone. It was determined that the N-O-N ligand was necessary, as the reaction without ligand, using solely copper tetrakis acetonitrile perchlorate and O_2 did not generate 3,5-DTBQ or D1, and only small levels of conversion were observed.

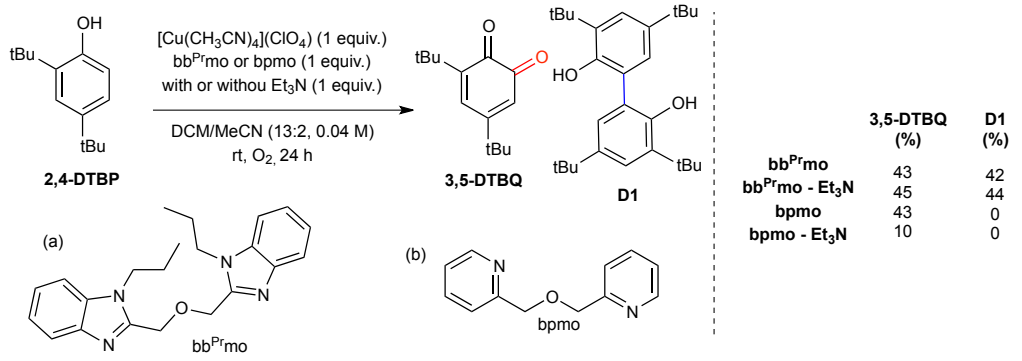

	3,5-DTBQ (%)	D1 (%)
$bb^{Pr}mo$	43	42
$bb^{Pr}mo$ - Et_3N	45	44
bpmo	43	0
bpmo - Et_3N	10	0

Scheme 1.4 (a) 1,3-bis(N-n-propylbenzimidazol-2-yl)-2-oxapropane ($bb^{Pr}mo$) ligand (b) 1,3-bis(pyrid-2-yl)-2-oxapropane (bpmo) ligand in 2,4-DTBP oxidations

B. Stoechiometric Models exhibiting a μ-η^2:η^2 –peroxo $Cu(II)_2$ binding geometry

In 1984, Karlin and coworkers reported the first synthetic model Tyrosinase system comprising an extensive ligand framework and demonstrating oxygenase type reactivity[46]. Upon exposure to O_2, Cu_2(XYL) complex **1.11** (Scheme 1.5) underwent oxygenation of the aromatic spacer of the ligand frame leading to a μ-hydroxo μ-peroxo complex. In 1989, Karlin proposed either a μ-η^2:η^2 –peroxo or a μ-*trans*-peroxo complex as the active catalyst species performing oxidation[47], and it was only a few months later that the first crystal structure of another side-on peroxo bridged dinuclear copper complex was solved[48], allowing further indication of the side-on peroxo binding mode of Karlin's Tyrosinase model complex.

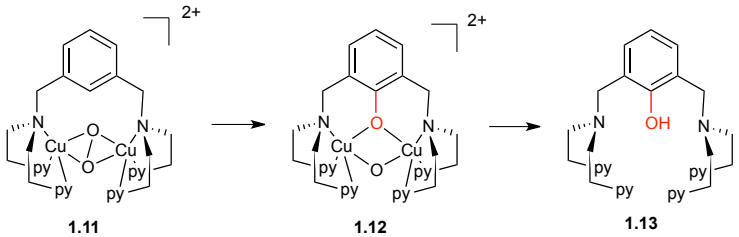

Scheme 1.5 Karlin's Cu_2(XYL) complex and aerobic reactivity (py = 2-pyridyl)

Since 1984, many other dinuclear copper systems capable of ligand hydroxylation have been reported, but most of these lack a thorough investigation of the copper-O_2 species effecting oxygenation[49-67]. Karlin's system remains one of the best studied, and has provided the basis for elucidation of the Tyrosinase oxygenase reactivity (*c.f.* Scheme 1.1)[27]. Experiments using $^{18}O_2$ revealed that both oxygen atoms of the peroxo-oxo complex are derived from O_2 (not H_2O). Careful study by Raman spectroscopy of the dicopper-O_2 species in solution revealed only peaks for a μ-η^2:η^2 –peroxo complex, and the upper limit of concentration for the amount of bis-μ-oxo isomer in 4mM solutions of dicopper-O_2 was calculated to be ~0.13%[27]. Although this does not exclude the possibility of bis-μ-oxo performing the hydroxylation, this reaction would have to be ~1000 times more reactive than that with the side-on peroxo system to significantly contritbute[27].

An important unresolved step of the analogous Tyrosinase catalytic cycle is how the oxygen atom is incorporated into the ligand arene (or, in Tyrosinase, the hydroxylation of phenol to a corresponding catechol). As electron withdrawing groups are incorporated into the Cu_2(XYL) system, the rate of hydroxylation of the ligand was decreased, suggesting an electrophilic aromatic substitution mechanism[68]. Further proof included the lack of a kinetic isotope effect when the hydrogen at the hydroxylated position was substituted for a deuterium atom (Scheme 1.6)[28]. Experiments when the hydrogen at the hydroxylation position is substituted for a methyl group have provided additional support for an electrophilic substitution mechanism (Scheme 1.7)[28]. Analysis of the products obtained from these substrates revealed a 1,2-methyl migration. This migration involves a cationic intermediate that would be generated after arene attack of the copper-peroxo adduct (Scheme 1.7).

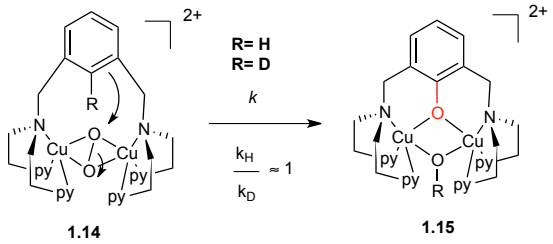

Scheme 1.6 Karlin's Cu_2(XYL-R) complex (R= H or D) undergoing oxygenation

In 1989, Kitajima reported the first x-ray crystal structure of of a μ-η^2:η^2 –peroxo dicopper species using $[Cu(HB(3,5\text{-}i\text{Pr}_2\text{pz})_3)]_2(O_2)$ (pz = pyrazole) (Scheme 1.8)[48]. Kitajima subsequently reported the system's oxygenase activity[69], demonstrating that under aerobic conditions, their complex was capable of acting as an oxidant on 2,4-DTBP, yielding a mixture

of diphenoquinone **1.21** and 3,5-di-*tert*-butyl *ortho* quinone (3,5-DTBQ) (in a ratio of 1700:18, expressed in percent with regards to the complex). Although this represented the first example of external phenolic hydroxylation to the *ortho*-quinone, and the first definitive evidence that a μ-η^2:η^2 –peroxo dicopper system could promote oxygenation, there remained a clear lack of selectivity. Diphenoquinones are believed to arise through dimerization of phenoxyl radicals, followed by two-electron oxidation of the 4,4'-biphenyl-diol.

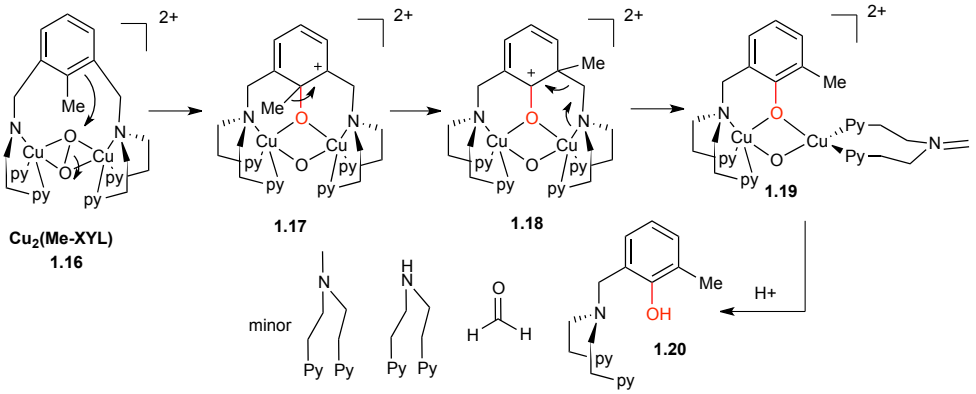

Scheme 1.7 Karlin's Cu_2(Me-XYL) complex undergoing 'NIH Shift'

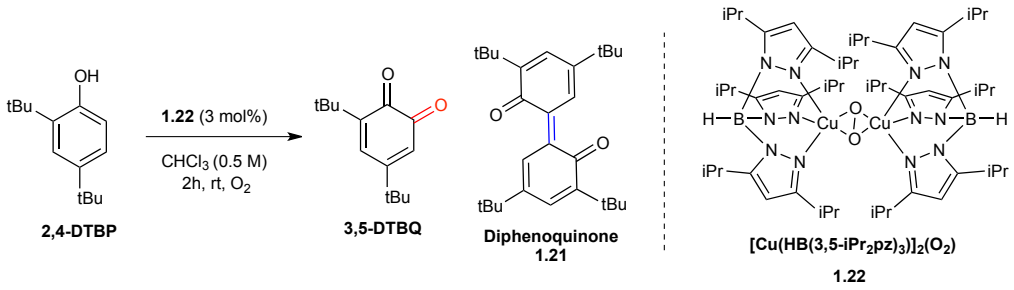

Scheme 1.8 Kitajima's reported copper-peroxo x-ray data and reactivity towards exogenous phenols

In 1991, Casella and co-workers published a dinuclear copper system, with ligand **L66**, capable of stoichiometric conversions of methyl-4-hydroxybenzoate to its corresponding catechol in 37% yield (Scheme 1.9)[70]. In a later report, Casella *et al.* effected systematic changes to ligands (Scheme 1.9), starting from **L66**, and investigated their respective reactivity towards the sodium salt of methyl-4-hydroxybenzoate[71]. Interestingly, the ligand with the highest spacer between the xylene bridge and the benzimidazole moiety worked best, demonstrating the importance of a flexible catalyst system, presumably to better accommodate the different preferred geometries of cuprous and cupric oxidation states necessary for oxidation. It was only in the year 2000 that Casella confirmed the copper-O_2 geometry of the active catalyst as a μ-η^2:η^2 –peroxo species[72].

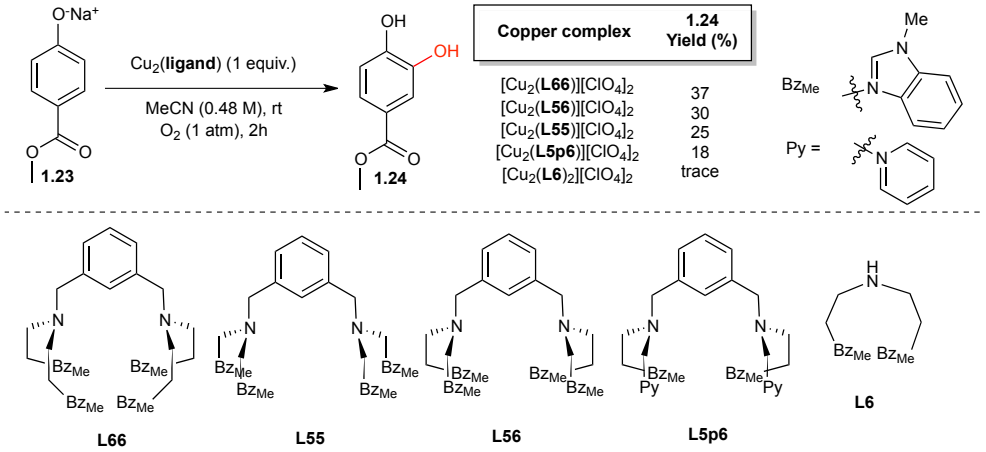

Scheme 1.9 Casella and co-workers' reported ligands and reactivity

Substituting a benzimidazole group for pyridine again reduces reactivity of the corresponding dicopper complex, which could be attributed to its increased acidity (pKa of 5.25 for the conjugate acid of pyridine versus a pKa of 16.5 for the conjugate acid of benzimidazoles)[73-74]. In effect, decreasing basicity will decrease the σ-donor ability of a given ligand, and thus its ability to stabilize a cupric state, necessary for oxidation. The backbonding ability of the ligands must also be considered, as a more accepting ligand will favor a cuprous state. Finally, the mononuclear complex formed using ligand **L6** showed almost no reactivity towards methyl-4-hydroxybenzoate. As mononuclear ligand frameworks have shown to catalyze oxygenations (discussed below), the nuclearity of the ligand cannot explain the reactivity difference. Rather, the presence of a secondary amine is significant.

Although Casella's systematic study evidenced crucial characteristics of an optimal copper-O_2 catalyst, such as the effect of reaction mixture pKa or ligand flexibility, the reaction conditions still included generation of the phenolate *in situ* from the corresponding phenol and sodium borohydride. Sodium borohydride is known to reduce *ortho*-quinones to their corresponding catechols. Exploring the reaction of Cu_2(**L-66**) with the same phenolate in non-reducing conditions at room temperature led to the isolation of the Micheal adduct, generated from phenolate addition to the initial *ortho*-quinone (Scheme 1.10)[71]. Reducing reaction temperature returned selectivity for the catechol, although incomplete conversion was observed, even with prolonged reaction times. Similar results were also demonstrated in 1994 by Sayre and co-workers, whose experiments refuted the intermediacy of catechols in the formation of *ortho*-

quinones, by showing that Casella's Cu_2(**L-66**) catalyst did not release the expected catechol in non-reducing conditions, and that catechols were unreactive under the reaction conditions[75].

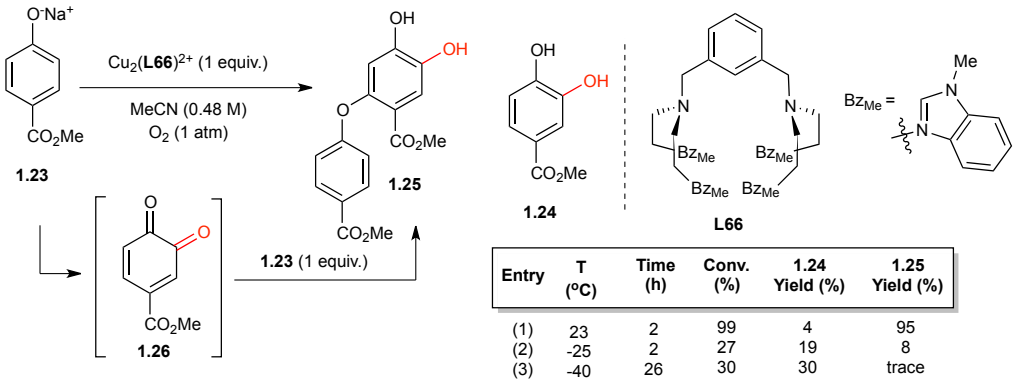

Entry	T (°C)	Time (h)	Conv. (%)	1.24 Yield (%)	1.25 Yield (%)
(1)	23	2	99	4	95
(2)	-25	2	27	19	8
(3)	-40	26	30	30	trace

Scheme 1.10 Non-selective oxygenation reactions with $Cu_2(L66)^{2+}$ in non-reducing conditions

In 1998, Casella *et al.* reported a system capable of selectively furnishing the catechol from the sodium salt of methyl-4-hydroxybenzoate at room temperature in non-reducing conditions (Scheme 1.11)[76]. Furthermore, although Cu_2(**L-66**) was unable to hydroxylate phenols (generating instead the corresponding biphenol), the novel Cu_2(**LB5**) was capable of *ortho*-oxygenation and furnished catechols in 17% yield (83% remaining starting material). This possibility was ascribed to the extra basic functionality of the ligand that could serve as a base to deprotonate the phenol before coordination to copper.

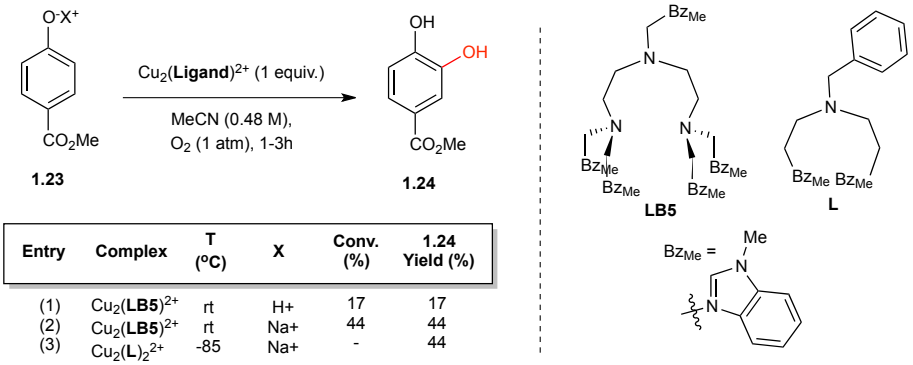

Entry	Complex	T (°C)	X	Conv. (%)	1.24 Yield (%)
(1)	$Cu_2(LB5)^{2+}$	rt	H+	17	17
(2)	$Cu_2(LB5)^{2+}$	rt	Na+	44	44
(3)	$Cu_2(L)_2^{2+}$	-85	Na+	-	44

Scheme 1.11 Casella's $Cu_2(LB5)^{2+}$ and $Cu_2(L)^{2+}$ complexes and reactivity towards phenolates and phenols

In 1996, Casella described a mononuclear copper(I) complex[71], Cu_2**L**$_2$ (Scheme 1.11) that was later shown to afford a μ-η^2:η^2–peroxo geometry upon oxygenation[77], but thought to be unreactive. In 2000, Sayre was able to utilize this complex to oxygenate the sodium salt of ethyl 4-hydroxybenzoate at room temperature to the corresponding phenol functionalized *o*-catechol[78].

In 2003, Casella and co-workers were also able to oxidize the sodium phenolate of methyl-4-hydroxybenzoate at low temperature to yield 88% yield of unsubstituted catechol (based on the amount of reactive dinuclear copper)[77]. At room temperature, results analogous to those of Sayre were obtained.

In 2005, a study was published by Casella on the oxygenation of a series of *para*-substituted phenols with a novel copper-ligand system, Cu_2(**Me-L66**), the 1,3,5-hemellitol-bridged version of previously published Cu_2(**L-66**), showing a μ-η^2:η^2 –peroxo geometry upon oxygenation[29]. This study provided additional support towards the electrophilic aromatic substitution mechanistic pathway previously proposed on the basis of studies of ligand hydroxylation reactions with copper O_2 systems, as electron poor phenols showed less reactivity than electron rich phenols.

Meanwhile, in 1991, the complex Cu(phen)(PPh_3)(BH_4), showing a side-on bridged peroxo binding geometry, was also demonstrated by the Rindone group to be capable of stoichiometric oxidation of several phenols to their corresponding catechols, with yields ranging from 30% (electron poor phenols) to 100%[79]. Based on the work of Sayre, it is likely that the borohydride of the pre-catalyst reduced the initially formed *ortho*-quinone, allowing for sole observation of catechols.

In 1995, Rindone systematically investigated the scope of μ-η^2:η^2 –peroxo dinuclear copper–mediated oxidations of *ortho*, *meta*, and *para*-substituted phenols using the Cu(phen)(PPh_3)(BH_4) complex reported in 1991[80]. *ortho*-Substituted phenols were found to provide decreased yields of the desired catechols, as expected due to potential steric interactions with the copper oxidant, while *meta*-substituted phenols were discovered to have a preference for yielding 3,4-catechols, *versus* 2,3-catechols.

In 2001, Itoh and co-workers reported benzyl-di-deuterium labeled $[Cu(PhCD_2Py_2)]^+$ complex **1.27**, which forms a μ-η^2:η^2 –peroxo complex upon oxygenation at low temperature (Scheme 1.12)[81]. Deuterium labeling was done in response to results showing that upon warming to room temperature under aerobic conditions, the hydrogen-substituted analogue, underwent benzylic hydroxylation and N-dealkylation. The heavier deuterium atom was expected to slow this reaction, which is undesired when intending to study reactivity towards external phenolic substrates. Effectively, reaction of the oxygenated deuterium labeled complex with lithium phenolates efficiently yielded catechols.

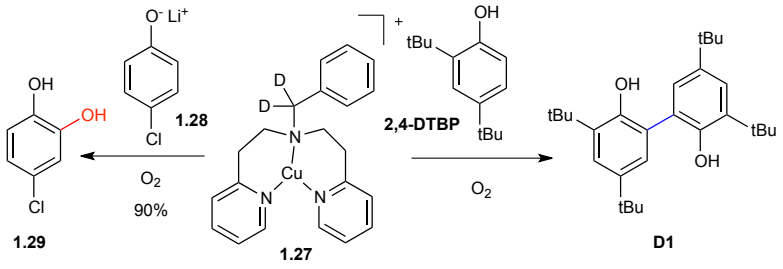

Scheme 1.12 Itoh's benzyl-di-deuterium labeled mononuclear copper complex

Interestingly, Itoh *et al.* investigated the reactivity of this complex towards neutral phenols only to find that neither *ortho*-quinones nor catechols were produced, but instead C-C coupled biphenols were obtained in very good yield. Formation of the dimers was attributed to copper acting as an outer-sphere oxidant generating phenoxyl radicals that recombine. Kushioka[82] reports biphenols as products of an inner sphere catalytic oxidation with copper, but there is wide agreement in the literature that C-C coupled products arise from radical coupling generated through an outer-sphere process of oxidation[1]. Kushioka bases the conclusion that biphenols are formed within the transition metal coordination sphere by studying the yields at different intervals of the oxidation of 2,4-DTBP with CuCl (4 mol%) and *N,N'*-di-*tert*-butylethylenediamine (8 mol%) in methanol at room temperature for 24 minutes under O_2.

Eleven years later, in 2012, Matsumoto and co-workers reported the synthesis and study of a new ligand-copper (I) system, namely *N,N',N''*-triisopropyl-cis,cis-1,3,5-triaminocyclohexane (*i*Pr$_3$TACH) in which the α carbon to the nitrogen is tertiary (Scheme 1.13)[83]. These complexes, upon oxygenation, directly provided a μ-η^2:η^2 –peroxo geometry. Interestingly, the same authors had previously reported oxygenation of analogous complexes bearing a secondary α carbon (R$_3$TACH where R= Et, *i*Bu, Bn) and yielding bis- μ-oxo complexes upon exposure to O_2 (Scheme 1.13). The difference is attributed to the decreased flexibility of the former system that would tighten the size of insertion of O_2 for binding. The reactivity of this complex towards sodium 2,4-di-*tert*-butyl phenolate was also investigated, exhibiting a 50% yield of the corresponding *ortho*-quinone based on the peroxide intermediate. This is in contrast to the complexes with ligands showing a secondary α carbon that were incapable of oxidizing phenolate.

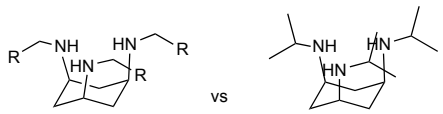

R_3TACH
R= Et, iBu, Bn

iPr_3TACH

Scheme 1.13 Matsumoto's R_3TACH and iPr_3TACH ligands

In 2012, Stack and co-workers published results whereby a self-assembled $Cu(Imidazole)_3X$ (Where X = SbF_6^- or PF_6^-) successfully mimicked oxygenase reactivity of Tyrosinase, and effected catalytic hydroxylations of several 2,4-disubstituted phenolates to the corresponding quinones and catechols[31]. Experiments revealed that the complexes afforded μ-η^2:η^2 –peroxo binding geometry with O_2 at low temperatures. Kinetic measurements again confirmed an electrophilic aromatic substitution mechanism for the oxygen insertion step of the reaction. This was the first report of a catalytic aerobic oxygenation with monodentate imidazole ligands.

Although the above reports suggest that the μ-η^2:η^2 –peroxo core is the geometry responsible for performing oxygenase type reactivity in synthetic systems and by analogy in Tyrosinase, few examples do exist whereby a bis-μ-oxo $Cu(III)_2$ binding geometry effects oxygenations. As previously stated, Tolman and co-workers have shown that there exists an equilibrium between the two O_2 binding geometries, although the equilibrium favors the side-on peroxo species[27]. Nevertheless, the presence of either species, when the other is characterized as the sole geometry spectroscopically, cannot be excluded.

C. Stoechiometric Models exhibiting a bis-μ-oxo - $Cu(III)_2$ binding geometry

In 2002, Stack and Solomon reported a μ-η^2:η^2 –peroxo complex formed by mixing a 2:1 mixture of *N,N'*-di-*tert*-butyl ethylene diamine (DBED) with $[Cu(CH_3CN)_4](X)$ where X= ($CF_3SO_3^-$, ClO_4^-, SbF_6^- or BF_4^-) (Scheme 1.14)[84]. Reaction of the lithium or sodium salt of 2,4-di-*tert*-butyl phenolate at 193 K formed a 1:1 mixture of the corresponding catechol and *ortho*-quinone, with overall 80% yield, as calculated from the oxidizing equivalents of the copper complex.

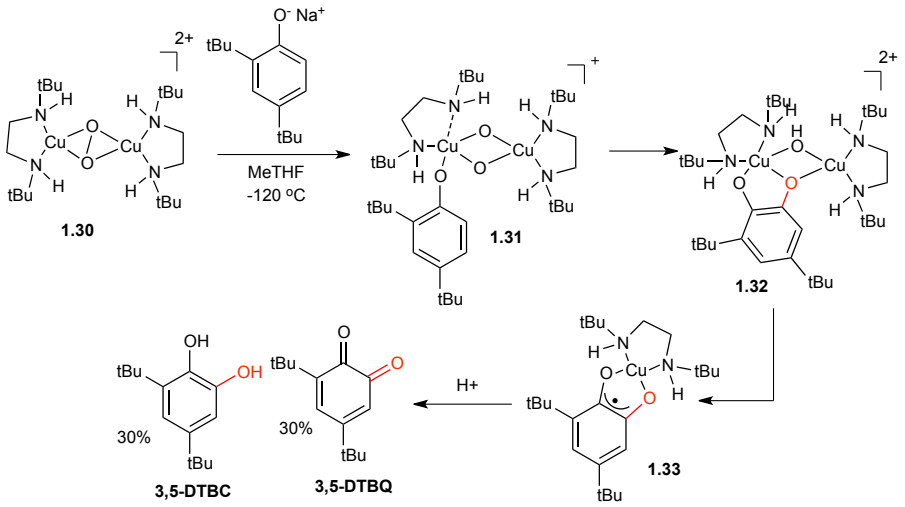

Scheme 1.14 Stack and Solomon's Cu2(DBED)2 mediated oxygenation of 2,4-DTBP

Stack and co-workers demonstrated that that phenolate binding to Cu/DBED peroxo-complex, triggers isomerization of the μ-η^2:η^2–peroxo **1.30** to bis-μ-oxo $Cu(III)_2$ **1.31** cleaving the O-O bond prior to oxygen atom transfer (Scheme 1.14)[85-86]. Oxygenation of the copper phenolate occurs, subsequently from the bis-μ-oxo geometry, to yield the chatecholate **1.32** which then leads to a 1:1 mixture of catechol and *ortho*-quinone following acid work-up. The authors also postulated the intermediacy of a copper-semiquinone species after oxygenation, which upon acid quenching disproportionates to form both the catechol and quinone in equal quantities.

Whereas almost all characterized bis-μ-oxo complexes had shown non-physiological C-C coupling towards external phenolic substrates[17], in 2008 Costas and co-workers reported a genuine bis-μ-oxo complex capable of performing hydroxylations of electron poor phenolates (Scheme 1.15)[87]. For example, this system selectively yielded the catechol **1.29** in 67% yield. Kinetic studies were performed on the Cu(I)(*m*-XYL^{MeAN}) system (Scheme 1.15a) and the Hammet plot constant indicated an electrophilic aromatic substitution pathway for the oxygenation step, as in the case of the side-on peroxo binding geometry. It is thus shown that both copper-O_2 geometries can oxygenate phenols selectively, and both show an electrophilic aromatic substitution mechanism. It is thus difficult to know which of the peroxo and oxo geometries of *oxy* -Tyrosinase is the one performing oxygenation *in situ.*

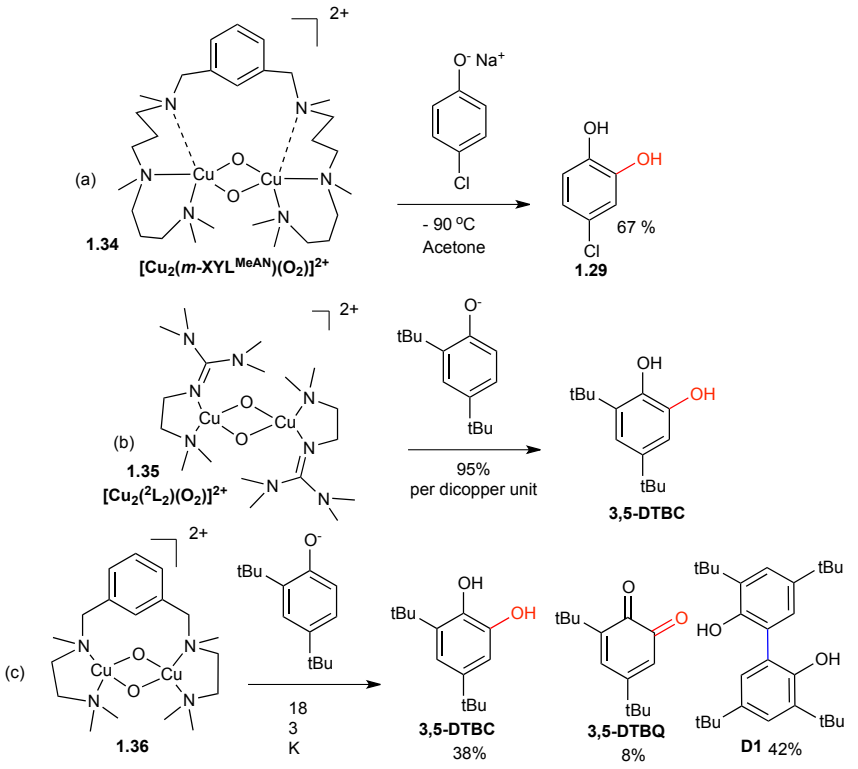

Scheme 1.15 (a) Costas' Cu $_2$(*m*-XYL^{MeAN}) complex and phenolate reactivity (b) Herres-Pawlis et al. guanidine derived mononuclear ligand complex and established phenolate reactivity (c) Mukherjee and co-workers' xylene bridged dinuclear bis-μ-oxo complex and reactivity towards external substrates

A year later, Stack and Herres-Pawlis published system **1.35** exhibiting bis-μ-oxo geometry with a permethylated amide-guanidine ligand ^{2}L (Scheme 1.15b), and performed hydroxylations of the sodium salt of 2,4-di-*tert*-butyl phenolate to give the corresponding catechol in 95% yield based on copper units[86].

In 2012, Mukherjee published xylil-bridged system **1.36** exhibiting a bis-μ-oxo geometry in aerobic conditions (Scheme 1.15c)[88], but the oxygenated complex's reactivity with phenolates at low temperatures lacked selectivity. Biphenols (42%), catechols (38%) and quinone (8%) were observed with 2 equivalents of phenolate relative to the catalyst for one hour in THF at 183 K. In the case of the last two studies, since unequal amounts of quinone and catechol are observed, the putative intermediate of a copper-semiquinone does not form or does not undergo disproportionation upon acid quenching, in contrast to Herres-Pawlis and Stack's Cu/DBED system.

D. Stoechiometric models with a *trans*-μ-η^1:η^1-peroxo $Cu(II)_2$ binding geometry

In 2010, Costas *et al.* showed that *trans*- μ-η^1:η^1-peroxo complexes were also capable of efficiently mimicking Tyrosinase oxygenase chemistry[89]. The $Cu(I)_2$(*m*-XYL^{N3N4}) complex **1.37** reacted with the sodium phenolate of *p*-chlorophenol to give the catechol **1.29** in 39% yield (Scheme 1.16).

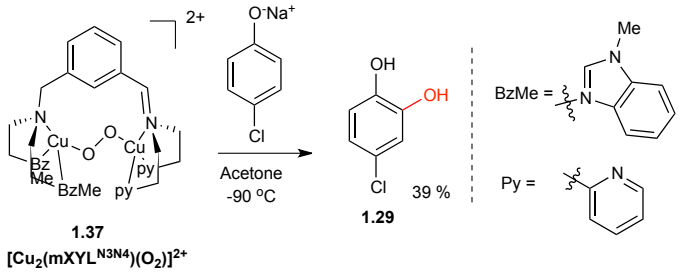

1.37
$[Cu_2(mXYL^{N3N4})(O_2)]^{2+}$

1.29

Scheme 1.16 Costas' trans-1,2-peroxo dinuclear copper complex and phenolate reactivity

Two years later, Costas further reinforced the fact that end-on peroxide can perform oxygenase chemistry by expanding the scope of $Cu(II)_2$(end-on O_2)(*m*-XYL^{N3N4}) to other *para*-substituted phenolates and *phenols* (bearing EWG and EDG)[30]. Electron-poor and bulky phenolates showed almost no reactivity, while electron rich and unhindered phenolates produced catechols in moderate yields. In contrast, phenols react only to form C-C coupled biphenols, which the authors associate with a PCET mechanism, in line with Itoh and Fukuzimi's observed reactivity of the $[Cu(PhCD_2Py_2)]^+$ complex towards phenols.

1.2.3 Catalytic synthetic models of Tyrosinase

Even more relevant to the action of the enzyme Tyrosinase is the *catalytic* conversion of phenols (phenolates) to *ortho*-quinones. The first such system was reported in 1984 by Bullowski in a patent, who used catalytic quantities of a binuclear copper complex, Cu_2(BiPh(impy)$_2$) (Scheme 1.17a) under basic and aerobic conditions to afford *ortho*-quinone and catechol, along with unreacted starting material and unknown derivatives, from 2,4-DTBP[90]. In 1990, Reglier optimized the same catalyst system, and obtained the *ortho*-quinone (along with biphenol) with a turnover number of 16 after one hour, as determined by kinetic (UV/Vis) experiments, using

1mol% catalyst and 2 equivalents of triethylamine in dichloromethane[91]. Importantly, when triethylamine was omitted from the reaction, only the biphenol was obtained.

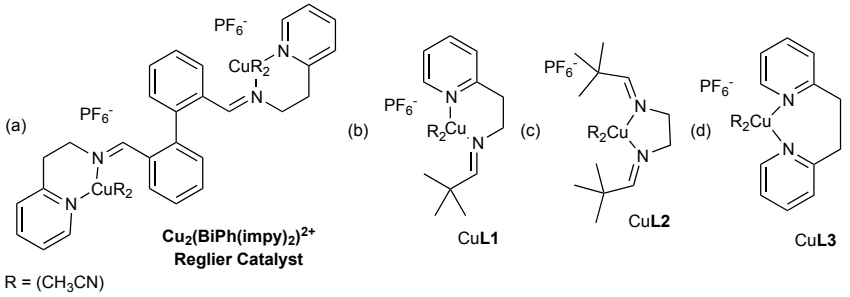

Scheme 1.17 (a) Reglier catalyst (b-d)Tuczek catalysts for 2,4-DTBP catalytic aerobic oxidation

Casella *et al.* also investigated the catalytic reaction of the extensively studied Cu_2(**L-66**) complex (*c.f.* Scheme 1.9)[70]. This system was not only shown to mediate stoichiometric hydroxylation of electron poor methyl 4-hydroxybenzoate to the corresponding catechol, but also to convert the sodium salt of 2,4-DTBP to the *ortho*-quinone, albeit along with unidentified byproducts, using a 1.5:1 ratio of phenolate to the preformed dinuclear Cu/O_2 complex in acetonitrile in 3 min, giving a turnover number greater than one.

In 2010, Tuczek and coworkers published a mono-nuclear catalyst, **L1** (Scheme 1.17b)[92], which, in combination with copper (I), triethylamine and O_2, was capable of effecting catalytic hydroxylation and subsequent two electron oxidation of 2,4-DTBP to the *ortho*-quinone with a turnover number of 18 (from kinetic studies of the quinone UV/Vis band appearance at 400 nm). The reaction was not selective however, and also yielded catechol and biphenol in 3% and 30% yield, respectively. Interestingly, the bisimine (**L2**) or bispyridine (**L3**) ligands did not show any reactivity (Scheme 1.17c-d)[92].

In 2013, Stack and Herres-Pawlis demonstrated that [Cu[bis(3-*tert*-butyl-pyrazolyl)pyridyl-methane)]]SbF_6^- was capable of oxygenating phenols and that the μ-η^2:η^2 – peroxo active catalyst was stable at room temperature. (Scheme 1.18)[93]. The authors reported room-temperature catalytic conversion of phenols, in basic aerobic media, to the corresponding *ortho*-quinones, with turnover numbers ranging from 8-14 in reaction times varying from 1-16 hours. In addition, *N*-acetyltyrosine methyl ester, a Tyrosinase substrate, was also oxidized to its dopaquinone form. Interestingly, room temperature results on oxidation of *p*-methoxy phenol showed the quinone as the product, yet at cold reaction temperatures (-78 ^oC) under

stoichiometric conditions, only the catechol was observed. The authors ascribe this difference in reactivity to catecholate binding inhibition at low temperatures. Control experiments without base (triethylamine) showed no reactivity at all, emphasizing the role of base as a proton shuttle. The authors propose a mechanism based on the discussed results (Scheme 1.19).

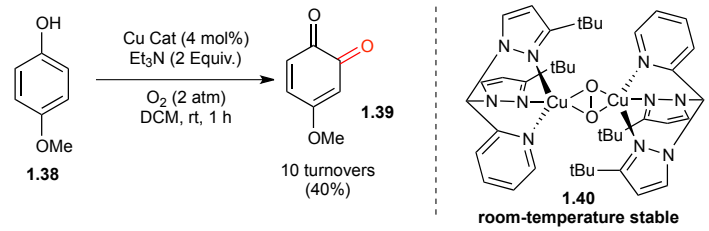

Scheme 1.18 Stack and Herres-Pawlis' catalyst for phenolic catalytic aerobic oxidation

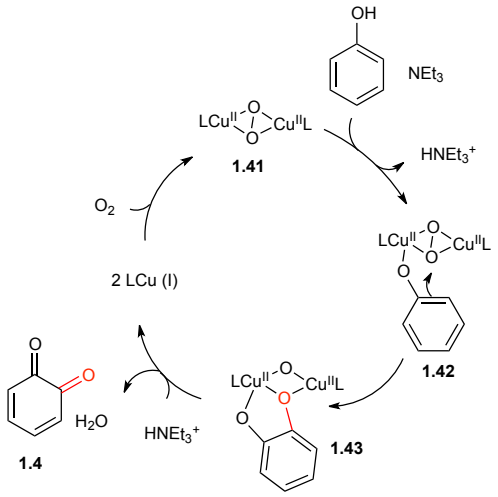

Scheme 1.19 Oxygenase chemistry mechanism as proposed by Herres-Pawlis and co-workers

At the end of 2013 and beginning of 2014, Tuczek published additional catalyst systems that performed hydroxylation of phenolic substrates under catalytic aerobic conditions[94-95]. These ligands contained imine and benzimidazole or pyrazole moieties, and in combination with a copper (I) source, triethylamine and O_2, furnished the *ortho*-quinone of the 2,4-di-*tert*-butyl phenol in turnover numbers up to 31 (Scheme 1.20), although C-C coupled unwanted byproducts are still observed. Kinetic measurements indicated that a higher reaction rate correlated with higher product yield, and this result was attributed to the diminished action of side reactions that destroy the catalyst when the desired reaction rate is faster.

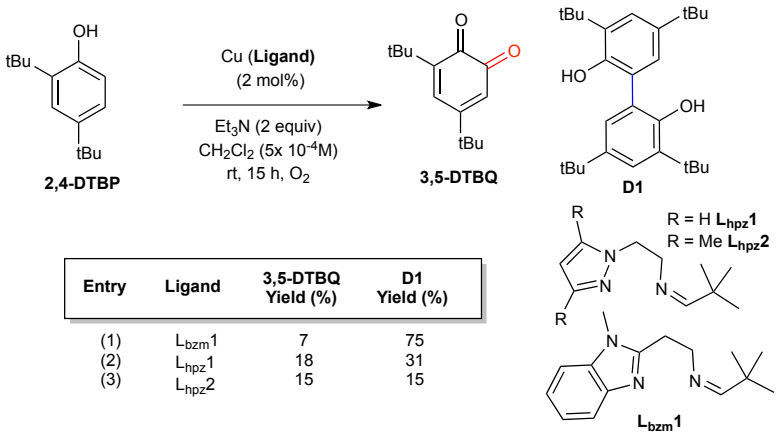

Entry	Ligand	3,5-DTBQ Yield (%)	D1 Yield (%)
(1)	$L_{bzm}1$	7	75
(2)	$L_{hpz}1$	18	31
(3)	$L_{hpz}2$	15	15

Scheme 1.20 Tuczek's pyrrazole and benzimidazole ligands and reactivity

While several catalytic systems for the aerobic *ortho*-oxygenation of phenols have been described, there remains a lack of synthetically useful conditions. In effect, all systems discussed above require very low reaction concentrations and superstoichiometric amounts of an amine base. Furthermore, more than a few of the discussed reactions are conducted at low temperatures and are limited to very small scales. Both catechols and quinone products are often obtained, and C-C coupled biphenols are also observed as byproducts. Overall, although genial advances have been made in the understanding of Tyrosinase and mimicking its activity with synthetic complexes, the development of an operationally simple, selective copper catalyzed aerobic phenol oxidation remains an unmet goal.

1.3 Oxepinobenzofurans: Discovery, Syntheses and Reactivity

Section 1.2 reveals that achieving selectivity for *ortho*-quinones *via* phenolic copper aerobic oxidations is challenging. A distinct mechanistic pathway for *ortho*-quinones *versus* the observed C-C coupled byproducts is evidenced[17], whereby the latter are thought to occur through an outer-sphere one-electron phenolic oxidation distinct from the copper-bound phenolic oxygenation pathway. The biphenols are the most ubiquitous C-C coupled byproducts observed in phenolic copper aerobic oxidations, along with their oxidized counterpart the oxepinobenzofurans (*c.f.* Chapter 2). A review of the discovery, syntheses and reactivity of the oxepinobenzofurans is given in Section 1.3, which will evidence the benefit of developing their

selective synthesis via copper aerobic phenolic oxidation, and demonstrate their unrealized potential as oxidation reagents.

1.3.1 Discovery and Characterization of Oxepinobenzofurans

In 1961, Muller and coworkers effected the basic potassium ferricyanide oxidation of 2,4-di-*tert*-butyl phenol to its corresponding C-C coupled product, 3,3',5,5'-tetra-*tert*-butyl-biphenyl-4,4'-diol[96]. Oxidation of the biphenol under identical conditions was found to yield a product never previously characterized. The oxidation could also be performed using 4-cyano-2,6-di-*tert*-butyl phenoxyl as the oxidant. With the obtained mass and IR spectra and knowing that reduction of the unknown product with lithium aluminum hydride provided the biphenol, the authors proposed three potential structures of the product (Scheme 1.21). Proton NMR showed four different butyl groups, evidencing the structure as asymmetric, and finally, by elimination, the spiro-quinol ether structure **1.46** was assigned as that of the unknown. This affirmation was reinforced by the analogy to the formation of homologous spiroquinol ethers[96].

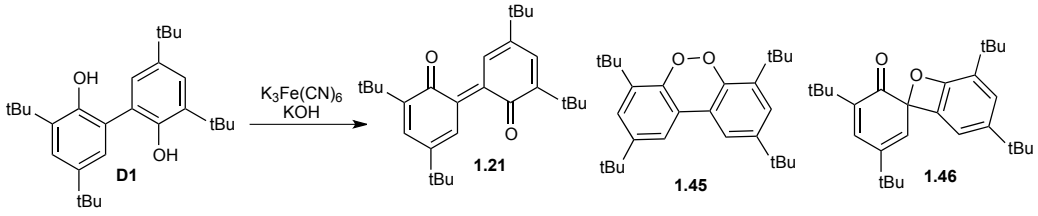

Scheme 1.21 Müller's proposed structures for unknown and assigned benzoxete structure 1.46

A radical mechanism was proposed for the formation of the spiro-quinol ether, whereby oxidation of the biphenol provides a diphenoquinone (**1.21**, Scheme 1.21) that subsequently rearranges *via* a cycloaddition to the proposed benzoxete. The diphenoquinone structure was proposed in accordance with an observed deep violet reaction color.

Baltes and Volbert, in 1955, reported the synthesis of an analogous benzoxete by ferricyanide oxidation of 4-methoxy-2-*tert*-butyl phenol (or its corresponding biphenol dimer)[97]. Primary formation of the diphenoquinone was hypothesized, and valence isomerization followed by precipitation yielded a supposed peroxide compound, analogous to **1.45** (Scheme 1.21). In 1964, Muller suggested a spiroquinol ether structure for this compound related to **1.46**[98].

In 1978, the Rieker group proposed a drastic reassignment of the spiro-quinol ether structure to that of oxepinobenzofurans[99]. By examination of the compounds derived from oxidations of biphenols **1.47a-1.47d** (Scheme 1.22), the authors found that the IR and ^{13}C NMR spectra discounted a spiro-quinol ether structure, based on carbonyl frequencies in comparison to compounds **1.53** and **1.54** (Scheme 1.22). Starting from the diphenoquinone, all asymmetric possible valence isomers were considered (Scheme 1.22). On the basis of NMR, IR, and an unreported crystal structure, the oxepinobenzofuran structure was finally concluded. It was not until 2013 that the x-ray crystal data of an oxepinobenzofuran was published.

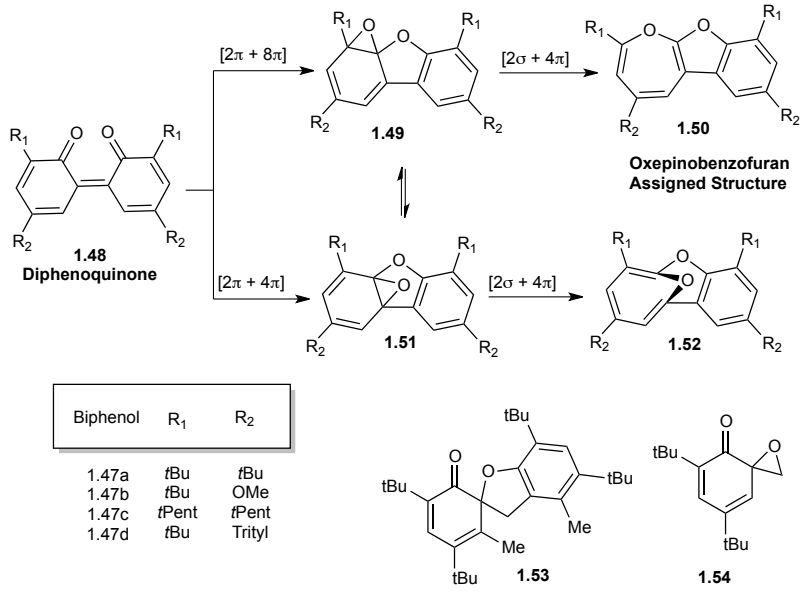

Scheme 1.22 Rieker's Structural reassignment of Spiroquinol ethers to Oxepinobenzofurans

1.3.2 Diphenoquinone – Oxepinobenzofuran Isomerism

From the very first synthesis of the oxepinobenzofurans, an equilibrium between blue-purple diphenoquinone and thermodynamically stable oxepinobenzofuran was hypothesized[97]. It was not until 1976 that such an unstable quinone was isolated, and its conversion to the oxepinobenzofuran measured[100]. Becker and Gustaffson reported the synthesis of 3,3'-di-*tert*-butyl-5,5'-di-trityl diphenoquinone from basic potassium ferricyanide oxidation of the corresponding phenol, and precipitation from water. Previous to that, only three reports of diphenoquinones existed[101-103], all alkoxy substituted, and none showed isomerization to the oxepinobenzofuran.

Upon solvation in ethanol or methanol, the diphenoquinone isomerized to the oxepinobenzofuran upon thermal treatment. This report provided confirmation of the intermediacy of the diphenoquinone in the synthesis of the oxepinobenzofuran. Knowing that the desired compound could also be obtained from the biphenol, a tentative mechanism was proposed. Becker suggested Zwitterionic species **1.55** as a reaction intermediate based on the accelerating effect of protic solvents (Scheme 1.23).

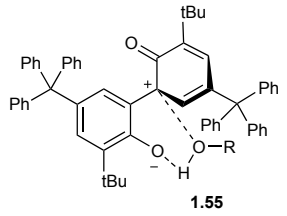

1.55

Scheme 1.23 Becker's proposed Zwitterionic intermediate in oxepinobenzofuran synthesis

In 1983, Hewgill and co-workers reported the rearrangement of an asymmetric diphenoquinone (Scheme 1.24a)[104]. In such an asymmetric system, the oxygen bearing the most negative charge can be expected to cyclize, giving a specific regioisomer, as was found to be the case. When the *ortho*-*tert*-butyl group is displaced to the *meta* position on one side of the biphenol (Scheme 1.24b), the produced diphenoquinone upon oxidation is very stable in non-polar solvents and does not rearrange to an oxepinobenzofuran. This can be explained by the work of Hayes *et al.*, who studied the equilibrium between arene oxides and oxepinobenzofurans, and found that substitution at C2, providing resonance or hyperconjugative stabilization favored the oxepinobenzofuran, whereas substituents at C3 favored the oxide[105]. This is well evidenced when considering the zwitterionic intermediate (Scheme 1.24): an electron donating group would resonance stabilize the positive charge, and enhance the equilibrium towards formation of this intermediate. It should be noted that here, the removed C2 substituent resides on the side of the biphenol that would bear the positive charge, based on earlier considerations.

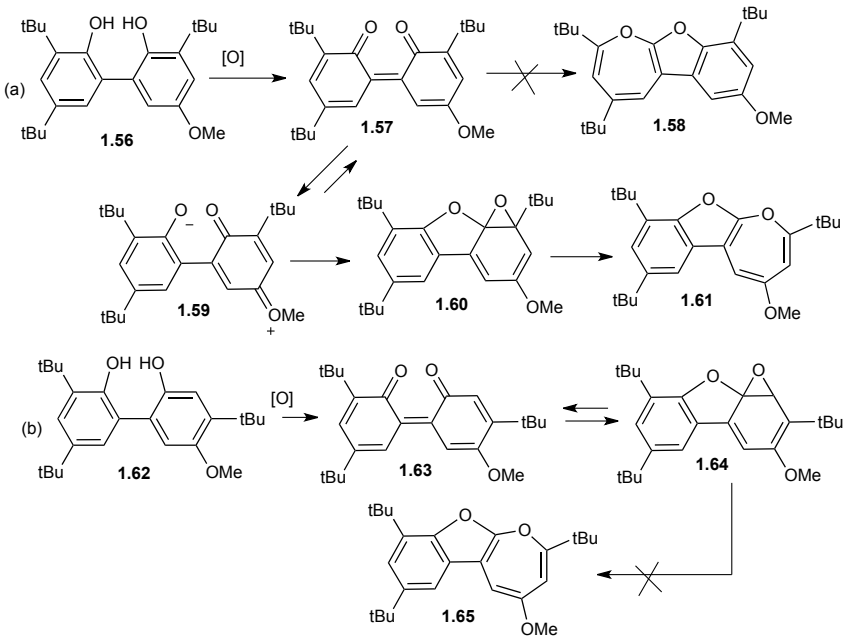

Scheme 1.24 (a) Regiochemistry of isomerization with asymmetric diphenoquinones (b) Effect of ortho-substituent on stability of diphenoquinone

Much later, in 2005, Rayne and co-workers found that photochemical treatment of dibenzo[1,4]dioxin yielded diphenoquinones (Scheme 1.25)[106], and subsequently measured the rates of decay of these compounds as a function of the attached substituents. A Hammet plot revealed two different pathways of degradation of diphenoquinones, depending on whether substitutents were electron withdrawing or donating groups. Benzofurans were generated with electron-withdrawing groups whereas oxepinobenzofurans were yielded with substrates bearing electron-donating groups. These results are consistent with the proposed mechanism (Schemes 1.23-1.24).

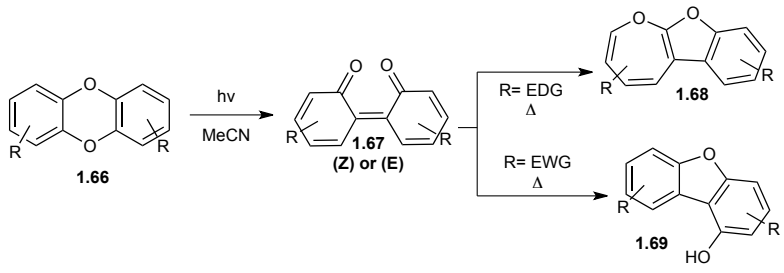

Scheme 1.25 Photochemical generation of diphenoquinones and subsequent thermal isomerizations

1.3.3 Syntheses of Oxepinobenzofurans

The first synthesis of oxepinobenzofurans proceeded through a two-step basic potassium ferricyanide mediated oxidation of 4-methoxy-2-*tert*-butyl phenol (MTBP)[97]. Later in 1961, the scope of this oxidation was expanded to 2,4-di-*tert*-butyl phenol and 2-iodo-4,6-di-*tert*-butyl phenol to produce, in both cases, 2,4,7,9-tetra-*tert*-butyl oxepinobenzofuran *via* the intermediate phenolic dimer (Scheme 1.26)[96].

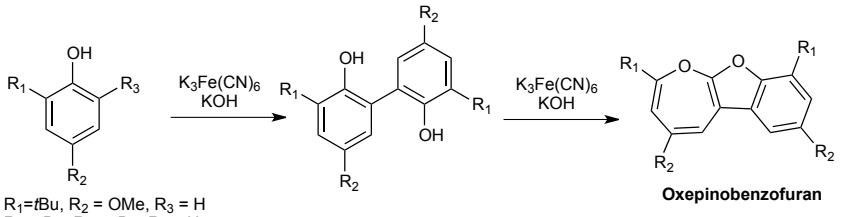

1.70 R_1=*t*Bu, R_2 = OMe, R_3 = H
1.71 R_1= *t*Bu, R_2 = *t*Bu, R_3 = H
1.72 R_1 = *t*Bu, R_2 = *t*Bu, R_3 = I

Scheme 1.26 First syntheses of oxepinobenzofurans

In 1968, Hewgill provided a novel synthesis of these compounds, consisting of base mediated radical coupling from halogenated phenols directly[107]. The authors proposed a mechanism (Scheme 1.27) involving initial base-catalyzed keto-enol tautomerization, of which the keto form and enol form can react and disproportionate to two phenoxyl radicals. Further C-C coupling can then occur to generate the intermediate biphenol, and radical propagation yields the intermediate diphenoquinone and desired oxepinobenzofuran isomer.

In 1969, Becker and Hay filed a patent describing catalytic aerobic conditions to prepare oxepinobenzofurans (then presumed to be benzoxetes), of any 2,4-di-alkyl substituted phenol[108]. The combination of CuCl and *N,N',N,N'*-tetra-methyl ethylene diamine in ethanol provided the products very cleanly but in low yield after precipitation from the cooled (0^oC) reaction mixtures (Scheme 1.28a). A year earlier, in 1968, Karpov and co-workers also reported the use of copper salts with amine ligands (or amine solvents) for phenolic oxidations but had misidentified the yielded compounds[109]. Using CuCl or $CuCl_2$ with pyridine, potassium hydroxide and O_2 for oxidation of 2,4-DTBP, the authors reported the isolation of compound **(1.81)** (Scheme 1.28b). In addition, compound **(1.82)** was the reported product of cuprous or cupric chloride and morpholine mediated aerobic oxidations (Scheme 1.28c). In fact, both structures were corrected by Hewitt in 1970, the former was reassigned as the oxepinobenzofuran (**1.50**) (then still

mistakenly assessed as the benzoxete **(1.46)** and the latter as compound (**1.83**) (Scheme 1.28)[110]. Compound **(1.83)** was later reassigned as structure **(1.84).**

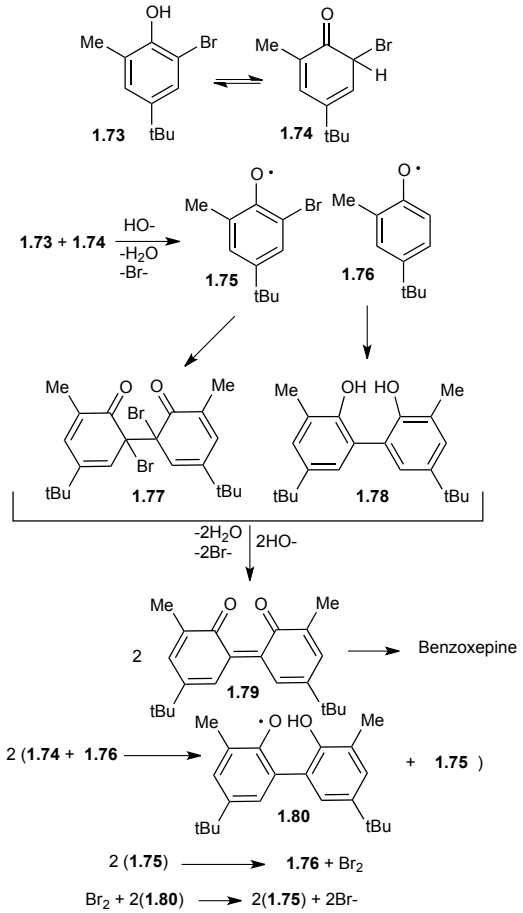

Scheme 1.27 Proposed mechanism for base-catalyzed oxepinobenzofuran synthesis

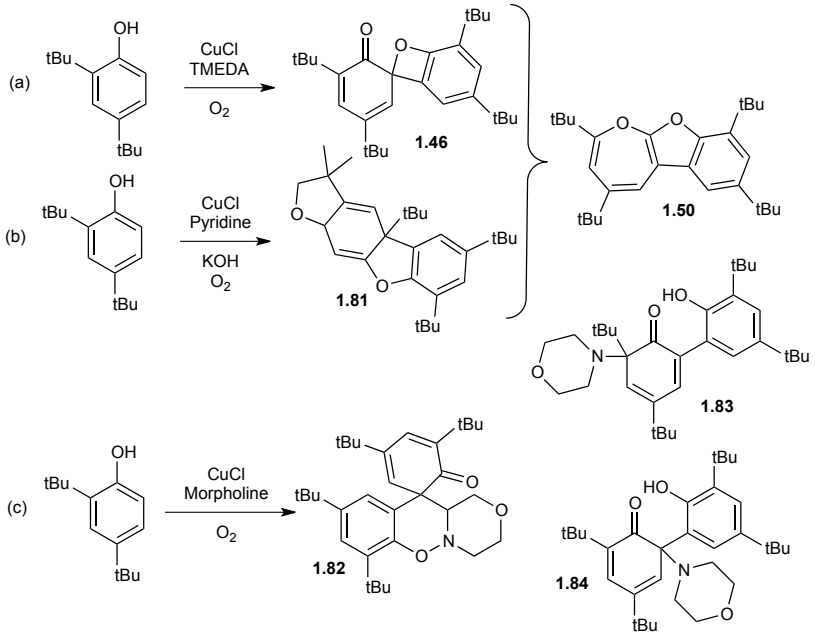

Scheme 1.28 (a) Hay's catalytic aerobic oxepinobenzofuran synthesis (b-c) Karpov and co-workers' copper-mediated aerobic oxidation of 2,4-DTBP

In 1983, Kushioka published a systematic study of amine bases as ligands to copper in the syntheses of biphenol **D1** and oxepinobenzofuran **OB1** (Scheme 1.29). The highest conversion and yield of oxepinobenzofuran was obtained using *N,N'*-di-*tert*-butyl ethylene diamine with Copper (II) chloride as a 2:1 ratio[111]. In subsequent articles, Kushioka was able to demonstrate the use of *tert*-butyl hydroperoxide or hydrogen peroxide as terminal oxidants in place of O_2, however these methods furnished solely the biphenol[112-113].

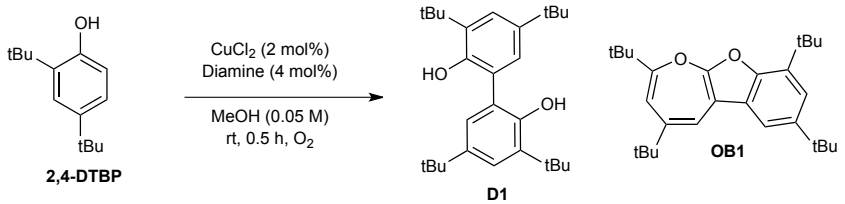

Entry	Diamine Alkyl Group[(a)]	D1 Yield (%)	OB1 Yield (%)
(1)	iC_3H_7	23	8
(2)	iC_4H_9	3	-
(3)	$secC_4H_9$	16	3
(4)	tC_4H_9	7	81

(a) Diamine = *N,N'*-dialkylethylene diamine

Scheme 1.29 Kushioka's copper aerobic oxepinobenzofuran synthesis

In 1984, Hewgill and co-workers completed the synthesis of morphenol by using the knowledge that diphenoquinones isomerize to the more stable oxepinobenzofurans[114]. The planar 1,3,6,8-tetra-*tert*-butyl-4,5-quinone, generated from silver oxide or lead dioxide oxidation of the corresponding biphenol (Scheme 1.30b), does not rearrange to the corresponding oxepinobenzofuran, but rather to the dienone which upon debutylation furnishes morphenol. The similar but non-planar 9,10-dihydroquinone isomerises directly to the oxepinobenzofuran (Scheme 1.30a).

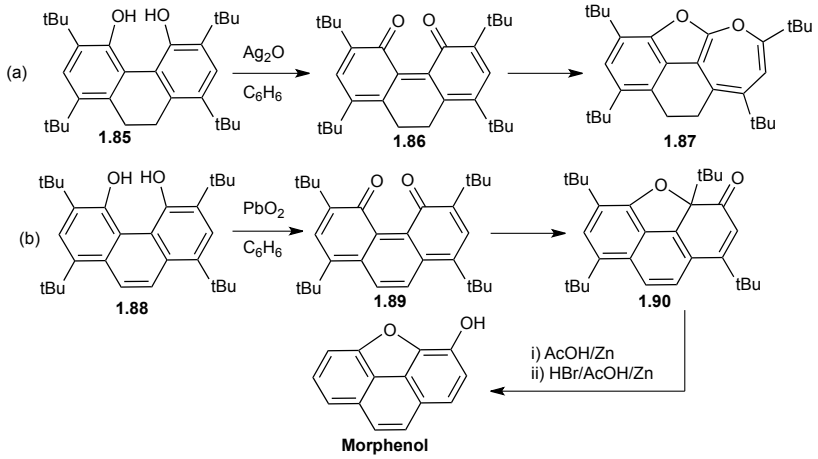

Scheme 1.30 Hewgill's synthesis of morphenol from diphenoquinones

In Section 1.2, the different reactivity patterns of dinuclear copper-O_2 complexes were discussed. The focus remained on *ortho*-quinone syntheses, in analogy to the enzyme Tyrosinase, however most of these examples arose from μ-η^2:η^2 –peroxo dinuclear copper complexes, and C-C coupled products, such as the biphenol and oxepinobenzofuran, arose more often from a bis-μ-oxo dinuclear copper geometry. In 2013, the Limberg group reported a Cu_2O binding mode of O_2 to copper (Scheme 1.31), capable of catalytically furnishing 2,4,7,9-tetra-*tert*-butyl oxepinobenzofuran in 15% yield, upon interaction with 2,4-DTBP under aerobic conditions[33].

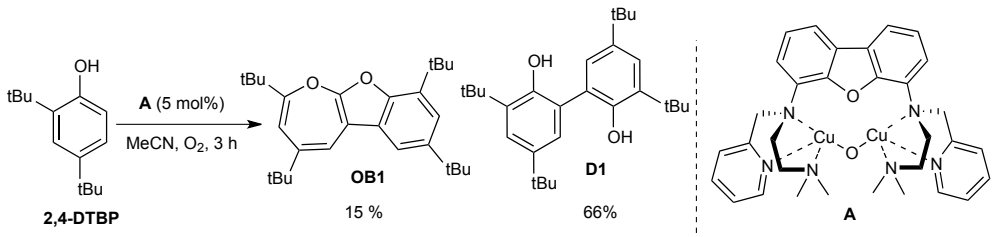

Scheme 1.31 Cu_2O catalytic aerobic synthesis of oxepinobenzofuran

Overall, although many reports of oxepinobenzofurans exist, no satisfactory synthetic method was developed, from the phenol directly, without the use of excess metal reagents, toxic oxidants or halogenated materials.

1.3.5 Reactivity of Oxepinobenzofurans

The first reaction effected with oxepinobenzofurans was a reduction[96]. Lithium Aluminium hydride reduction at room temperature of 2,4,7,9-tetra-*tert*-butyl oxepinobenzofuran provided the corresponding biphenol. Hydrogen Iodide mediated reduction yielded a furan (Scheme 1.32)[96]. Hewgill and co-workers tried a zinc/acetic acid reduction of 2,9-di-*tert*-butyl-4,7-di-methoxy oxepinobenzofuran, which provided a mixture of mono-acetylated biphenol and a similar benzofuran as Muller's (Scheme 1.32)[115]. In a patent, Hay again evidenced the ability of oxepinobenzofurans (then believed to be benzoxets) to act as oxidants, by showing that heating a mixture of 2,4-di-alkyl substituted phenol with oxepinobenzofurans furnished the corresponding biphenols (Scheme 1.32)[108].

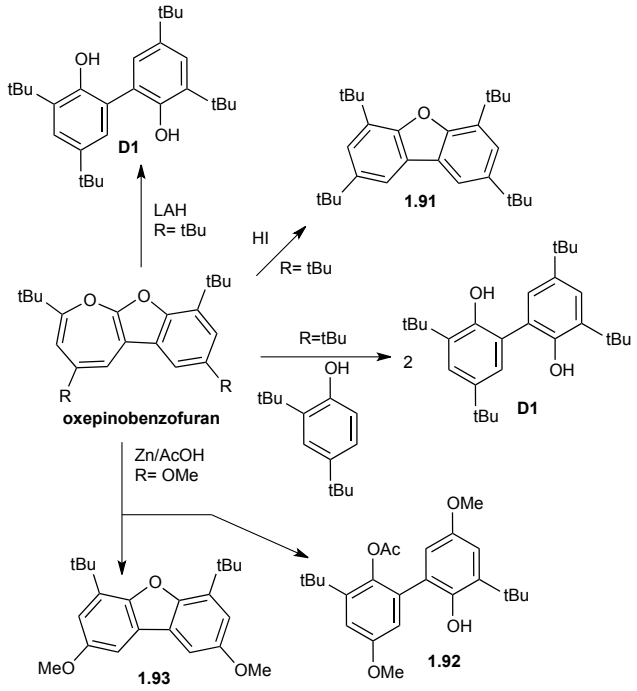

Scheme 1.32 Oxepinobenzofuran reduction products

In 1967, Hewgill's group reported the lead dioxide oxidation of 2,9-di-*tert*-butyl-4,9-di-methoxy oxepinobenzofuran[115], affording an acetylated benzoxete (Scheme 1.33). At this time however, the starting material was still believed to be a spiro-quinol ether, the product structure was mainly determined based on its reduction products, thus indicating the compound structure should be revised.

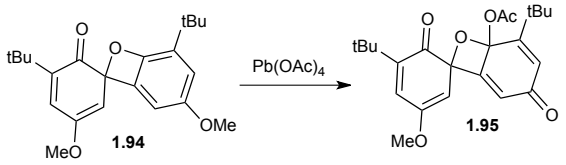

Scheme 1.33 Lead tetraacetate mediated oxidation of oxepinobenzofuran, formerly believed to be benzoxetes

In 1982, Becker and co-workers reported the DDQ mediated oxidation of oxepinobenzofurans, as a preliminary step in the synthesis of isoxindigos (Scheme 1.34a)[116]. This reaction was previously reported, although directly from the phenol, and the intermediacy of the oxepinobenzofuran was not shown[117]. At the time, the reaction was reported to yield a lactone that underwent further oxidation with DDQ in methanol to another lactone (Scheme 1.34b). The structures of the lactones **(1.99)** and **(1.100)** (Scheme 1.34c) were later revised as

compounds **(1.97)** and **(1.98),** respectively[118-119]. Becker, using an alkoxy substituted oxepinobenzofuran, obtained benzofuranylidenones upon DDQ oxidations, either in methanol or dioxane (Scheme 1.34).

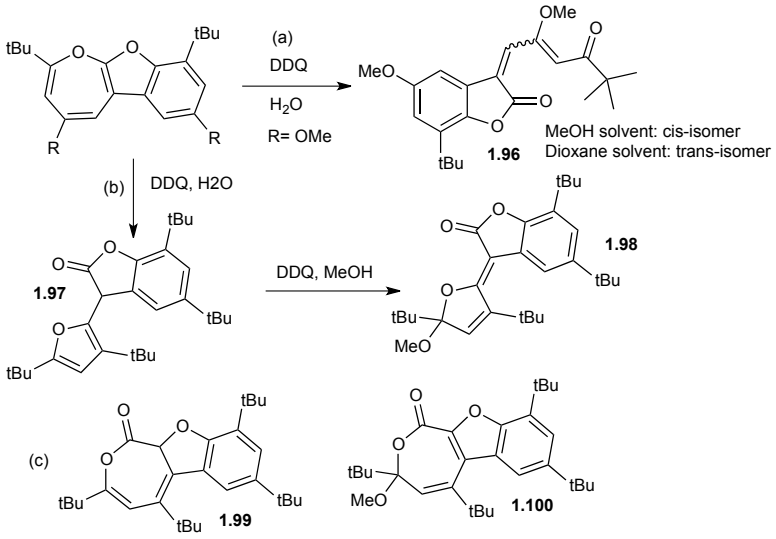

Scheme 1.34 DDQ mediated oxepinobenzofuran oxidations, and structural reasssignments

In 1989, Byrne published the sensitized photo-oxidation of oxepinobenzofuran **(1.101),** reacting with one equivalent of O_2 to yield product **(1.105)** in 42 % yield (Scheme 1.35)[120]. Methanol in this case acts as both solvent and nucleophile, on an initial endoperoxide as proposed by the authors.

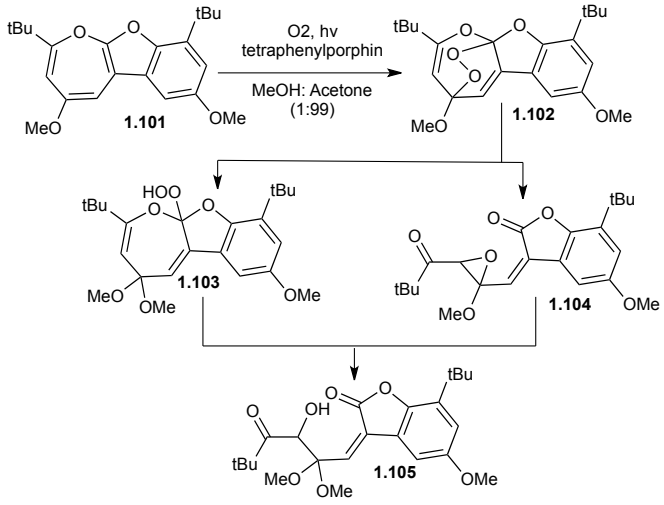

Scheme 1.35 Byrne's dioxygen photo-oxidation of oxepinobenzofuran

The reactivity of oxepinobenzofurans that was most explored is its capacity to act as an electrophile. Starting in 1966, Hewgill published the acid-catalyzed hydrolysis of a oxepinobenzofuran, using silica gel or *p*-toluene sulfonic acid, to yield a hemi-acetal (Scheme 1.36)[121].

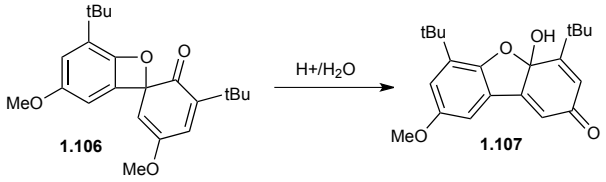

Scheme 1.36 Acid catalyzed hydrolysis of oxepinobenzofurans, still believed to be benzoxetes

When using methanol as a nucleophile, interesting results were obtained[115, 122]. Isolated compounds were the alkoxylated benzofuran and equal amounts of the biphenol (Scheme 1.37). These findings suggested methanol addition, and reoxidation by another molecule of oxepinobenzofuran, generating alkoxy substituted oxepinobenzofuran, and biphenol.

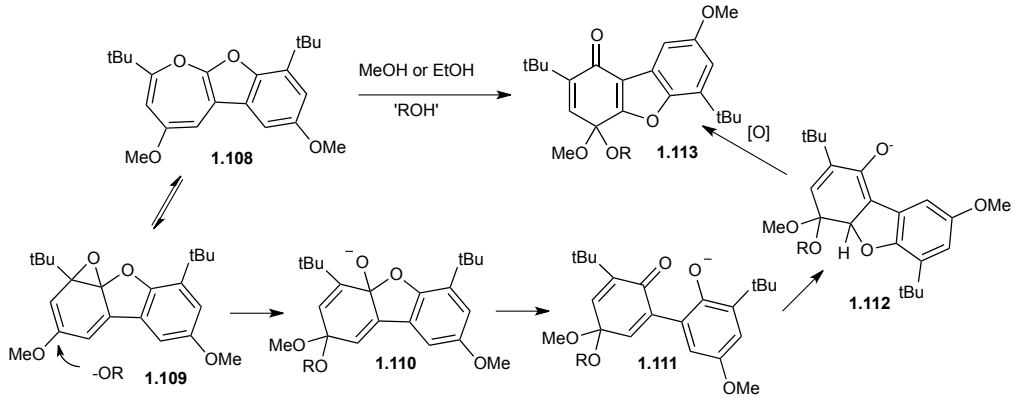

Scheme 1.37 Nucleophilic addition of alcohols to oxepinobenzofurans

In 1976, Becker investigated the addition of secondary and primary amines to 'benzoxetes'[123]. The authors were able to obtain azepinones with primary amines, and suggested an intermediate arene aziridine intermediate (Scheme 1.38).

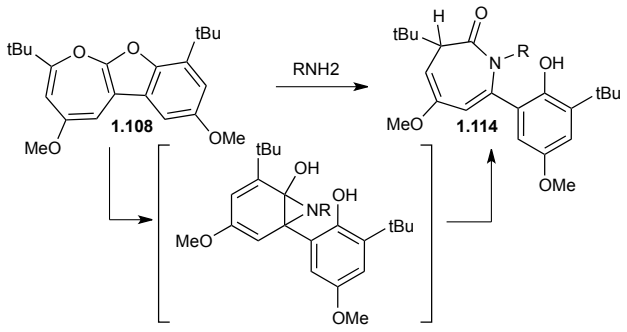

Scheme 1.38 Nucleophilic addition of amines to oxepinobenzofurans: Synthesis of azepinones

1.4 Outline of Thesis

Catalytic aerobic oxidations of phenols are fundamentally important in Nature, as exemplified by the enzyme Tyrosinase, and the enzyme's efficiency has driven extensive studies towards mimicking its reactivity with synthetic model systems[1]. Success in mimicry of the catalytic reactivity of the enzyme would allow a better understanding of the enzymatic machinery, and provide a useful and benign methodology for phenolic oxidations,.

The historical issue in Tyrosinase mimicry, as seen in Section 1.2, is one of selectivity between *ortho*-oxygenation and unphysiological C-C and C-O coupled products. Furthermore, to date, laboratory copper catalyzed phenolic oxidations are typically substrate driven, due to the facile autoxidation of phenols to phenoxyl radicals, limiting reactivity to substrates undergoing selective radical chemistry. Nevertheless, phenolic oxidations have the potential for providing easy access to a wide range of structurally different compounds from readily available, cheap starting materials.

We therefore set out to develop catalytic in copper aerobic oxidations of phenols allowing access to the different possible products, by effecting changes to the catalytic system. Chapter two will describe efforts towards this goal, starting with Tyrosinase mimicry for the selective generation of *ortho*-quinones. In the course of optimization, oxepinobenzofurans and biphenols were often obtained as byproducts, and the optimization of reaction conditions for their selective syntheses is also described in Chapter Two.

Oxepinobenzofurans are known since 1955, yet very few reports exist of their utility in synthetic methods[97]. Chapter Three will evidence the promise of oxepinobenzofurans as oxidants

performing hydrogen abstraction. Preliminary efforts towards a mechanistic understanding of this reactivity will also be described.

1.5 References and Bibliography

1. Allen, S. E.; Walvoord, R. R.; Padilla-Salinas, R.; Kozlowski, M. C. *Chem. Rev.* **2013,** *113* (8), 6234-6458.
2. Ye, X.; Johnson, M. D.; Diao, T.; Yates, M. H.; Stahl, S. S. *Green Chem.* **2010,** *12* (7), 1180-1186.
3. Company, A. O2 Reactivity at Model Copper Systems: Mimicking Tyrosinase Activity. In *Ideas in Chemistry and Molecular Sciences*, Wiley-VCH Verlag GmbH & Co. KGaA: 2010; pp 265-289.
4. Yoshizawa, K. Theoretical Aspects of Dioxygen Activation in Dicopper Enzymes. In *Copper-Oxygen Chemistry*, John Wiley & Sons, Inc.: 2011; pp 197-224.
5. Greene, J. F.; Hoover, J. M.; Mannel, D. S.; Root, T. W.; Stahl, S. S. *Org. Proc. Res. & Dev.* **2013,** *17* (10), 1247-1251.
6. Parmeggiani, C.; Cardona, F. *Green Chem.* **2012,** *14* (3), 547-564.
7. *The Chemistry of Phenols*. John Wiley & Sons, Ltd.: England, 2003.
8. Holm, R. H.; Kennepohl, P.; Solomon, E. I. *Chem. Rev.* **1996,** *96* (7), 2239-2314.
9. Klinman, J. P. *Chem. Rev.* **1996,** *96* (7), 2541-2562.
10. During, A.; Debouche, C.; Raas, T.; Larondelle, Y. *J. Nutr.* **2012,** *142* (10), 1798-1805.
11. Hwang, B.; Lee, J.; Liu, Q.-H.; Woo, E.-R.; Lee, D. G. *Molecules* **2010,** *15*, 3507-3516.
12. Pickel, B.; Schaller, A. *Appl. Microbiol. Biotechnol.* **2013,** *97* (19), 8427-8438.
13. Umezawa, T. *Phytochemistry Reviews* **2003,** *2* (3), 371-390.
14. Solomon, E. I.; Sundaram, U. M.; Machonkin, T. E. *Chem. Rev.* **1996,** *96* (7), 2563-2606.
15. Hay, A. S.; Blanchard, H. S.; Endres, G. F.; Eustance, J. W. *J. Am. Chem. Soc.* **1959,** *81* (23), 6335-6336.
16. Hay, A. S. Process for producing high molecular weight polymers from impure 2,6-xylenol. Google Patents: 1969.
17. Rolff, M.; Schottenheim, J.; Decker, H.; Tuczek, F. *Chem. Soc. Rev.* **2011,** *40* (7), 4077-4098.
18. Itoh, S.; Fukuzumi, S. *Acc. Chem. Res.* **2007,** *40* (7), 592-600.
19. Magnus, K. A.; Hazes, B.; Ton-That, H.; Bonaventura, C.; Bonaventura, J.; Hol, W. G. J. *Proteins: Structure, Function, and Bioinformatics* **1994,** *19* (4), 302-309.
20. Gerdemann, C.; Eicken, C.; Krebs, B. *Acc. Chem. Res.* **2002,** *35* (3), 183-191.
21. Ismaya, W. T.; Rozeboom, H. t. J.; Weijn, A.; Mes, J. J.; Fusetti, F.; Wichers, H. J.; Dijkstra, B. W. *Biochemistry* **2011,** *50* (24), 5477-5486.
22. Decker, H.; Schweikardt, T.; Tuczek, F. *Angew. Chem. Int. Ed.* **2006,** *45* (28), 4546-4550.
23. van Holde, K. E.; Miller, K. I. Hemocyanins. In *Adv. Protein Chem.*, C.B. Anfinsen, F. M. R. J. T. E.; David, S. E., Eds. Academic Press: 1995; Vol. Volume 47, pp 1-81.
24. Solomon, E. I.; Chen, P.; Metz, M.; Lee, S.-K.; Palmer, A. E. *Angew. Chem. Int. Ed.* **2001,** *40* (24), 4570-4590.
25. Mayer, A. M. *Phytochemistry* **2006,** *67* (21), 2318-2331.

26. Decker, H.; Tuczek, F. *Trends Biochem. Sci* **2000,** *25* (8), 392-397.
27. Lewis, E. A.; Tolman, W. B. *Chem. Rev.* **2004,** *104* (2), 1047-1076.
28. Nasir, M. S.; Cohen, B. I.; Karlin, K. D. *J. Am. Chem. Soc.* **1992,** *114* (7), 2482-2494.
29. Palavicini, S.; Granata, A.; Monzani, E.; Casella, L. *J. Am. Chem. Soc.* **2005,** *127* (51), 18031-18036.
30. Garcia-Bosch, I.; Ribas, X.; Costas, M. *Chem. - Eur. J.* **2012,** *18* (7), 2113-2122.
31. Citek, C.; Lyons, C. T.; Wasinger, E. C.; Stack, T. D. P. *Nat Chem* **2012,** *4* (4), 317-322.
32. Maumy, M.; Capdevielle, P. *J. Mol. Catal. A: Chem.* **1996,** *113* (1-2), 159-166.
33. Haack, P.; Kärgel, A.; Greco, C.; Dokic, J.; Braun, B.; Pfaff, F. F.; Mebs, S.; Ray, K.; Limberg, C. *J. Am. Chem. Soc.* **2013,** *135* (43), 16148-16160.
34. Itoh, S. Chemical Reactivity of Copper Active-Oxygen Complexes. In *Copper-Oxygen Chemistry*, John Wiley & Sons, Inc.: 2011; pp 225-282.
35. Q. Hatcher, L.; D. Karlin, K. Ligand Influences in Copper-Dioxygen Complex-Formation and Substrate Oxidations. In *Adv. Inorg. Chem.*, Eldik, R. v.; Reedijk, J., Eds. Academic Press: 2006; Vol. Volume 58, pp 131-184.
36. Hatcher, L.; Karlin, K. *J. Biol. Inorg. Chem.* **2004,** *9* (6), 669-683.
37. Osako, T.; Ohkubo, K.; Taki, M.; Tachi, Y.; Fukuzumi, S.; Itoh, S. *J. Am. Chem. Soc.* **2003,** *125* (36), 11027-11033.
38. Brackman, W.; Havinga, E. *Recl. Trav. Chim. Pays-Bas* **1955,** *74*, 937.
39. Brackman, W.; Havinga, E. *Recl. Trav. Chim. Pays-Bas* **1955,** *74*, 1107.
40. Brackman, W.; Havinga, E. *Recl. Trav. Chim. Pays-Bas* **1955,** *74*, 1100.
41. Brackman, W.; Havinga, E. *Recl. Trav. Chim. Pays-Bas* **1955,** *74*, 1070.
42. Brackman, W.; Havinga, E. *Recl. Trav. Chim. Pays-Bas* **1955,** *74*, 1021.
43. Capdevielle, P.; Maumy, M. *Tet. Lett.* **1982,** *23* (15), 1573-1576.
44. Capdevielle, P.; Maumy, M. *Tet. Lett.* **1982,** *23* (15), 1577-1580.
45. Cheng, Y.-T.; Chen, H.-L.; Tsai, S.-Y.; Su, C.-C.; Tsang, H.-S.; Kuo, T.-S.; Tsai, Y.-C.; Liao, F.-L.; Wang, S.-L. *Eur. J. Inorg. Chem.* **2004,** (10), 2180-2188.
46. Karlin, K. D.; Hayes, J. C.; Gultneh, Y.; Cruse, R. W.; McKown, J. W.; Hutchinson, J. P.; Zubieta, J. *J. Am. Chem. Soc.* **1984,** *106* (7), 2121-2128.
47. Tyeklar, Z.; Karlin, K. D. *Acc. Chem. Res.* **1989,** *22* (7), 241-248.
48. Kitajima, N.; Fujisawa, K.; Morooka, Y.; Toriumi, K. *J. Am. Chem. Soc.* **1989,** *111* (24), 8975-8976.
49. Casella, L.; Gullotti, M.; Pallanza, G.; Rigoni, L. *J. Am. Chem. Soc.* **1988,** *110* (13), 4221-4227.
50. Gelling, O. J.; van Bolhuis, F.; Meetsma, A.; Feringa, B. L. *J. Chem. Soc., Chem. Commun.* **1988,** (8), 552-554.
51. La Monica, G.; Angaroni, M. A.; Cariati, F.; Cenini, S.; Ardizzoia, G. A. *Inorg. Chim. Acta* **1988,** *148* (1), 113-118.
52. Menif, R.; Martell, A. E. *J. Chem. Soc., Chem. Commun.* **1989,** (20), 1521-1523.
53. Reglier, M.; Amadei, E.; Tadayoni, R.; Waegell, B. *J. Chem. Soc., Chem. Commun.* **1989,** (8), 447-450.
54. Menif, R.; Martell, A. E.; Squattrito, P. J.; Clearfield, A. *Inorg. Chem.* **1990,** *29* (23), 4723-4729.
55. Sorrell, T. N.; Vankai, V. A.; Garrity, M. L. *Inorg. Chem.* **1991,** *30* (2), 207-210.
56. Sorrell, T. N.; Garrity, M. L. *Inorg. Chem.* **1991,** *30* (2), 210-215.
57. Sorrell, T. N.; Vankai, V. A. *Inorg. Chem.* **1990,** *29* (9), 1687-1692.

58. Casella, L.; Gullotti, M.; Bartosek, M.; Pallanza, G.; Laurenti, E. *J. Chem. Soc., Chem. Commun.* **1991,** (18), 1235-1237.
59. Kitajima, N.; Moro-oka, Y. *Chem. Rev.* **1994,** *94* (3), 737-757.
60. Ghosh, D.; Lal, T. K.; Ghosh, S.; Mukherjee, R. *Chem. Commun.* **1996,** (1), 13-14.
61. Mahapatra, S.; Kaderli, S.; Llobet, A.; Neuhold, Y.-M.; Palanché, T.; Halfen, J. A.; Young, V. G.; Kaden, T. A.; Que, L.; Zuberbühler, A. D.; Tolman, W. B. *Inorg. Chem.* **1997,** *36* (27), 6343-6356.
62. Ryan, S.; Adams, H.; Fenton, D. E.; Becker, M.; Schindler, S. *Inorg. Chem.* **1998,** *37* (9), 2134-2140.
63. Holland, P. L.; Rodgers, K. R.; Tolman, W. B. *Angew. Chem. Int. Ed.* **1999,** *38* (8), 1139-1142.
64. Ohi, H.; Tachi, Y.; Itoh, S. *Inorg. Chem.* **2006,** *45* (26), 10825-10835.
65. De, A.; Mandal, S.; Mukherjee, R. *J. Inorg. Biochem.* **2008,** *102* (5–6), 1170-1189.
66. Sander, O.; Henß, A.; Näther, C.; Würtele, C.; Holthausen, M. C.; Schindler, S.; Tuczek, F. *Chem. - Eur. J.* **2008,** *14* (31), 9714-9729.
67. Martinez-Calvo, M.; Vazquez, L. M.; Pedrido, R.; Gonzalez-Noya, A. M.; Bermejo, M. R.; Monzani, E.; Casella, L.; Sorace, L. *Chem. - Eur. J.* **2010,** *16* (47), 14175-14180, S14175/1-S14175/10.
68. Karlin, K. D.; Nasir, M. S.; Cohen, B. I.; Cruse, R. W.; Kaderli, S.; Zuberbuehler, A. D. *J. Am. Chem. Soc.* **1994,** *116* (4), 1324-1336.
69. Kitajima, N.; Koda, T.; Iwata, Y.; Morooka, Y. *J. Am. Chem. Soc.* **1990,** *112* (24), 8833-8839.
70. Casella, L.; Gullotti, M.; Radaelli, R.; Di Gennaro, P. *J. Chem. Soc., Chem. Commun.* **1991,** (22), 1611-1612.
71. Casella, L.; Monzani, E.; Gullotti, M.; Cavagnino, D.; Cerina, G.; Santagostini, L.; Ugo, R. *Inorg. Chem.* **1996,** *35* (26), 7516-7525.
72. Santagostini, L.; Gullotti, M.; Monzani, E.; Casella, L.; Dillinger, R.; Tuczek, F. *Chem. - Eur. J.* **2000,** *6* (3), 519-522.
73. Linnell, R. *J. Org. Chem.* **1960,** *25* (2), 290-290.
74. Walba, H.; Isensee, R. W. *J. Org. Chem.* **1961,** *26* (8), 2789-2791.
75. Sayre, L. M.; Nadkarni, D. V. *J. Am. Chem. Soc.* **1994,** *116* (7), 3157-8.
76. Monzani, E.; Quinti, L.; Perotti, A.; Casella, L.; Gullotti, M.; Randaccio, L.; Geremia, S.; Nardin, G.; Faleschini, P.; Tabbì, G. *Inorg. Chem.* **1998,** *37* (3), 553-562.
77. Battaini, G.; Carolis, M. D.; Monzani, E.; Tuczek, F.; Casella, L. *Chem. Commun.* **2003,** (6), 726-727.
78. Mandal, S.; Macikenas, D.; Protasiewicz, J. D.; Sayre, L. M. *J. Org. Chem.* **2000,** *65* (16), 4804-4809.
79. Chioccara, F.; Di Gennaro, P.; La Monica, G.; Sebastiano, R.; Rindone, B. *Tetrahedron* **1991,** *47* (25), 4429-4434.
80. Chioccara, F.; Chiodini, G.; Farina, F.; Orlandi, M.; Rindone, B.; Sebastiano, R. *J. Mol. Catal. A: Chem.* **1995,** *97* (3), 187-194.
81. Itoh, S.; Kumei, H.; Taki, M.; Nagatomo, S.; Kitagawa, T.; Fukuzumi, S. *J. Am. Chem. Soc.* **2001,** *123* (27), 6708-6709.
82. Kushioka, K. *J.Org.Chem.* **1984,** *49*, 4456-4459.
83. Matsumoto, J.; Kajita, Y.; Masuda, H. *Eur. J. Inorg. Chem.* **2012,** *2012* (26), 4149-4158, S4149/1-S4149/3.

84. Mirica, L. M.; Vance, M.; Rudd, D. J.; Hedman, B.; Hodgson, K. O.; Solomon, E. I.; Stack, T. D. P. *J. Am. Chem. Soc.* **2002,** *124* (32), 9332-9333.
85. Mirica, L. M.; Vance, M.; Rudd, D. J.; Hedman, B.; Hodgson, K. O.; Solomon, E. I.; Stack, T. D. P. *Science* **2005,** *308* (5730), 1890-1892.
86. Op't Holt, B. T.; Vance, M. A.; Mirica, L. M.; Heppner, D. E.; Stack, T. D. P.; Solomon, E. I. *J. Am. Chem. Soc.* **2009,** *131* (18), 6421-6438.
87. Company, A.; Palavicini, S.; Garcia-Bosch, I.; Mas-Ballesté, R.; Que, L.; Rybak-Akimova, E. V.; Casella, L.; Ribas, X.; Costas, M. *Chem. - Eur. J.* **2008,** *14* (12), 3535-3538.
88. Mandal, S.; Mukherjee, J.; Lloret, F.; Mukherjee, R. *Inorg. Chem.* **2012,** *51* (24), 13148-13161.
89. Garcia-Bosch, I.; Company, A.; Frisch, J. R.; Torrent-Sucarrat, M.; Cardellach, M.; Gamba, I.; Güell, M.; Casella, L.; Que, L.; Ribas, X.; Luis, J. M.; Costas, M. *Angew. Chem. Int. Ed.* **2010,** *49* (13), 2406-2409.
90. Bullowski, J. E. 4545937, 1984.
91. Reglier, M.; Jorand, C.; Waegell, B. *J. Chem. Soc., Chem. Commun.* **1990,** (24), 1752-1755.
92. Rolff, M.; Schottenheim, J.; Peters, G.; Tuczek, F. *Angew. Chem. Int. Ed.* **2010,** *49* (36), 6438-6442.
93. Hoffmann, A.; Citek, C.; Binder, S.; Goos, A.; Rübhausen, M.; Troeppner, O.; Ivanović-Burmazović, I.; Wasinger, E. C.; Stack, T. D. P.; Herres-Pawlis, S. *Angew. Chem. Int. Ed.* **2013,** *52* (20), 5398-5401.
94. Hamann, J. N.; Tuczek, F. *Chem. Commun.* **2014**.
95. Schottenheim, J.; Fateeva, N.; Thimm, W.; Krahmer, J.; Tuczek, F. *Z. Anorg. Allg. Chem.* **2013,** *639* (8-9), 1491-1497.
96. Müller, E.; Mayer, R.; Narr, B.; Rieker, A.; Scheffler, K. *Just. Lieb. Ann. Chem.* **1961,** *645* (1), 25-35.
97. Baltes, J.; Volbert, R. E. *Fette, Seifen, Anstrichm* **1955,** *57*, 660.
98. Müller, E.; Kaufmann, H.; Rieker, A. *Just. Lieb. Ann. Chem.* **1964,** *671* (1), 61-70.
99. Meier, H. S., Hans-Peter; Rieker, Anton; Hitchcock, Peter B. *Angew. Chem.* **1978,** *90* (2), 128-129.
100. Becker, H.-D.; Gustafsson, K. *Tet. Lett.* **1976,** *17* (52), 4883-4886.
101. Schulte-Frohlinde, D.; Erhardt, F. *Just. Lieb. Ann. Chem.* **1964,** *671* (1), 92-97.
102. Adderley, C. J. R.; Hewgill, F. R. *J. Chem. Soc. C* **1968,** (0), 1434-1438.
103. Hewgill, F. R.; Hewitt, D. G. *J. Chem. Soc. C* **1967,** (0), 723-725.
104. Hewgill, F. R.; La Greca, B.; Legge, F.; Roga, P. E. *J. Chem. Soc., Perkin Trans. 1* **1983,** (0), 131-134.
105. Hayes, D. M.; Nelson, S. D.; Garland, W. A.; Kollman, P. A. *J. Am. Chem. Soc.* **1980,** *102* (4), 1255-1262.
106. Rayne, S.; Sasaki, R.; Wan, P. *Photochem Photobiol Sci* **2005,** *4* (11), 876-86.
107. Bowman, D. F.; Hewgill, F. R. *Chem. Comm. (London)* **1968,** (9), 524-525.
108. Hay, A. S.; Becker, H. D. Biphenols and spiroquinol ethers. DE1900680A, 1969.
109. Karpov, V. V.; Puchkov, V. A.; Khidekel, M. L. *Zhur. Org. Khim.* **1968,** *4*, 1594.
110. Hewitt, D. G. *J. Chem. Soc. D: Chem. Comm.* **1970,** (4), 227-228.
111. Kushioka, K. *J. Org. Chem.* **1983,** *48*, 4948-4950.
112. Kushioka, K. T., I. *J. Chem. Soc. Perkin. Trans. II* **1989**, 1303-1308.

113. Kushioka, K.; Tanimoto, I.; Maruyama, K. *Bull. Chem. Soc. Jpn.* **1989,** *62* (4), 1147-1153.
114. Hewgill, F. R. S., J.M. *J. Chem. Soc., Chem. Commun.* **1984**, 1419-1420.
115. Hewgill, F. R.; Hewitt, D. G. *J. Chem. Soc. C* **1967,** (0), 726-730.
116. Becker, H.-D. L., H. *J. Org. Chem.* **1982,** *47*, 1095-1101.
117. Becker, H. D. *J. Org. Chem.* **1969,** *34* (5), 1198-1203.
118. Becker, H.; Hall, S.; White, A. *Aust. J. Chem.* **1978,** *31* (4), 927-931.
119. Hall, S.; Raston, C.; Skelton, B.; White, A. *Aust. J. Chem.* **1978,** *31* (4), 923-926.
120. Byrne, L. T. E., L.M.; Hewgill, F.R.; Skelton, B.W.; White, A.H. *J. Chem. Soc. Perkin. Trans. I* **1989**, 133-142.
121. Hewgill, F. R.; Kennedy, B. R. *J. Chem. Soc. C* **1966,** (0), 362-366.
122. Schneider, H.-P.; Winter, W.; Rieker, A. *J. Chem. Research (S)* **1978**, 336-337.
123. Becker, H.-D.; Gustafsson, K. *Tet. Lett.* **1976,** *17* (20), 1705-1708.

CHAPTER TWO

CONTROLLING THE CATALYTIC AEROBIC OXIDATION OF PHENOLS

2.1 Background and Motivation

Catalytic aerobic oxidations are extensively utilized in biological systems to yield a wide array of useful natural products and materials (Section 1.1)[1-2]. In the case of phenols, the large resonance stabilization by the aryl ring explains the facile one-electron oxidation to generate a phenoxyl radical. A wide range of products can be envisioned to arise from a single starting phenol, given the several reaction pathways that the aroxyl possesses (Section 1.1, Figure 1.1). No prefunctionalization is required to achieve reactivity at a given phenol regiochemical site, which further enhances the attractiveness of phenolic one-electron oxidations as synthetic methodologies.

Industrial phenol syntheses include the addition-elimination reaction of hydroxide with benzene sulfonic acid, or addition of water to benzyne, after elimination of HCl from chlorobenzene (Scheme 2.1a-b)[3]. Contemporarily, the prevalent phenol synthesis consists of the acidic oxidation of benzene (Scheme 2.1c)[3-4]. In the presence of a Lewis acid catalyst, benzene and propylene undergo addition to yield cumene at high pressure. Oxidation of the benzylic C-H bond with O_2 forms a stabilized benzylic radical, which forms the hydroperoxide upon bonding with another molecule of O_2. In acidic medium, the Hock rearrangement provides phenol and the commodity chemical acetone as the only by-product. Phenols are typically considered to be readily available and relatively inexpensive starting materials, synthesized industrially by an addition reaction followed by O_2 mediated oxidation, with only useful waste generated.

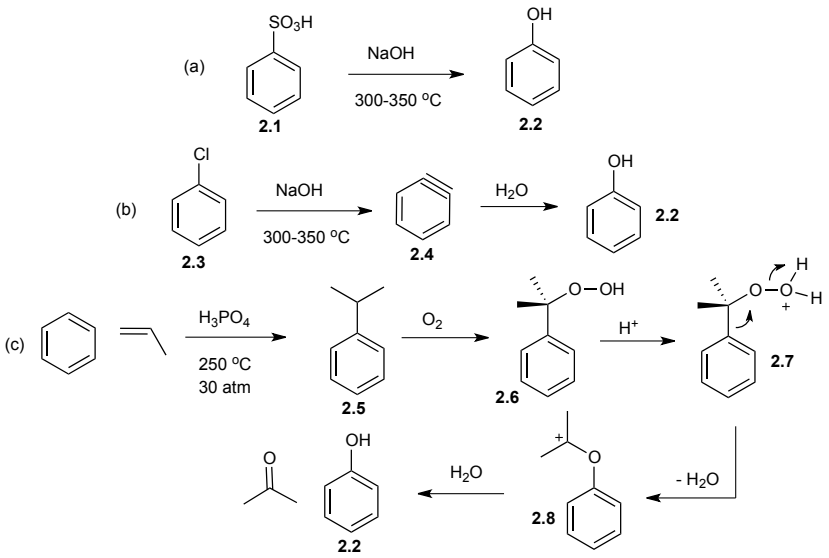

Scheme 2.1 Industrial Processes for Phenol Synthesis (a) addition-elimination of sulfonic acid (b) elimination of chlorobenzene followed by hydration (c) Hock Cumene Process

The availability of phenols, their ease of oxidation, and the potential for many useful products have led to a large development of phenolic catalytic aerobic oxidations. Despite much effort, these oxidations remain plagued with competitive non-selective autoxidation of phenols, yielding complex mixtures of C-C coupled products (Section 1.2)[5]. In contrast, regio- and chemo- selectivity is achieved by metalloenzymes by activating O_2 and effecting substrate oxidation within the confinement to the active site[6]. The competing oxidation pathways, 'inner'-sphere (metal bound) versus 'outer'- sphere were well demonstrated by Hay, while optimizing the synthesis of polypropylene ether (PPE)[5, 7]. Oxidation of 2,6-di-methyl phenol or 2,6-di-*tert*-butyl phenol with catalytic amounts of CuCl and pyridine yield the PPE-polymer **2.12** and diphenoquinone **2.11** respectively (Scheme 2.2). This drastic difference in reactivity was attributed to the two alternate mechanistic pathways, inner versus outer sphere catalytic oxidations. The bulkiness of the *tert*-butyl substituents disfavors the inner sphere mechanistic pathway due to steric interactions with the catalyst.

Presently the substrate dictates the oxidation products, by biasing between the two mechanisms of oxidation. Additionally the substitution pattern on the starting material will dictate regio- and chemo-selectivity of the oxidation in a radical based, outer-sphere pathway[5]. While selectivity for a product can be achieved with a given substrate, it remains inherent to that substrate. Catalyst control will provide versatility by ensuring a given oxidative mechanism for a range of phenols, thus allowing selectivity to be achieved over a wide range of substrates. Due to the great variety of products potentially synthesized, and the innate efficiency of catalytic aerobic

oxidations, we set out to access catalyst-controlled aerobic phenolic oxidations. Specifically, we became interested in accessing selective inner-sphere oxidations of phenols, by optimizing the catalytic aerobic oxidation of phenols to *ortho*-quinones, which are characteristic products from 'inner-sphere' catalytic aerobic oxidations (*c.f.* Section 1.2).

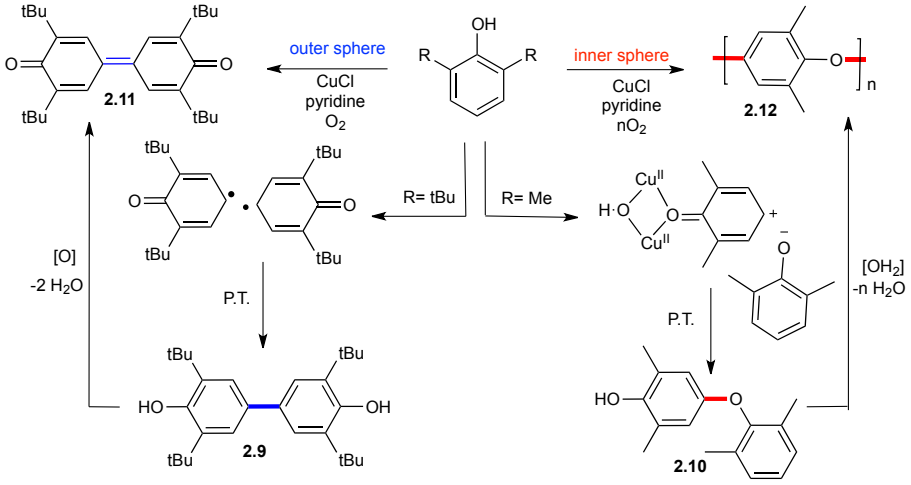

Scheme 2.2 Substrate bias for inner or outer-sphere mechanistic pathways of oxidation

2.2 Catalyst-Controlled Phenol Catalytic Aerobic Oxidation

The Lumb group recently reported that catalytic amounts of $[Cu(CH_3CN)_4]PF_6$ and triethylamine, with the addition of molecular sieves, catalyze the aerobic oxidation of mono-substituted phenols to the corresponding di-substituted *ortho*-quinones (Scheme 2.3)[8]. Alternatively, the reaction can also be run using the more robust *N,N'*-di-tert-butyl ethylene diamine (DBED) ligand, eliminating the need for dessicant. Using DBED, the reaction proceeds through the formation of a semiquinone radical **SQ**, followed by addition of a second equivalent of starting material, and re-oxidation[9]. We became interested in applying these conditions to more demanding substrates, such as the sterically encumbered 2,4-di-*tert*-butylphenol (2,4-DTBP), and using these as probes for clarifying factors influencing selectivity and efficacy of reaction.

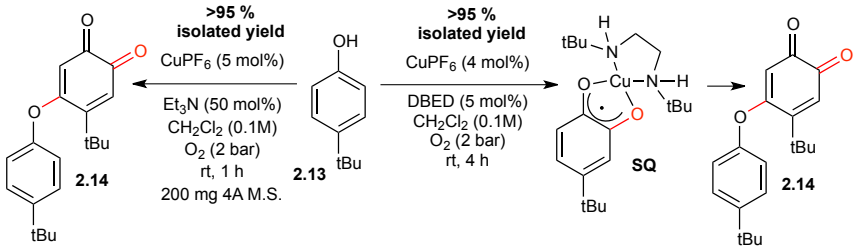

Scheme 2.3 Controlled Melanogenic Functionalization (CMF)

2,4-DTBP was oxidized using copper hexafluorophosphate, triethylamine, and molecular sieves in dichloromethane at 0.1 M and room temperature (Table 2.1). After 4 hours, with either 100 mg or 200 mg of molecular sieves, the reaction shows complete conversion. A loss of mass balance is observed however, that diminishes as the dessicant amount is reduced. The dessicant is shown to play a crucial role in the reaction, with an optimal loading of 100 mg and higher or lower amounts proving deleterious to reaction performance. An improved 80% *ortho*-quinone yield was obtained by reducing reaction time to 1 hour, although with a concomitant increased yield of biphenol **D1**. Although triethylamine is shown to be necessary for oxidation, increasing loadings do not induce a change in yield or selectivity. Finally, the copper salt amount is a crucial determinant of reaction performance, with highly decreased selectivity with lower catalyst loadings. The Lumb group was later able to obtain 3,5-DTBQ selectively in quantitative from 2,4-DTBP (1 mmol), using 8 mol% of copper hexafluorophosphate, 50 mol% of triethylamine and 200 mg molecular sieves under 2 atm of O_2 pressure in 1 hour at room-temperature (Table 2.1, Entry 10).

Table 2.1 Reaction optimization of 2,4-DTBP catalytic aerobic oxidation to 3,5-DTBQ[a]

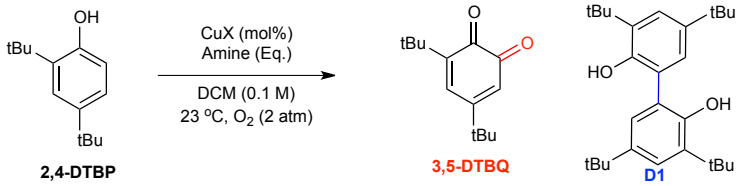

Entry	CuX (mol%)	Amine (Eq.)	Time (h)	4Å Mol. Sieves. (Amount)	Conversion[b] (%)	Yield[b] (%) 3,5-DTBQ/D1
(1)	$CuPF_6$ (20)	Et_3N (0.5)	4	200 mg	100	40 / 2
(2)	$CuPF_6$ (20)	Et_3N (0.5)	4	100 mg	100	53 / 0
(3)	$CuPF_6$ (20)	Et_3N (0.5)	1	100 mg	97	80 / 12
(4)	$CuPF_6$ (20)	Et_3N (0.5)	0.25	100 mg	64	48 / 10
(5)	$CuPF_6$ (20)	Et_3N (0.5)	1	50 mg	75	55 / 12
(6)	$CuPF_6$ (20)	Et_3N (0.1)	1	100 mg	1	0 / 0.5
(7)	$CuPF_6$ (20)	Et_3N (0.9)	1	100 mg	95	73 / 10
(8)	$CuPF_6$ (10)	Et_3N (0.5)	1	100 mg	95	35 / 20
(9)	$CuPF_6$ (5)	Et_3N (0.5)	1	100 mg	78	17 / 37
(10)	$CuPF_6$ (8)	Et_3N (0.5)	1	200 mg	100[c]	> 95[c] / 0[c]

(a) Reactions were performed on 0.25 mmol 2,4-DTBP (b) Product yield & conversion determined by ^1H NMR spectroscopy using hexamethylbenzene as an internal standard (c) Reaction performed on 1 mmol of 2,4-DTBP by Kenneth Virgel N. Esguerra

The loss of mass balance indicates that the *ortho*-quinone is unstable to the reaction conditions, thus lower reaction times show an increased yield by preventing decomposition from

occurring. It is also possible that molecular sieves cause some product decomposition, as lower loadings return higher yields. Yet if too little dessicant is used decreased reaction efficiency is observed. In this case water could be deleterious to the reaction by quenching catalytic activity. This hypothesis is reinforced by noting that selectivity is not affected when using very low molecular sieves loadings.

Next, the optimized conditions for 4-*tert*-butylphenol oxygenation (Scheme 2.3) with DBED as ligand were applied to 2,4-DTBP. Remarkably, a complete reversal of selectivity was observed. Instead of 3,5-DTBQ, the oxepinobenzofuran **OB1** was obtained quantitatively (Table 2.2). Use of a copper salt with a more coordinating anion such as CuCl with DBED still yields the oxepinobenzofuran **OB1**. Cuprous chloride in combination with triethylamine, however, furnishes biphenol **D1** selectively.

Table 2.2 Catalyst-controlled aerobic oxidation of 2,4-disubstituted phenol to ortho-quinone[(a)], biphenol[(b)] or oxepinobenzofuran[(c)]

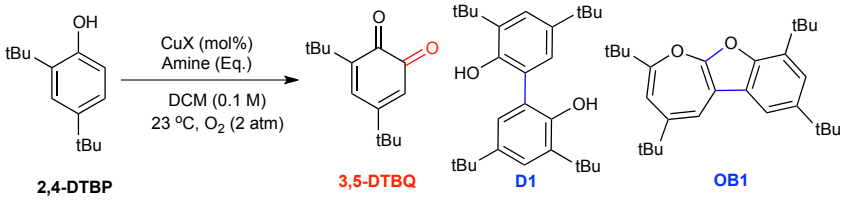

2,4-DTBP | 3,5-DTBQ | D1 | OB1

Entry	CuX (mol%)	Amine (Eq.)	Time (h)	4Å Mol. Sieves. (Amount)	Yield (%) 3,5-DTBQ	Yield(%) D1	Yield(%) OB1
(1)	$CuPF_6$ (8)	Et_3N (0.5)	1	200 mg	> 95[(e)(f)]	-	-
(2)	$CuPF_6$ (4)	DBED (0.05)	4	-	-	-	> 95[(e)]
(3)	CuCl (10)	DBED (0.05)	1	-	-	-	> 95[(e)]
(4)	CuCl (10)	Et_3N (1)	1	-	-	> 95[(d)]	-

(a) Reactions were performed on 1 mmol of 2,4-DTBP (b) Reactions were performed on 0.25 mmol of 2,4-DTBP (c) Reactions were performed on 2 mmol of 2,4-DTBP (d) Isolated yield of product (e) NMR yield of product as determined with hexamethylbenzene as an internal standard (f) Reaction performed by Kenneth Virgel N. Esguerra DBED = N,N'-di-tert-butylethylenediamine

When switching from triethylamine to DBED, there is a shift from an inner-sphere dominated pathway yielding *ortho*-quinones, to an outer-sphere process whereby only oxepinobenzofuran is generated (Table 2.2, Entry 2). This complete change in reactivity is ascribed to steric factors, whereby the more sterically encumbered DBED ligand disfavors an inner-sphere oxygenation pathway by accelerating dissociation of a phenoxyl radical. Although bulky, triethylamine is a monodentate ligand and it is likely that only one or two triethylamine molecules are present per copper atom during catalytic activity, to accommodate ligation of the starting material. With CuCl, the more coordinating anion prevents the formation of a peroxo

species (*c.f.* Section 1.2), thus yields biphenol and oxepinobenzofuran products selectively, depending on the oxidant strength. The clear effects of steric bulk of the catalyst complex and of the coordinating strength of the copper anion reinforce the hypothesis that biphenol and oxepinobenzofurans are derived from 'outer-sphere' oxidations, thus also contradict Kushioka's findings that both biphenols and oxepinobenzofurans syntheses necessitate an intermediate peroxo[10]. Overall, these results evidence a powerful catalyst control, unachieved previously, in copper-catalyzed aerobic oxidations.

2.3 Biphenols – Synthesis Optimization and Reaction Scope

2.3.1 Biphenol Synthesis Optimization

The 2,2'-biphenol structure is prominent in natural products[11], as well as in drugs and drug candidates[12]. For example, the structurally simple Magnolol (Figure 2.1) shows high activity as an anti-oxidant[13]. An important 2,2'-biphenol containing molecule is the antibiotic Vancomycin (Figure 2.3), currently utilized as a last resort drug in the treatment of *Staphylococcus aureus* [12]. As synthetic reagents, the *o,o*'-biaryls in general are well recognized as an important class of ligands for asymmetric synthesis in a broad range of reactions, such as the Bayer-Villiger, Diels-Alder and many more[11].

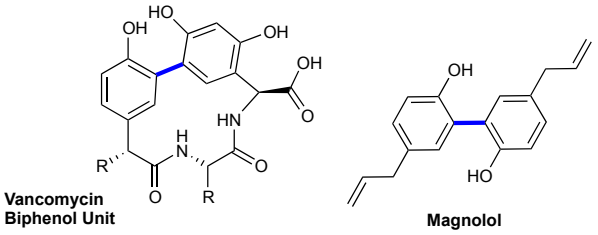

Vancomycin Biphenol Unit **Magnolol**

Figure 2.1 O,o'-biphenols and biaryls in natural products and drug candidates

The optimization of reaction conditions for catalytic aerobic biphenol synthesis provides insight into several mechanistic considerations (Table 2.3). Reactions were performed using 10 mol% of a copper chloride salt and one equivalent or less of an amine base in dichloromethane at room temperature under 2 atm of O_2. Notably, as the amount of triethylamine is lowered below one equivalent, a significant decrease in reaction rate is observed (Entries 1-5). Higher

concentrations also decrease the reaction rate (Entries 6-9). Additionally, although a copper (II) source formed *in situ* is likely to perform the discussed phenolic oxidation, starting with $CuCl_2$ shows no reactivity at all (Entry 10). Limited catalytic ability is observed when switching the amine ligand to 1,10-phenanthroline, morpholine or DIPEA (Entries 11-14). With morpholine, 20% yield of cyclohexadienone **1.84** (*c.f.* Scheme 1.28) is observed, showing that the catalyst complex can overoxidize the biphenol. Interestingly, however, the combination of cuprous chloride and pyridine seems potent in delivering oxepinobenzofuran (Entries 15-17).

Table 2.3: Optimization of 2,4-DTBP catalytic aerobic oxidation to Biphenol D1[(a)]

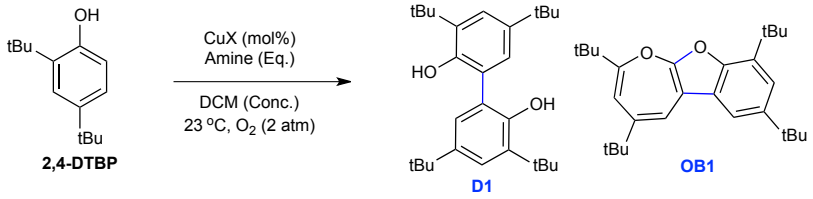

Entry	CuX (mol%)	Amine (Eq.)	Conc.	Time (h)	Conversion[(b)] (%)	Yield[(b)] (%) D1/OB1
(1)	CuCl (10)	Et_3N (1)	0.1 M	1	99	99 / 0
(2)	CuCl (10)	Et_3N (0.75)	0.1 M	1	81	81 / 0
(3)	CuCl (10)	Et_3N (0.5)	0.1 M	1	80	80 / 0
(4)	CuCl (10)	Et_3N (0.1)	0.1 M	1	79	79 / 0
(5)	CuCl (10)	Et_3N (0.05)	0.1 M	1	72	68 / 0
(6)	CuCl (10)	Et_3N (1)	0.25 M	1	80	80 / 0
(7)	CuCl (10)	Et_3N (1)	0.33 M	1	76	75 / 0
(8)	CuCl (10)	Et_3N (1)	0.75 M	1	70	70 / 0
(9)	CuCl (10)	Et_3N (1)	1.0 M	1	57	60 / 0
(10)	$CuCl_2$ (10)	Et_3N (1)	0.1 M	1	0	0 / 0
(11)	CuCl (10)	Phenanthroline (1)	0.1 M	1	5	5 / 0
(12)	CuCl (10)	Phenanthroline (0.1)	0.1 M	1.5	60	60 / 0
(13)	CuCl (10)	Morpholine (1)	0.1 M	1	95	60 / 0
(14)	CuCl (10)	DIPEA (1)	0.1 M	1	60	33 / 0
(15)	CuCl (10)	Pyridine (1)	0.1 M	1	100	10 / 90
(16)	CuCl (10)	Pyridine (1)	0.1 M	0.5	100	15 / 85
(17)	CuCl (10)	Pyridine (1)	0.1 M	1.5	100	0 / 100

(a) Reactions were performed on 0.25 mmol of 2,4-DTBP (b) Product yield & conversion determined by 1H NMR spectroscopy using hexamethylbenzene as an internal standard DIPEA = diisopropylethylamine

To form the desired biphenol, two equivalents of phenol must be oxidized to the corresponding phenoxyl radicals by two equivalents of a Cu(II) source. Starting from CuCl, dioxygen can oxidize copper (I) chloride as shown in Figure 2.2, necessitating two equivalents of proton to generate water as the byproduct. Although the active catalyst remains unknown, the

proposed redox reactions evidence the role of triethylamine as a proton shuttle in the catalytic cycle. Reducing the amount of triethylamine can slow the catalytic process by decreasing the rate of re-oxidation of copper (I) chloride (limit the rate of line (1) Figure 2.2). Although triethylamine proves the best ligand and base for 2,4-DTBP oxidation to the corresponding biphenol, Hunig's base and phenanthroline are also able to furnish the desired product. Reduced yields with Hunig's base could be due to increased steric bulk of the catalytic complex. The lower pKa of phenanthroline (4.8-5.2 of the conjugate acid)[14] suggest that only a small amount of starting phenol (pKa ~11.56)[14] will be deprotonated. For example, the phenolic proton could be deprotonated following coordination to copper, as ligation to copper will dramatically increase the acidity of the phenol. Although the reaction works, it is much slower than with triethylamine, potentially due to the decreased liability of the bidentate ligand, as well as the lower basicity of the ligand.

Figure 2.2 Role of the Base (B) as proton shuttle in catalytic aerobic phenol oxidation (PhO- = deprotonated 2,4-DTBP)

Overall, an efficient aerobic catalytic oxidation of 2,4-DTBP to its corresponding biphenol was successfully devised, showing for the first time that triethylamine can be used simultaneously as the base and ligand in oxidative catalytic biaryl formation. Through reaction optimization, the choice of ligand was found to be crucial for chemo-selectivity, demonstrating a catalyst-control previously unachieved in phenolic catalytic aerobic oxidations.

2.3.2 Catalytic Aerobic Biphenol Synthesis Scope

Investigation of the reaction scope reveals that our synthesis of biphenols is amenable to a variety of 2,4-disubstituted phenols (Table 2.4).

Increased steric bulk is tolerated by the catalytic system, as evidenced by the ability to oxidize *t*Amyl, Cumyl and Trityl substituted biphenols (Table 2.4, Entries 2-6). We attribute the decreased yields to steric hindrance between the starting phenol and catalyst. The reaction is

chemoselective for phenolic oxidation in the presence of a secondary benzylic proton (Table 2.4, Entry 7). *para*-Phenyl-*ortho*-*tert*-butyl phenol works well under our standard conditions, providing the corresponding biphenol in 94% isolated yield after one hour. Likewise, electron donating and withdrawing substituents are tolerated on the 4-aryl substituent.

Table 2.4: Substrate scope for the catalytic aerobic biphenol synthesis[a]

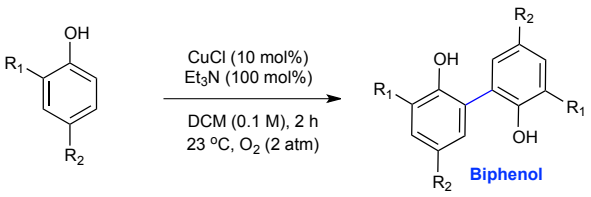

Entry	R_1	R_2	Yield[b] (%) Biphenol
(1)	tBu	tBu	99
(2)	tBu	tAmyl	87
(3)	tAmyl	tAmyl	85
(4)	tBu	Cumyl	69
(5)	Cumyl	Cumyl	55
(6)	tBu	Trityl	67
(7)	tBu	iPr	83
(8)	tBu	Ph	94[c]

(a) Reactions were performed on 0.25 mmol of phenol (b) Isolated product yield & conversion (c) Reaction was run for 1 h

Table 2.5: Substrate scope for the catalytic aerobic Aryl substituted biphenol synthesis[a]

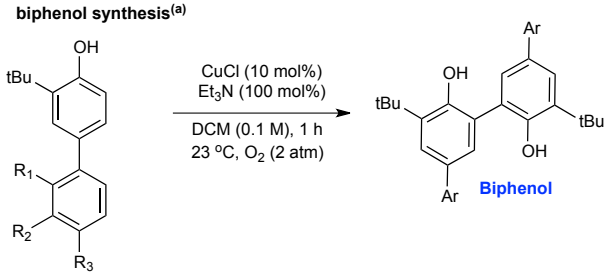

Entry	R_1	R_2	R_3	Yield[b] (%) Biphenol
(1)	Me	H	H	70
(2)	H	Me	H	96
(3)	H	H	Me	97
(4)	OMe	H	H	81
(5)	H	OMe	H	90
(6)	H	H	OMe	95
(7)	H	H	F	92
(8)	Ar = 2 - naphthyl			> 95

(a) Reactions were performed on 0.25 mmol of phenol (b)Isolated product yield & conversion

Overall, an efficient and operationally simple method for biphenol synthesis was developed, the optimization of which permitted the gathering of valuable information on the steric and electronic requirements for the aerobic oxidative coupling of phenols to biphenols. We anticipate that our method will be applicable to the synthesis of biphenols in a variety of contexts.

2.4 Oxepinobenzofurans – Synthesis Optimization and Reaction Scope

2.4.1 Oxepinobenzofuran structural determination

When first obtained from $CuPF_6$/DBED mediated aerobic oxidation of 2,4-DTBP, the oxepinobenzofuran structure was unknown. Extensive spectroscopic studies were not successful for structural determination, but a crystal structure was obtained by growing single crystals of the oxepinobenzofuran at 4^{o}C overnight in a mixture of dichloromethane and methanol (Figure 2.3).

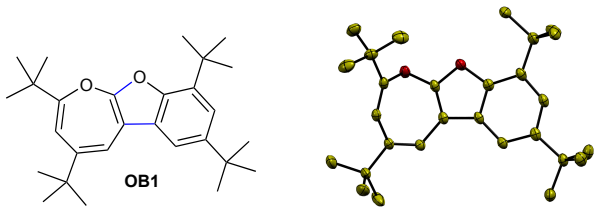

Figure 2.3 Crystal Structure of Oxepinobenzofuran OB1

2.4.2 Oxepinobenzofuran Synthesis Optimization

With the intuition that a more coordinating anion would favor outer-sphere type pathways, thus formation of either biphenol or oxepinobenzofuran, optimization of oxepinobenzofuran synthesis was started with copper salts such as cuprous chloride (Table 2.6).

2,4-DTBP was oxidized to the corresponding oxepinobenzofuran in aerobic media, at room temperature and high concentration (1 M), with a copper salt and TMEDA as the catalytic agents. Using CuCl, TMEDA and O_2 administered through a double-layered balloon, the desired oxepinobenzofuran **OB1** was obtained in 54% yield as a solid which precipitates from the

reaction mixture. Increasing O_2 to 1 bar overpressure, and changing the reaction vessel to a Radley tube increased the yield of **OB1** to 77% (Table 2.6, Entry 3).

Table 2.6: Optimization of 2,4-DTBP catalytic aerobic oxidation with TMEDA to Oxepinobenzofuran OB1[(a)]

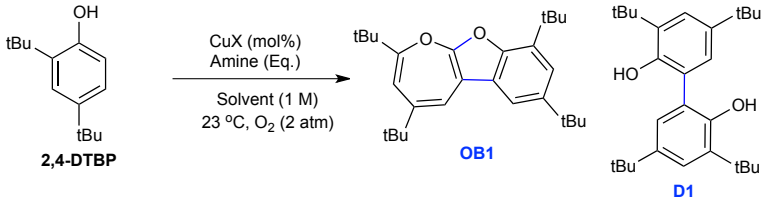

Entry	CuX (mol%)	Amine (Eq.)	Solvent	Time (h)	Conversion[(b)] (%)	Yield[(b)] (%) **OB1/D1**
(1)	CuCl (10)	TMEDA (0.1)	EtOH	6	-	54[(c,d,e)] / -
(2)	CuCl (10)	TMEDA (0.1)	EtOH	6	-	18[(c,e)] / -
(3)	CuCl (10)	TMEDA (0.05)	EtOH	6	-	77[(c)] / -
(4)	CuCl (10)	TMEDA (0.2)	EtOH	6	-	76[(c)] / -
(5)	CuCl (5)	TMEDA (0.025)	EtOH	6	-	62[(c)] / -
(6)	CuCl (5)	TMEDA (0.05)	EtOH	6	85	63 / 7
(7)	CuCl (5)	TMEDA (0.1)	EtOH	6	90	57 / 5
(8)	CuCl (10)	TMEDA (0.05)	Acetone	3	73	7 / 15
(9)	CuCl (10)	TMEDA (0.05)	DCM	3	100	0 / 22
(10)	CuCl (10)	TMEDA (0.05)	PhMe	3	80	0 / 30
(11)	CuCl (10)	TMEDA (0.05)	THF	3	65	0 / 13
(12)	CuBr (10)	TMEDA (0.05)	EtOH	6	70	22 / 40
(13)	CuI (10)	TMEDA (0.05)	EtOH	6	90	60 / 12
(14)	CuCl (10)	TMEDA (0.05)	EtOH	15	99	83 / 0

(a) Reactions were performed on 2.0 mmol of 2,4-DTBP (b) Product yield & conversion determined by ^{1}H NMR spectroscopy using hexamethylbenzene as an internal standard (c) Isolated yield of product (d) Double-layered baloon utilized for O_2 input (e) Reaction performed on 10 mmol of 2,4-DTBP TMEDA = *N,N,N′,N′*-tetramethylethylenediamine DCM = dichloromethane THF = tetrahydrofuran

Increasing the ligand loading (Table 2.6, Entry 4) has little effect on the reaction outcome, whereas lowering the amount of copper leads to decreased conversion and product yield. (Table 2.6, Entries 5-7). This effect appears to be independent of the amount of ligand that is present.

The use of polar or nonpolar aprotic solvents (Table 2.6, Entries 8-11) has a negative impact on the isolated yield of **OB1**, and instead, selectivity for biphenol **D1** is observed. Although conversion in apolar solvents is moderate to good, only low yields of the biphenol are observed. We attribute these results to the ability of these solvents to serve as reductants.

Larger anions to copper, as in the cuprous iodide and cuprous bromide salts, show a decreased rate of reaction using the best available conditions with CuCl (Table 2.6, Entry 6, Entries 12-13).

Finally, we found that using TMEDA, the reaction worked best in ethanol, and furnished the product in 83% yield after 15 hours. It should be noted that the oxepinobenzofurans are unstable to acidic or basic reaction media, and decompose very quickly when slightly impure or in solution. It is likely that the product yield, and a complete conversion of starting material, reflects some amount of decomposition.

Next, replacing TMEDA with DBED was investigated (Table 2.7, Entry 2). In 6 hours, the reaction shows complete conversion and a yield of 75% product, with no biphenol observable. Cuprous bromide works as well as cuprous chloride with DBED as the ligand however the use of cuprous iodide induces a significant decrease in reaction rate, with a 40% yield of oxepinobenzofuran and 35% yield of biphenol (Table 2.7, Entries 3-4).

Table 2.7: Optimization of 2,4-DTBP catalytic aerobic oxidation with DBED to Oxepinobenzofuran OB1[(a)]

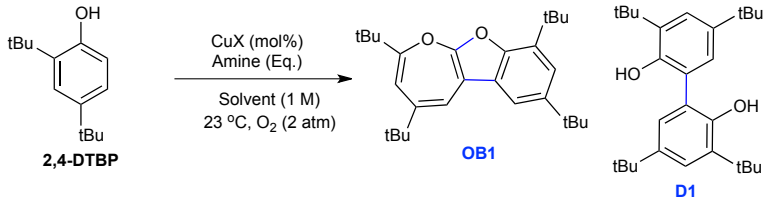

Entry	CuX (mol%)	Amine (Eq.)	Solvent	Time (h)	Conversion[(b)] (%)	Yield[(b)] (%) **OB1/D1**
(1)	CuCl (10)	TMEDA (0.05)	EtOH	15	99	83 / 0
(2)	CuCl (10)	DBED (0.05)	EtOH	6	100	75 / 0
(3)	CuBr (10)	DBED (0.05)	EtOH	6	100	80 / 0
(4)	CuI (10)	DBED (0.05)	EtOH	6	100	40 / 35
(5)	CuCl (10)	DBED (0.05)	EtOH	3	100	80 / 0
(6)	CuCl (5)	DBED (0.025)	EtOH	3	100	80 / 0
(7)	CuCl (2.5)	DBED (0.0125)	EtOH	3	100	80 / 0
(8)	CuCl (1)	DBED (0.005)	EtOH	3	100	80 / 0
(9)	CuCl (1)	DBED (0.005)	EtOH	1	90	62 / 16
(10)	CuCl (10)	DBED (0.05)	EtOH	15	100	80 / 0
(11)	CuCl (10)	DBED (0.05)	HFIP	15	100	0 / 100
(12)	CuCl (5)	DBED (0.05)	EtOH	3	100	75 / 0
(13)	CuCl (5)	DBED (0.1)	EtOH	3	100	86 / 0

(a) Reactions were performed on 2.0 mmol of phenol (b) Product yield & conversion determined by ^{1}H NMR spectroscopy using hexamethylbenzene as an internal standard TMEDA = *N,N,N′,N′*-tetramethylethylenediamine DBED = *N,N′*-ditertbutylethylenediamine HFIP = hexafluoroisopropanol

Since complete conversion is observed with 10mol% copper in six hours, shorter reaction times and reduced catalyst loadings were investigated (Table 2.7, Entries 5-9). Gratifyingly, the reaction still performed to full conversion and 80% yield of product with 1mol% cuprous chloride and 0.5mol% DBED in three hours. The DBED loading has little effect on reaction efficiency (Table 2.7, Entries 12-13).

Although in ethanol the reaction proceeds to full conversion with 80% yield of product, running the reaction under otherwise identical conditions in hexafluoroisopropanol (HFIP) yields the biphenol quantitatively, with no trace of oxepinobenzofuran even after prolonged reaction time (Table 2.7, Entries 10-11). We attribute this change in selectivity to the decreased pka of the fluorinated solvent.

Optimization of oxepinobenzofuran synthesis by copper catalyzed aerobic oxidation of phenols was successful. The above results demonstrate high catalyst-control, with complete bias for an outer-sphere oxidation pathway and high chemo-selectivity between biphenols and oxepinobenzofurans *via* ligand tuning.

2.4.2 Catalytic Aerobic Oxepinobenzofuran Synthesis Scope

With optimized conditions for the synthesis of oxepinobenzofurans using either TMEDA or DBED as a ligand to Cu, we investigated the reaction scope of these two reactions.

Similarly to biphenol synthesis, optimized conditions for catalytic aerobic oxepinobenzofuran synthesis tolerate increased steric bulk, as shown by the reasonable yields of *t*Amyl, Cumyl and Trityl substited phenols (Table 2.8, Entries 2-6). Remarkably, the oxidation of 2-*tert*-butyl-4-*iso*-propyl phenol furnishes the corresponding oxepinobenzofuran in 97% yield (Table 2.8, Entry 7). Electron rich and electron-poor aryl substituted phenols are also oxidized, albeit in lower yields (Table 2.9). Although no large effect is noticed on oxepinobenzofuran yields upon changing starting material electronic properties, yields tend to slightly decrease as the substituent moves from an *ortho* position on the aryl (blocking a planar conformation and large resonance stabilization of phenoxyl radicals) to the *para*-position.

Table 2.8: Substrate scope for the catalytic aerobic oxepinobenzofuran synthesis[a]

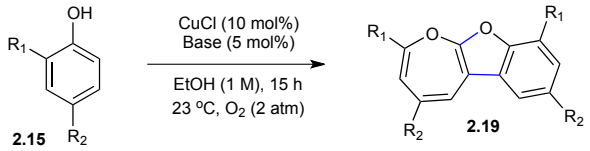

Entry	R_1	R_2	Yield (%) DBED[b]	Yield (%) TMEDA[c]
(1)	*t*Bu	*t*Bu	83	82
(2)	*t*Bu	*t*Amyl	87	63
(3)	*t*Amyl	*t*Amyl	66	60
(4)	*t*Bu	Cumyl	73	-
(5)	Cumyl	Cumyl	73	-
(6)	*t*Bu	Trityl	72	0
(7)	*t*Bu	*i*Pr	97	-
(8)	*t*Bu	Ph	50	20[d]

(a) Reactions were performed on 2 mmol of phenol (b) Isolated yields (c) NMR yields determined using hexamethylbenzene as internal standard (d) reaction was run on 4.2 mmol

Table 2.9: Substrate scope for the catalytic aerobic Aryl substituted oxepinobenzofuran synthesis[a]

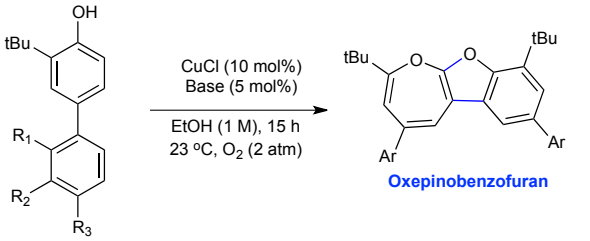

Entry	R_1	R_2	R_3	Yield (%) DBED[b]	Yield (%) TMEDA[c]
(1)	Me	H	H	65	25
(2)	H	Me	H	59	22
(3)	H	H	Me	55	33
(4)	OMe	H	H	83	26
(5)	H	OMe	H	72	20
(6)	H	H	OMe	75	23
(7)	H	H	F	53	22
(8)	Ar = 2 - naphthyl			> 95	0

(a) Reactions were performed on 2 mmol of phenol (b) Isolated yield of product (c) NMR yield determined using hexamethylbenzene as internal standard

Typically, the reaction is less efficient with TMEDA than with DBED, which can be attributed to added steric bulk of the catalytic system. In effect, no reaction is observed using TMEDA with the bulkier Trityl substituted starting phenol (Table 2.8, Entry 6). Changing

substituents of an aryl group on starting phenols also evidences the superiority of CuCl/DBED as catalytic system for oxepinobenzofuran synthesis (Table 2.9).

Assignments of oxepinobenzofurans structures were made through spectroscopic assesments and by analogy to the obtained x-ray crystal structure of **OB1.** In addition, single crystals of 2,9-di-*tert*-butyl-4,7-di-phenyl oxepinobenzofuran (OB8) were obtained by dissolving **OB8** in a mixture of dichloromethane and methanol (Figure 2.4).

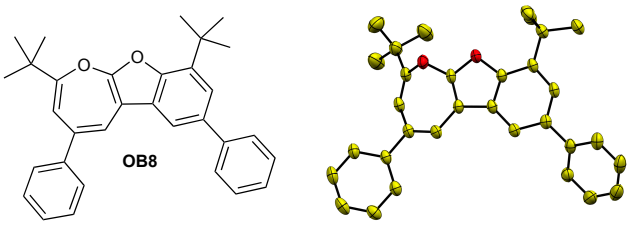

Figure 2.4 Crystal Structure of Oxepinobenzofuran OB8

2.5 Conclusions

Phenolic catalytic aerobic oxidations have historically been unselective due to overwhelming substrate control of reactivity[5], limiting their use to starting materials able to undergo clean radical reactions. Finally, for the first time a definite catalyst control in phenolic aerobic oxidations is shown, capable of furnishing useful biphenols and oxepinobenzofurans from a single phenol by subtle ligand and metal couterion tuning.

The optimized biphenol synthesis conditions have the potential for a broader substrate scope, and intra-molecular phenolic coupling should be looked into. In the case of the oxepinobenzofurans, the decomposition pathway evidences a new mode of reactivity of these molecules, and warrants more investigation, particularly as new H-abstraction agents.

2.6 Supporting Information

2.6.1 General Experimental

Chemicals and solvents were purchased from Sigma Aldrich, Alfa Aesar, Strem Chemicals or TCI. Solvents were dried and purified using a PureSolv MD 7 (from Innovative Technology) or

MB SPS 800 (from MBraun). We have not observed differences in the reaction outcome using either of these preparation methods. Triethylamine and *N*,*N*′-di-*tert*-butylethylenedimaine (DBED) were distilled over CaH_2 or activated 4Å Molecular Sieves under N_2 prior to use. Molecular sieves were flame-dried with a torch in the reaction vessel immediately prior to use. Unless otherwise noted, reactions were performed in flame-dried glassware under a positive pressure of nitrogen using standard synthetic organic, inert atmosphere techniques. All oxidation reactions were set-up in flame-dried, 25 mL Radley tubes with a Teflon-coated stir bar under a nitrogen atmosphere (*Praxair*, N_2 pre-purified). The reaction vessels were then connected to a cylinder of O_2 (Praxair), purged three times with O_2 and then pressurized to +1.0 atm.

Proton nuclear magnetic resonance (^{1}H NMR) spectra were acquired using Varian Inova 400 MHz and Varian Mercury 300 MHz spectrometers. Chemical shifts (δ) are reported in parts per million (ppm) and are calibrated to the residual solvent peak. Coupling constants (*J*) are reported in Hz. Multiplicities are reported using the following abbreviations: *s* = singlet; *d* = doublet; *t* = triplet; *q* = quartet; *m* = multiplet (range of multiplet is given). Carbon nuclear magnetic resonance (^{13}C NMR) spectra were acquired using Varian Inova 100 MHz and Varian Mercury 75 MHz spectrometers. Chemical shifts (δ) are reported in parts per million (ppm) and are calibrated to the residual solvent peak. High resolution mass spectra (HRMS) were recorded using a Bruker maXis Impact TOF mass spectrometer by electrospray ionization or chemical ionization time of flight reflectron experiments. Fourier-transform infrared (FT-IR) spectra were recorded on a Perkin-Elmer FT-IR ATR spectrometer. Analytical thin-layer chromatography was performed on pre-coated 250 mm layer thickness silica gel 60 F_{254} plates (EMD Chemicals Inc.). Visualization was performed by ultraviolet light and/or by staining with potassium permanganate or iodine. Purifications by column chromatography were performed using standard column chromatography using silica gel (40-63 μm, 230-400 mesh).

2.6.2 Synthesis of Phenolic Substrates S1-S20

General Procedure A for the Synthesis of S1-S8

Para-aryl phenols S1-S8 were prepared following the method of Hirao et Al.[15]

Para-iodophenol (1 equiv.), 10% palladium on carbon (0.3 mol%), K_2CO_3 (3 equiv.) and arylboronic acid (1 equiv.) were added to a round-bottom flask equipped with a Teflon coated

stir bar. DI water (0.1 M) was added by syringe and the flask was capped with a rubber septum. The heterogeneous mixture was stirred vigorously at room temperature for 13 hours. Upon completion, the mixture was quenched with 1.5 M HCl to precipitate a white solid. Vacuum filtration allowed recovery of crude product and Pd/C catalyst. The filtrate was washed with H_2O thoroughly. Product was separated from Pd/C by extraction with EtOAc. The organic fraction was dried over $MgSO_4$, filtered and concentrated *in vacuo* to afford *para*-arylphenols.

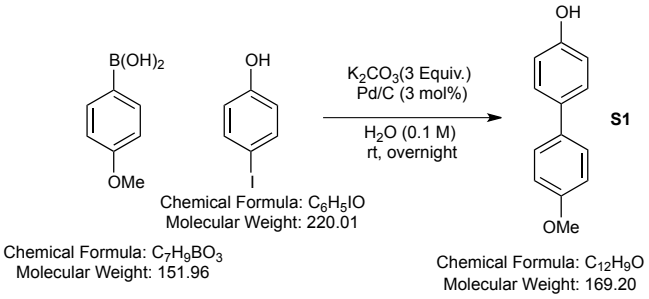

The reaction was carried out in accordance with general procedure **A** using *p*-methoxyphenylboronic acid (3.45 g, 22.73 mmol, 1 equiv.) as the coupling partner to afford **S1** (4504.9 mg, 99%).

***R*$_f$:** 0.58 (silica gel, 5/1 Hexanes/EtOAc) **IR ν_{max} (cm^{-1}):** 3378.6, 2834.3, 1606.6, 1496.8, 1374.0. **^{1}H NMR** ($CDCl_3$, 400 MHz): δ 7.47 (d, *J* = 8 Hz, 2H), 7.41 (d, *J* = 8 Hz, 2H), 6.94 (d, *J* = 8 Hz, 2H), 6.87 (d, *J* = 8 Hz, 2H), 4.84 (s, 1H) 3.84 (s, 3H). **^{13}C NMR** ($CDCl_3$, 75 MHz): δ 158.6, 154.5, 133.68, 133.41, 127.94, 127.69, 115.56, 114.14, 55.33

Analytical data matches that reported in the literature.[16]

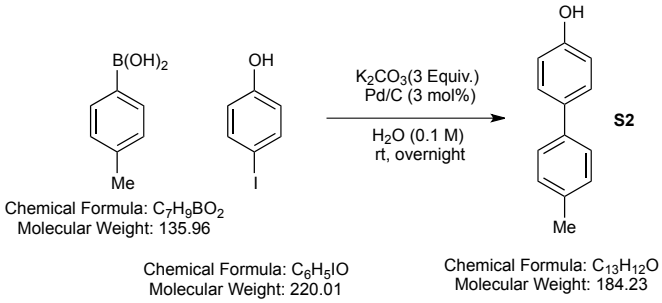

The reaction was carried out in accordance with general procedure **A** using *p*-methylphenylboronic acid (3.09 g, 22.73 mmol, 1 equiv.) as the coupling partner to afford **S2** (3.65 g, 87%).

R_f: 0.29 (silica gel, 5/1 Hexanes/EtOAc) **IR ν_{max} (cm^{-1}):** 3243.4, 1607.8, 1497.7, 1453.8, 1248.7 **^{1}H NMR** ($CDCl_3$, 300 MHz): δ 7.45 (m, 4H), 7.22 (d, *J* = 7.5 Hz, 2H), 6.89 (d, *J* = 9.9 Hz, 2H), 4.8 (br s, 1H), 2.34 (s, 3H). **^{13}C NMR** ($CDCl_3$, 75 MHz): δ 154.80, 137.87, 136.40, 133.97, 129.43, 128.17, 126.55, 115.58, 21.04.

Analytical data matches that reported in the literature.[17]

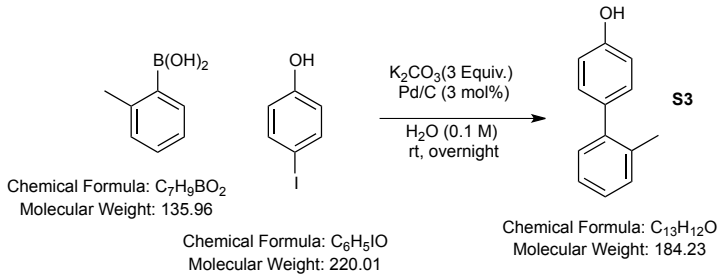

The reaction was carried out in accordance with general procedure **A** using *o*-methylphenylboronic acid (3.09 g, 22.73 mmol, 1 equiv.) as the coupling partner to afford **S3** (4.12 g, 98%).

R_f: 0.33 (silica gel, 5/1 Hexanes/EtOAc) **IR ν_{max} (cm^{-1}):** 3261.3, 1594.3, 1513.4, 1480.1, 1436.8, 1378.0 **^{1}H NMR** ($CDCl_3$, 400 MHz): δ 7.25 (m, 6H), 6.93 (d, *J* = 9 Hz, 2H), 5.08 (br s, 1H), 2.31 (s, 3H) **^{13}C NMR** ($CDCl_3$, 75 MHz): δ 154.31, 141.47, 135.21, 134.53, 130.83, 130.51, 129.91, 127.06, 125.80, 115.00, 20.56

Analytical data matches that reported in the literature.[16]

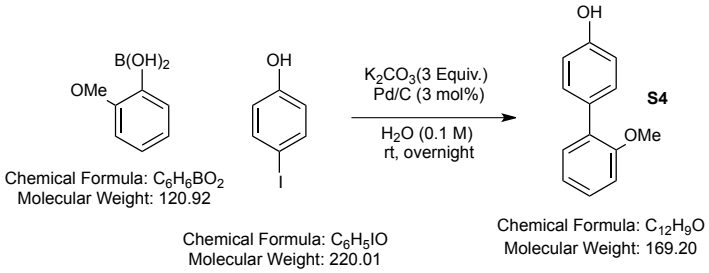

The reaction was carried out in accordance with general procedure **A** using *o*-methoxyphenylboronic acid (3.45 g, 22.73 mmol, 1 equiv.) as the coupling partner to afford **S4** (3.60 g, 80%).

R_f: 0.23 (silica gel, 5/1 Hexanes/EtOAc) **IR ν_{max} (cm^{-1}):** 3410.9, 2831.4, 1593.8, 1514.0, 1481.8, 1464.2, 1175.1, 1121.0 **^{1}H NMR** ($CDCl_3$, 400 MHz): δ 7.42 (d, *J* = 9 Hz, 2H), 7.30 (m, 2H),

7.02 (m, 2H), 6.86 (d, *J* = 9 Hz, 2H), 3.82 (s, 3H). **^{13}C NMR** ($CDCl_3$, 75 MHz): δ 156.38, 154.54, 131.9, 130.81, 130.67, 130.24, 128.22, 120.85, 114.93, 111.23, 55.56.

Analytical data matches that reported in the literature.[18]

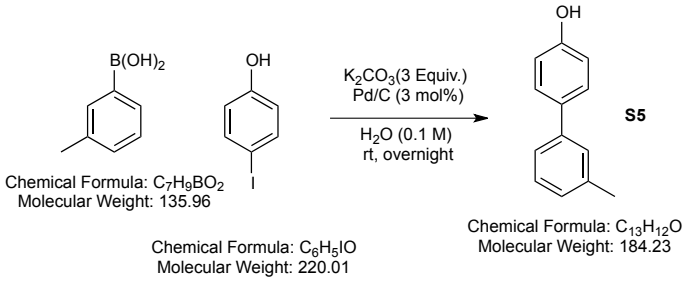

The reaction was carried out in accordance with general procedure **A** using *m*-methylphenylboronic acid (3.09 g, 22.73 mmol, 1 equiv.) as the coupling partner to afford **S5** (3.60 g, 86%).

***R*$_f$:** 0.33 (silica gel, 5/1 Hexanes/EtOAc) **IR ν_{max} (cm^{-1}):** 3270.0, 1596.6, 1513.9, 1482.0, 1373.3, 1238.1, 1176.5, 1106.2 **^{1}H NMR** ($CDCl_3$, 400 MHz): δ 7.48 (d, *J* = 9 Hz, 2H), 7.34 (d, *J* = 9 Hz, 2H), 7.31 (s, 1H), 7.13 (d, *J* = 6 Hz, 1H), 6.90 (d, *J* = 6 Hz, 2H), 4.88 (br s, 1H), 2.41 (s, 3H). **^{13}C NMR** ($CDCl_3$, 75 MHz): δ 154.99, 140.74, 138.30, 134.11, 128.64, 128.40, 127.55, 127.46, 123.83, 115.60, 21.55.

Analytical data matches that reported in the literature.[19]

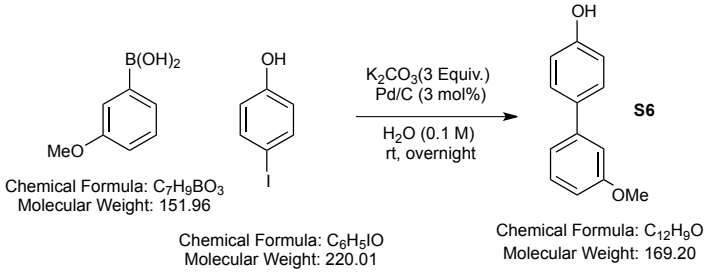

The reaction was carried out in accordance with general procedure **A** using *m*-methoxyphenylboronic acid (3.45 g, 22.73 mmol, 1 equiv.) as the coupling partner was used to afford **S6** (3.05 g, 67%).

***R*$_f$:** 0.19 (silica gel, 5/1 Hexanes/EtOAc) **IR ν_{max} (cm^{-1}):** 3382.0, 1609.6, 1576.8, 1518.8, 1481.3, 1456.2, 1295.1, 1262.7, 1174.7 **^{1}H NMR** ($CDCl_3$, 400 MHz): δ 7.50 (d, *J* = 9 Hz, 2H), 7.36 (t, *J* = 6 Hz, 1H), 7.16 (d, *J* = 6 Hz, 2H), 7.11 (s, 1H), 6.93 (d, *J* = 9 Hz, 2H), 5.46 (br s, 1H), 3.89 (s,

3H). **^{13}C NMR** ($CDCl_3$, 75 MHz): δ 159.82, 155.22, 142.33, 133.78, 129.77, 128.46, 119.40, 115.68, 112.54, 112.14, 55.37.

Analytical data matches that reported in the literature.[15]

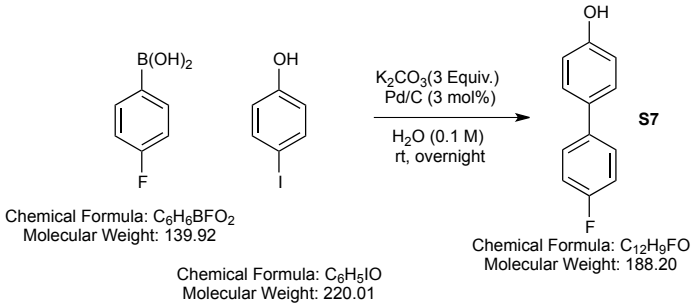

The reaction was carried out in accordance with general procedure **A** using *p*-fluorophenylboronic acid (3.18 g, 22.73 mmol, 1 equiv.) as the coupling partner to afford **S7** (3839.8 mg, 90%).

***R*$_f$:** 0.27 (silica gel, 5/1 Hexanes/EtOAc) **IR ν_{max} (cm^{-1}):** 3403.9, 1598.3, 1497.7, 1448.5, 1238.5, 1162.4 **^{1}H NMR** ($CDCl_3$, 300 MHz): δ 7.48 (dd, *J* = 6, 3 Hz, 2H), 7.42 (d, *J* = 6 Hz, 2H), 7.10 (t, *J* = 6 Hz, 2H), 6.91 (d, *J* = 9 Hz, 2H), 4.77 (br s, 1H). **^{13}C NMR** ($CDCl_3$, 75 MHz): δ 163.74, 160.48, 155.0, 136.89, 136.86, 128.27, 128.15, 115.68, 115.39, 110.01.

Analytical data matches that reported in the literature.[20]

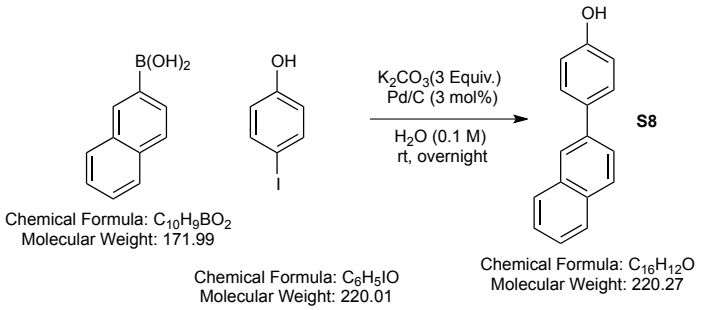

The reaction was carried out in accordance with general procedure **A** using 2-naphthylboronic acid (3.83 g, 22.73 mmol, 1 equiv.) as the coupling partner was used to afford **S8** (4440 mg, 91%).

***R*$_f$:** 0.27 (silica gel, 5/1 Hexanes/EtOAc) **IR ν_{max} (cm^{-1}):** 3051.2, 1593.6, 1519.2, 1499.9, 1460.9, 1249.3, 1179.8, 1200.6 **^{1}H NMR** ($CDCl_3$, 300 MHz): δ 7.99 (s, 1H), 7.88 (m, 3H), 7.71 (d, *J* = 6 Hz, 1H), 7.62 (d, *J* = 9 Hz, 2H), 7.48 (m, 2H), 6.96 (d, *J* = 9 Hz, 2H). **^{13}C NMR** ($CDCl_3$, 75

MHz): δ 155.23, 138.08, 133.82, 133.71, 132.30, 128.65, 128.34, 128.03, 127.61, 126.23, 125.66, 125.41, 125.02, 115.76.

Analytical data matches that reported in the literature.[18]

General Procedure B for the Synthesis of S9-S12

Phenol (1 equiv.) was added to a round bottom flask equipped with a Teflon coated cross stir bar. Acetic Acid (1.12 M) was added by syringe. Conc. Sulfuric Acid (10.12 M) was added by syringe. Tert-butanol (2.5 equiv.) was added dropwise by syringe. The flask was capped with a rubber septum and allowed to stir at 60 ^{o}C for 3 days. Upon completion, the mixture was diluted with aqueous saturated sodium bicarbonate and EtOAc. The organic phase was washed with saturated sodium bicarbonate three times. The organic phase was dried over $MgSO_4$, filtered and concentrated *in vacuo* to afford a dark orange residue. The crude was purified by column chromatography (10% EtOAc in Hexanes) to afford pure product.

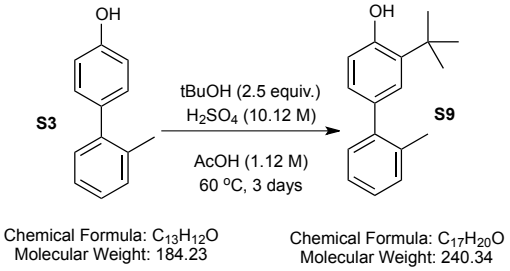

The reaction was carried out in accordance with general procedure **B** using **S3** (1.00 g, 5.43 mmol, 1 equiv.) to afford **S9** (754 mg, 58%).

***R*$_f$:** 0.60 (silica gel, 5/1 Hexanes/EtOAc) **HRMS (ESI$^-$, *m/z*):** Calcd for $C_{17}H_{19}O$ [M-H] 239.1441 Found 239.1450 **IR ν_{max} (cm^{-1}):** 3535.0, 2867.4, 1506.9, 1456.9, 1400.4, 1362.9, 1247.9, 1178.2, 1083.6. **^{1}H NMR** ($CDCl_3$, 300 MHz): δ 7.26 (m, 5H), 7.02 (d, J = 9 Hz, 1H), 6.71 (d, J = 9 Hz, 1H), 4.87 (br s, 1H), 2.29 (s, 3H), 1.44 (s, 9H). **^{13}C NMR** ($CDCl_3$, 75 MHz): δ 153.06, 142.05, 135.54, 135.46, 134.12, 130.29, 129.92, 128.25, 127.50, 126.80, 125.71, 116.12, 34.63, 29.66, 20.62.

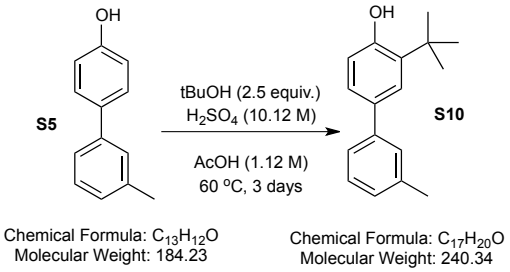

The reaction was carried out in accordance with general procedure **B** using **S5** (1.00 g, 5.42 mmol, 1 equiv.) to afford **S10** (769 mg, 59%).

R_f: 0.47 (silica gel, 5/1 Hexanes/EtOAc) **HRMS (ESI$^+$, *m/z*):** calcd for $C_{17}H_{20}NaO$ $[M+Na]^+$ 263.1406 Found 263.1406. **IR ν_{max} (cm^{-1}):** 3532.6, 2953.7, 2866.5, 1605.9, 1507.9, 1482.2, 1455.4, 1400.1, 1362.3, 1327.6, 1246.7, 1177.1, 1139.9, 1083.0, 1035.6 **^{1}H NMR** ($CDCl_3$, 300 MHz): δ 7.23 (m, 5H), 7.03 (d, *J* = 8.4 Hz, 1H), 6.71 (d, *J* = 8.1 Hz, 1H), 4.95 (br s, 1H), 2.29 (s, 3H), 1.43 (s, 9H). **^{13}C NMR** ($CDCl_3$, 75 MHz): δ 153.12, 142.08, 135.57, 135.49, 134.13, 130.32, 129.95, 128.27, 127.53, 126.83, 125.74, 116.15, 34.65, 29.68, 20.64.

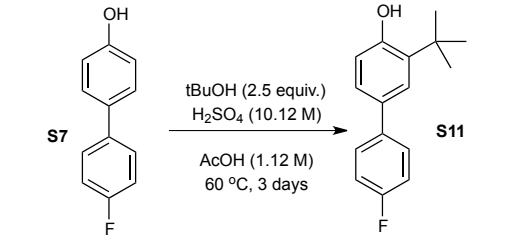

Chemical Formula: $C_{12}H_9FO$
Molecular Weight: 188.20

Chemical Formula: $C_{16}H_{17}FO$
Molecular Weight: 244.30

The reaction was carried out in accordance with general procedure **B** using **S7** (1.00 g, 5.32 mmol, 1 equiv.) to afford **S19** (636.0mg, 49%).

R_f: 0.49 (silica gel, 5/1 Hexanes/EtOAc) **HRMS (ESI$^-$, *m/z*):** Calcd for $C_{16}H_{16}FO$ [M-H] 243.1191 Found 243.1187 **IR ν_{max} (cm^{-1}):** 3585.6, 2957.3, 1603.6, 1493.3, 1466.1, 1421.8, 1386.4, 1363.5, 1340.8, 1250.7, 1208.3, 1189.7, 1158.4, 1143.6, 1099.9, 1083.2. **^{1}H NMR** ($CDCl_3$, 300 MHz): δ 7.47 (m, 3H), 7.23 (s, 1H), 7.10 (t, *J* = 6 Hz, 2H), 6.73 (d, *J* = 9 Hz, 1H), 4.85 (br s, 1H), 1.46 (s, 9H). **^{13}C NMR** ($CDCl_3$, 75 MHz): δ 163.63, 153.74, 136.42, 132.75, 128.32, 128.22, 126.02, 125.46, 116.92, 115.58, 115.29, 109.98, 34.68, 29.57.

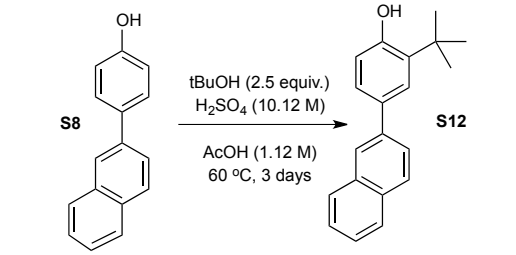

Chemical Formula: $C_{16}H_{12}O$
Molecular Weight: 220.27

Chemical Formula: $C_{20}H_{20}O$
Molecular Weight: 276.37

The reaction was carried out in accordance with general procedure **B** using **S8** (1.00 g, 4.54 mmol, 1 equiv.) was used to afford **S12** (1004 mg, 80%).

R_f: 0.49 (silica gel, 5/1 Hexanes/EtOAc) **HRMS (ESI$^+$, *m/z*):** Calcd for $C_{20}H_{20}NaO$ $[M+Na]^+$ 299.1406 Found 299.1408 **IR ν_{max} (cm^{-1}):** 3565.8, 2955.5, 1495.6, 1477.3, 1404.8, 1361.0, 1327.4, 1250.3, 1201.9, 1180.3, 1149.8, 1083.0. **^{1}H NMR** ($CDCl_3$, 300 MHz): δ 7.99 (s, 1H), 7.89 (t, *J* = 9 Hz, 3H), 7.72 (d, *J* = 8.7 Hz, 1H), 7.65 (s, 1H), 7.46 (m, 3H), 6.78 (d, *J* = 7.8 Hz, 1H), 4.95 (br s, 1H), 1.52 (s, 9H). **^{13}C NMR** ($CDCl_3$, 75 MHz): δ 153.92, 138.82, 136.49, 133.76, 133.58, 132.37, 128.29, 128.04, 127.64, 126.44, 126.21, 125.93, 125.66, 125.58, 125.06, 117.05, 34.77, 29.65.

General Procedure C for the Synthesis of S13-S20

Tert-butanol (1 equiv.) was added by syringe to a flame dried 25 mL round bottom flask equipped with a Teflon coated stir bar. Dry and degassed DCM (0.083 M) was added by syringe. $BF_3.OEt_2$ (0.5 equiv.) was added by syringe. Phenol (3 equiv.) was added at once to the DCM solution. The mixture was allowed to stir at room temperature for 5 minutes. The mixture was heated to reflux with rapid stirring for 12 hours under Argon. Upon completion, the mixture was concentrated to dryness *in vacuo*. The crude was purified by column chromatography (17% Ethyl Acetate in Hexanes) to afford pure product.

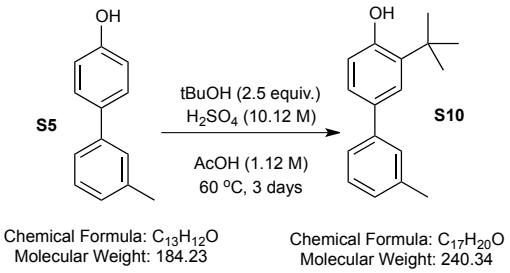

The reaction was carried out in accordance with general procedure **C** using 4-phenylphenol (255.1 mg, 1.50 mmol, 3 equiv.) to afford **S13** (112.5 mg, 99%).

R_f: 0.55 (silica gel, 5/1 Hexanes/EtOAc) **IR ν_{max} (cm^{-1}):** 2955.1, 1604.9, 1485.9, 1449.0, 1400.8, 1364.2, 1252.0, 1202.7, 1142.7, 1083.4, 1043.2 **^{1}H NMR** ($CDCl_3$, 400 MHz): δ 7.61 (m, 3H), 7.48 (t, *J* = 6 Hz, 2H), 7.36 (m, 2H), 6.79 (d, *J* = 9 Hz, 1H), 5.61 (br s, 1H), 1.55 (s, 9H). **^{13}C NMR** ($CDCl_3$, 75 MHz): δ 154.19, 141.61, 136.40, 133.45, 128.72, 126.89, 126.52, 126.16, 125.61, 116.94, 34.78, 29.66.

Analytical data matches that reported in the literature.[21]

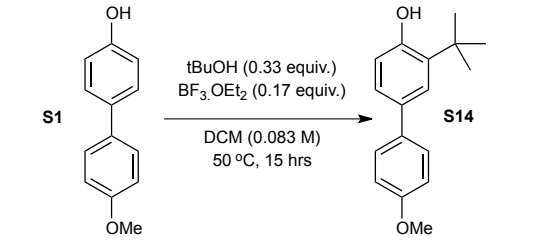

The reaction was carried out in accordance with general procedure **C** using **S1** (1.00 g, 4.99 mmol, 1 equiv.) to afford **S14** (527 mg, 41%).

R_f: 0.35 (silica gel, 5/1 Hexanes/EtOAc) **HRMS (ESI$^-$, *m/z):*** Calcd for $C_{17}H_{19}O_2$ [M-H] 255.1391 Found 255.1392. **IR ν_{max} (cm^{-1}):** 3415.5, 2950.8, 1602.4, 1495.4, 1395.3, 1202.4, 1181.8, 1143.0, 1015.6. **^{1}H NMR** ($CDCl_3$, 400 MHz): δ 7.51 (m, 3H), 7.27 (d, *J* = 9 Hz, 1H), 6.99 (d, *J* = 6 Hz, 2H), 6.73 (d, *J* = 9 Hz, 1H), 4.96 (br s, 1H), 3.88 (s, 3H), 1.50 (s, 9H). **^{13}C NMR** ($CDCl_3$, 75 MHz): δ 158.53, 153.40, 136.31, 134.23, 133.33, 127.86, 125.80, 125.22, 116.90, 114.16, 55.40, 34.71, 29.64.

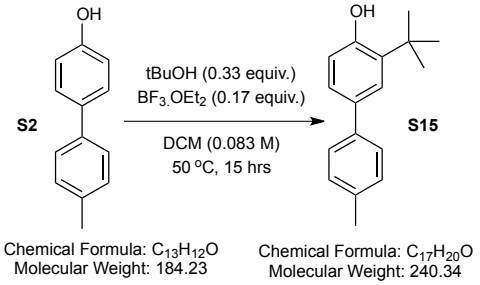

The reaction was carried out in accordance with general procedure **C** using **S2** (2.09 g, 11.36 mmol, 3 equiv.) to afford **S15** (821 mg, 90%).

R_f: 0.61 (silica gel, 5/1 Hexanes/EtOAc) **HRMS (ESI$^-$, *m/z):*** Calcd for $C_{17}H_{19}O$ [M-H] 239.1441 Found 239.1435 **IR ν_{max} (cm^{-1}):** 3509.8, 2950.3, 2912.1, 1865.4, 1604.1, 1495.3, 1387.9, 1364.4, 1339.1, 1257.4, 1189.6, 1143.7, 1081.9, 1048.6, 1018.1. **^{1}H NMR** ($CDCl_3$, 300 MHz): δ 7.48 (d, *J* = 2 Hz, 1H), 7.43 (d, *J* = 9 Hz, 2H), 7.27 (d, *J* = 9 Hz, 1H), 7.22 (d, *J* = 9 Hz, 2H), 6.72 (d, *J* = 9 Hz, 1H), 4.80 (br s, 1H), 2.39 (s, 3H), 1.46 (s, 9 H). **^{13}C NMR** ($CDCl_3$, 75 MHz): δ 153.56, 138.61, 136.24, 136.19, 133.65, 129.37, 126.69, 126.01, 125.40, 116.86, 35.68, 29.61, 21.05.

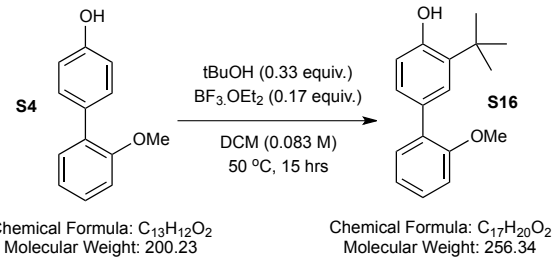

The reaction was carried out in accordance with general procedure **C** using **S4** (2402.8 mg, 12.00 mmol, 3 equiv.) to afford **S16** (947 mg, 92%).

R**f*: 0.51 (silica gel, 5/1 Hexanes/EtOAc) **HRMS (ESI⁻, *m/z): Calcd for $C_{17}H_{19}O_2$ [M-H] 255.1391 Found 255.1402. **IR ν_{max} (cm^{-1}):** 3522.7, 2953.7, 1598.7, 1509.1, 1483.5, 1462.0, 1399.6, 1362.6, 1247.6, 1178.1, 1141.8, 1121.3, 1083.8, 1023.8 **^{1}H NMR** ($CDCl_3$, 300 MHz): δ 7.44 (d, *J* = 3 Hz, 1H), 7.29 (t, *J* = 9 Hz, 3H), 7.03 (d, *J* = 6 Hz, 1H), 6.98 (d, *J* = 6 Hz, 1H), 6.71 (d, *J* = 6 Hz, 1H), 4.76 (br s, 1H), 3.80 (s, 3H), 1.44 (s, 9H) **^{13}C NMR** ($CDCl_3$, 75 MHz): δ 156.42, 153.42, 143.48, 135.53, 130.91, 130.80, 130.55, 128.55, 128.05, 120.90, 116.21, 110.87, 55.59, 34.66, 29.71.

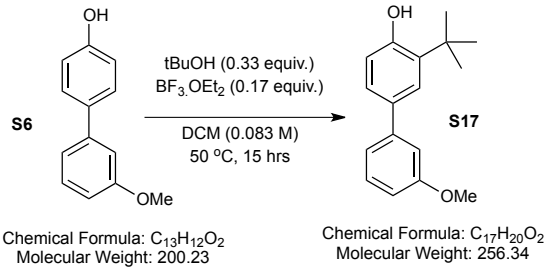

The reaction was carried out in accordance with general procedure **C** using **S6** (2151.5 mg, 10.75 mmol, 3 equiv.) to afford **S17** (735.7 mg, 80%).

R**f:* 0.23 (silica gel, 5/1 Hexanes/EtOAc) **HRMS (ESI⁻, *m/z): Calcd for $C_{17}H_{19}O_2$ [M-H] 255.1391 Found 255.1393. **IR ν_{max} (cm^{-1}):** 3530.3, 2954.5, 1605.8, 1575.7, 1510.8, 1481.5, 1388.3, 1253.1, 1169.3, 1142.0, 1082.4, 1036.6. **^{1}H NMR** ($CDCl_3$, 300 MHz): δ 7.49 (s, 1H), 7.34 (d, *J* = 6 Hz, 1H), 7.29 (d, *J* = 6 Hz, 1H), 7.13 (d, *J* = 6 Hz, 1H), 7.07 (d, *J* = 6 Hz, 1H), 6.85 (d, *J* = 6 Hz, 1H), 6.73 (d, *J* = 6 Hz, 1H), 4.83 (br s, 1H), 3.86 (s, 3H), 1.45 (s, 9H) **^{13}C NMR** ($CDCl_3$, 75 MHz): δ 159.82, 153.99, 143.07, 136.34, 133.45, 129.66, 126.21, 125.64, 119.49, 116.87, 112.78, 111.77, 55.32, 34.62, 29.01

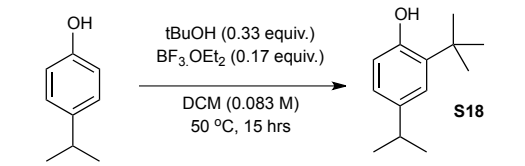

Chemical Formula: $C_9H_{12}O$
Molecular Weight: 136.19

Chemical Formula: $C_{13}H_{20}O$
Molecular Weight: 192.30

The reaction was carried out in accordance with general procedure **C** using 4-*iso*-propyl phenol (1.63 g, 12.0 mmol, 3 equiv.) to afford **S18** (676.2 mg, 88%).

R_f: 0.46 (silica gel, 5/1 Hexanes/EtOAc). **HRMS (ESI$^-$, *m/z):*** Calcd for $C_{13}H_{19}O$ [M-H] 191.1441 Found 191.1434 **IR *ν_{max}* (cm^{-1}):** 2956.4, 1503.7, 1460.9, 1417.5, 1362.0, 1323.2, 1249.1, 1177.2, 1082.9 **^{1}H NMR** ($CDCl_3$, 400 MHz): δ 1.24 (s, 3H), 1.27 (s, 3H), 1.41 (s, 9H), 2.83 (m, 1H), 4.59 (br s, 1H), 6.59 (d, *J* = 8 Hz, 1H), 6.92 (d, *J* = 8 Hz, 1H), 7.11 (s, 1H). **^{13}C NMR** ($CDCl_3$, 75 MHz): δ 152.04, 140.74, 135.63, 125.38, 124.22, 116.27, 34.53, 33.56, 29.63, 24.28.

This compound has been reported previously.[22] No analytical data was provided.

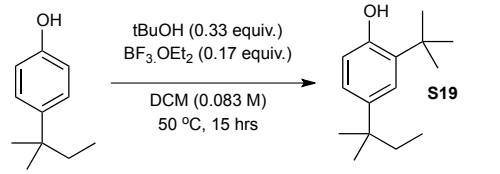

Chemical Formula: $C_{11}H_{16}O$
Molecular Weight: 164.24

Chemical Formula: $C_{15}H_{24}O$
Molecular Weight: 220.35

The reaction was carried out in accordance with general procedure **C** using 4-*tert*-Amyl phenol (1.48 g, 6.0 mmol, 3 equiv.) to afford **S19** (646.2 mg, 98%).

R_f: 0.56 (silica gel, 5/1 Hexanes/EtOAc) **HRMS (ESI$^-$, *m/z):*** Calcd for $C_{15}H_{23}O$ [M-H] 219.1754 Found 219.1763. **IR *ν_{max}* (cm^{-1}):** 3531.8, 2960.0, 2870.4, 1605.8, 1505.2, 1462.0, 1405.0, 1361.6, 1252.4, 1179.2, 1148.5, 1083.3.s **^{1}H NMR** ($CDCl_3$, 400 MHz): δ 0.68 (t, *J* = 7.6 Hz, 3H), 1.25 (s, 6H), 1.41 (s, 9H), 1.60 (q, *J* = 7.6 Hz, 2H), 4.68 (br s, 1H), 6.59 (d, *J* = 8.4 Hz, 1H), 6.99 (d, *J* = 8.4 Hz, 1H), 7.22 (s, 1H). **^{13}C NMR** ($CDCl_3$, 75 MHz): δ 151.63, 141.27, 135.04, 124.63, 124.15, 115.82, 37.41, 36.98, 34.68, 29.67, 28.56, 9.15.

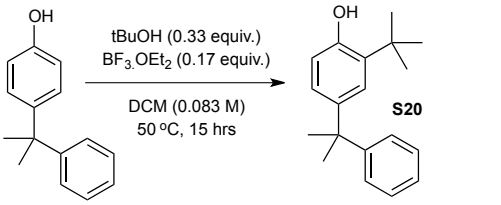

Chemical Formula: $C_{15}H_{16}O$
Molecular Weight: 212.29

Chemical Formula: $C_{19}H_{24}O$
Molecular Weight: 268.39

This compound has been reported previously.[23] No analytical data was provided.

The reaction was carried out in accordance with general procedure **C** using 4-cumyl phenol (3.82 g, 18.0 mmol, 3 equiv.) to afford **S20** (1766.6 mg, 73%).

R_f: 0.63 (silica gel, 5/1 Hexanes/EtOAc) **HRMS (ESI$^-$, *m/z):*** Calcd for $C_{19}H_{23}O$ [M-H] 267.1754 Found 267.1764. **IR ν_{max} (cm^{-1}):** 3533.2, 2963.0, 1601.1, 1493.5, 1443.8, 1405.9, 1361.8, 1183.2, 1083.8. **^{1}H NMR** ($CDCl_3$, 400 MHz): 7.30-7.23 (m, 5H), 7.15 (s, 1H), 6.88 (d, J = 8.4 Hz, 1H), 6.55 (d, J = 8 Hz, 1H), 4.70 (br s, 1H), 1.66 (s, 6H), 1.36 (s, 9H) **^{13}C NMR** ($CDCl_3$, 75 MHz): δ 151.86, 151.01, 142.50, 135.08, 127.85, 126.71, 125.47, 125.41, 125.27, 116.12, 42.49, 34.65, 30.96, 29.55.

Analytical data matches that reported in the literature.[24]

2.6.4 Synthesis of Phenolic Substrate: S21

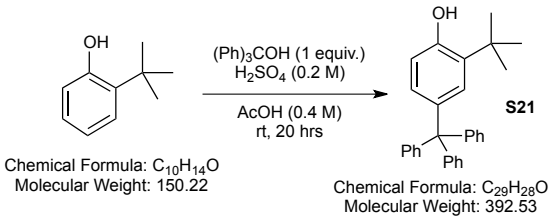

Triphenylcarbinol (26.0 g, 0.0998 mol, 1 equiv.) was added to a 500 mL round bottom flask equipped with a Teflon coated stir bar. Acetic acid (250 mL, 0.4 M) was poured into the flask. 2-tertbutylphenol (15.3 mL, 15.0 g, 0.0998 mol, 1 equiv.) was added by syringe. The flask was heated to 50^{o}C with stirring. Concentrated H_2SO_4 (5 mL) was added by syringe to the stirring solution. The heating bath was removed and the solution was stirred vigorously for 20 hours. Upon completion, the precipitate formed was filtered and washed extensively with water to afford pure **S20** (32.86 g, 84%)**.**

R_f: 0.53 (silica gel, 5:1 hexanes/EtOAc) **IR ν_{max} (cm^{-1}):** 3538.9, 2946.2. **^{1}H NMR** ($CDCl_3$, 400 MHz): δ 7.25-7.15 (m, 15H), 7.09 (d, J= 2.4 Hz, 1H), 6.85 (dd, J= 8.4, 2.4 Hz, 1H), 6.53 (d, J= 8.4Hz, 1H), 4.62 (br s, 1H), 1.25 (s, 9H). **^{13}C NMR** ($CDCl_3$, 75 MHz): δ 151.9, 147.2, 138.7, 134.5, 131.1, 130.5, 129.5, 127.3, 125.7, 115.3, 64.5, 34.6, 29.6.

Analytical data matches that reported in the literature.[25]

2.6.3 Catalytic Aerobic Phenol Oxidations for Biphenol Syntheses

General Procedure D for Synthesis of Biphenols D1-D16 (Table 2.4 & Table 2.5) Phenol (0.25 mmol, 1 equiv.) and CuCl (2.5 mg, 0.025 mmol, 10 mol%) were added to a flame dried and cooled Radley tube equipped with a Teflon coated cross stir bar and capped with a rubber septum. Dry and degassed DCM (2.5 mL, 0.1 M) was added to the Radley tube with stirring. Triethylamine (10 μL, 8.62 mg, 0.25 mmol, 1 equiv.) was added to the Radley tube by syringe. Under a high pressure of Argon, the rubber septum was replaced by a Radley cap. The mixture was allowed to stir at room temperature for 1 or 2 h under O_2 overpressure (1 bar). Upon completion, the mixture was quenched with 10% $NaHSO_4$ solution (25 mL). The aqueous phase was extracted with DCM three times. The combined organic phases were dried over $MgSO_4$, filtered and concentrated *in vacuo* to afford crude product. Column chromatography (Hexanes/Ethyl Acetate) was performed to yield pure biphenols.

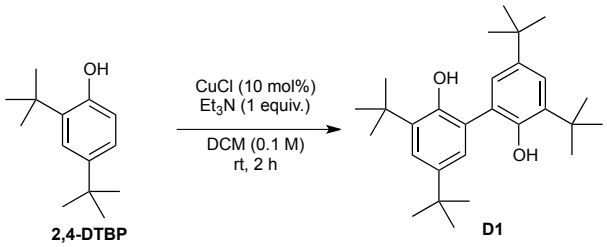

The reaction was carried out in accordance with general procedure **D** using phenol **2,4-DTBP** (51.6 mg, 0.25 mmol, 1 equiv.) for 2 h to afford pure **D1** (50.3 mg, 99%).

R_f: 0.85 (silica gel, 5/1 Hexanes/EtOAc) **IR ν_{max} (cm^{-1}):** 3522.9, 2956.4, 1475.3, 1434.3, 1361.2, 1332.4, 1281.1, 1228.5, 1199.7, 1168.8, 1093.7 **^{1}H NMR** ($CDCl_3$, 400 MHz): δ 7.39 (d, *J* = 2.4 Hz, 2H), 7.11 (d, *J* =2.8 Hz, 2H), 5.21 (br s, 2H), 1.45 (s, 18H), 1.32 (s, 18H). **^{13}C NMR** ($CDCl_3$, 75 MHz): δ 149.74, 142.95, 136.20, 125.26, 124.81, 122.29, 35.18, 34.44, 31.62, 29.65.

Analytical data matches that reported in the literature.[26]

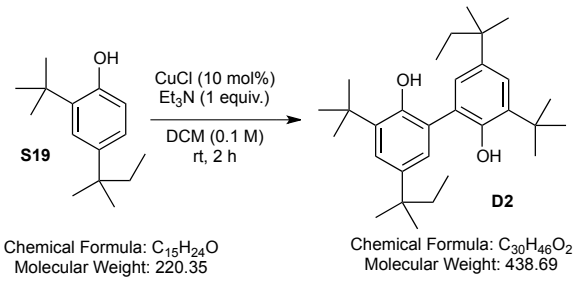

The reaction was carried out in accordance with general procedure **D** using **S19** (55.1 mg, 0.25 mmol, 1 equiv.) for 2 h. Purification by column chromatography (Silica Gel, 9/1 Hexanes/Ethyl Acetate) afforded **D2** (47.7 mg, 87%).

R_f: 0.75 (silica gel, 5/1 Hexanes/EtOAc). **HR-MS (ESI$^-$, *m/z):*** Calcd for $C_{30}H_{45}O_2$ [M-H] 437.3425 Found 437.3446 **IR ν_{max} (cm^{-1}):** 3526.2, 2958.7, 2916.2, 2870.6, 1433.5, 1360.9, 1268.5, 1214.6, 1197.8 1176.1, 1094.3. **^{1}H NMR** ($CDCl_3$, 300 MHz): δ 7.33 (s, 2H), 7.05 (s, 2H), 5.20 (br s, 2H), 1.62 (q, *J* = 7.5 Hz, 4H), 1.45 (s, 18 H), 1.27 (s, 12H), 0.075 (t, *J* = 7.5 Hz, 6H). **^{13}C NMR** ($CDCl_3$, 75 MHz): δ 149.63, 141.38, 136.10, 125.85, 125.33, 122.18, 37.58, 36.91, 35.16, 29.68, 28.48, 9.27.

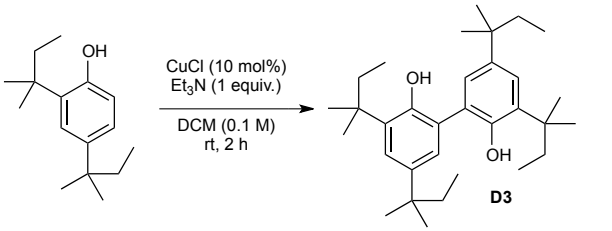

Chemical Formula: $C_{16}H_{26}O$
Molecular Weight: 234.38

Chemical Formula: $C_{32}H_{50}O_2$
Molecular Weight: 466.74

The reaction was carried out in accordance with general procedure **D** using 2,4-di-*tert*-amyl phenol (58.6 mg, 0.25 mmol, 1 equiv.) for 2 h. Purification by column chromatography (Silica Gel, 7/1 Hexanes/Ethyl Acetate) afforded **D2** (49.6 mg, 85%).

R_f: 0.84 (silica gel, 5/1 Hexanes/EtOAc) **HR-MS (ESI$^-$, *m/z):*** Calcd for $C_{32}H_{49}O_2$ [M-H] 465.3738 Found 465.3748 **IR ν_{max} (cm^{-1}):** 3526.2, 2874.8, 1457.3, 1436.2, 1361.6, 1328.9, 1235.9, 1214.3, 1197.4, 1166.4, 1094.9. **^{1}H NMR** ($CDCl_3$, 300 MHz): δ 7.25 (d, *J* = 1.8 Hz, 2H), 7.02 (d, *J* = 2.1 Hz, 2H), 5.13 (br s, 2H), 1.96-1.79 (m, 4H), 1.62 (q, *J* = 7.2 Hz, 4H), 1.40 (s, 12H), 1.28 (s, 12H), 0.73 (q, *J* = 7.2 Hz, 12H) **^{13}C NMR** ($CDCl_3$, 75 MHz): δ 149.58, 141.12, 134.45, 126.73, 125.78, 122.09, 38.79, 37.53, 37.01, 33.09, 28.62, 27.62, 9.59, 9.24.

Analytical data matches that reported in the literature.[27]

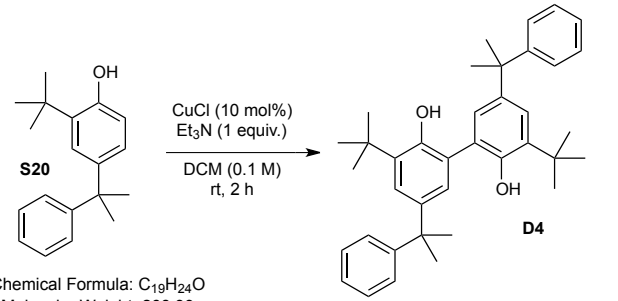

Chemical Formula: $C_{19}H_{24}O$
Molecular Weight: 268.39

Chemical Formula: $C_{38}H_{46}O_2$
Molecular Weight: 534.77

The reaction was carried out in accordance with general procedure **D** using **S20** (67.1 mg, 0.25 mmol, 1 equiv.) for 2 h. Purification by column chromatography (Silica Gel, 9/1 Hexanes/Ethyl Acetate) afforded **D4** (46.1 mg, 69%).

R_f: 0.70 (silica gel, 5/1 Hexanes/EtOAc) **HR-MS (ESI$^-$, *m/z):*** Calcd for $C_{38}H_{45}O_2$ [M-H] 533.3425 Found 533.3446 **IR ν_{max} (cm^{-1}):** 3526.2, 2961.3, 2869.5, 1599.3, 1434.5, 1361.7, 1330.4, 1275.1, 1237.3, 1199.0, 1175.5, 1092.4, 1029.8 **^{1}H NMR** ($CDCl_3$, 300 MHz): δ 7.28-7.26 (m, 10H), 7.17 (s, 2H), 6.94 (s, 2H), 5.20 (br s, 2H), 1.67 (s, 18H), 1.36 (s, 12H). **^{13}C NMR** ($CDCl_3$, 75 MHz): δ 150.62, 149.76, 142.64, 136.21, 127.94, 126.69, 126.63, 126.45, 125.55, 122.12, 42.63, 35.10, 30.99, 29.60.

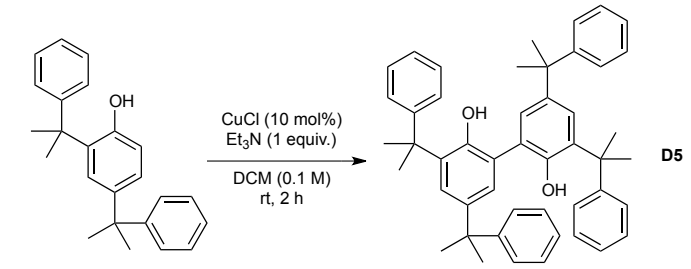

The reaction was carried out in accordance with general procedure **D** using 2,4-di-cumyl phenol (82.6 mg, 0.25 mmol, 1 equiv.) for 2 h. Purification by column chromatography (Silica Gel, 7/1 Hexanes/Ethyl Acetate) afforded **D5** (45.6 mg, 55%).

R_f: 0.68 (silica gel, 5/1 Hexanes/EtOAc) **HR-MS (ESI$^-$, *m/z):*** Calcd for $C_{48}H_{49}O_2$ [M-H] 657.3738 Found 657.3729 **IR ν_{max} (cm^{-1}):** 3519.9, 3494.5, 2959.7, 2924.6, 2869.2, 1597.6, 1492.1, 1441.1, 1362.0, 1195.7, 1148.5, 1028.1 **^{1}H NMR** ($CDCl_3$, 300 MHz): δ 7.28-7.02 (m, 22H), 6.92 (d, J = 3 Hz, 2H), 5.06 (br s, 2H), 1.71 (s, 12H), 1.58 (s, 12H). **^{13}C NMR** ($CDCl_3$, 75 MHz): δ 150.76, 149.73, 148.60, 142.48, 135.48, 128.36, 127.89, 126.78, 125.86, 125.67, 125.58, 125.55, 125.50, 115.51, 42.64, 42.19, 31.00, 29.69.

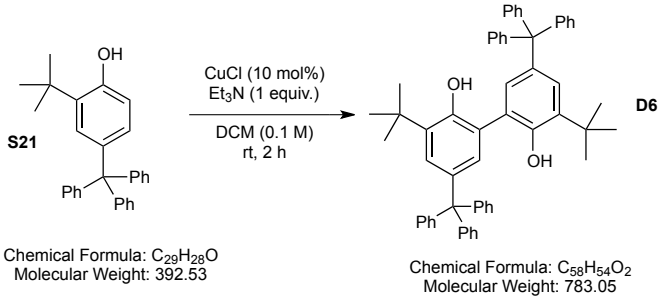

The reaction was carried out in accordance with general procedure **D** using **S21** (98.1 mg, 0.25 mmol, 1 equiv) for 2 h. Purification by column chromatography (Silica Gel, 5/1 Hexanes/Ethyl Acetate) afforded **D6** (65.5 mg, 67%).

R_f: 0.71 (silica gel, 5/1 Hexanes/EtOAc) **IR ν_{max} (cm^{-1}):** 2958.8, 1594.7, 1491.7, 1442.0, 1033.9. **^{1}H NMR** ($CDCl_3$, 300 MHz): δ 7.22-7.15 (m, 32H), 6.91 (s, 2H), 5.19 (br s, 2H), 1.24 (s, 18H) **^{13}C NMR** ($CDCl_3$, 75 MHz): δ 149.8, 147.0, 138.7, 135.8, 131.1, 130.9, 130.5, 129.5, 125.8, 122.2, 64.6, 35.1, 29.6.

Analytical data matches that reported in the literature.[28]

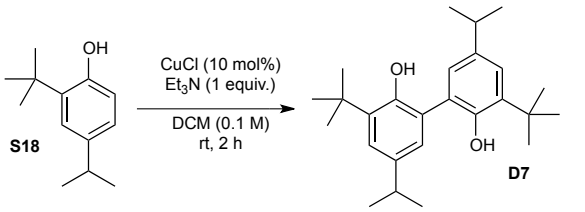

Chemical Formula: $C_{13}H_{20}O$
Molecular Weight: 192.30

Chemical Formula: $C_{26}H_{38}O_2$
Molecular Weight: 382.58

The reaction was carried out in accordance with general procedure **D** using **S18** (48.1 mg, 0.25 mmol, 1 equiv.) for 2 h. Purification by column chromatography (Silica Gel, 7/1 Hexanes/Ethyl Acetate) afforded **D7** (39.7 mg, 83%).

R_f: 0.86 (silica gel, 5/1 Hexanes/EtOAc) **HR-MS (ESI$^-$, *m/z*):** Calcd for $C_{26}H_{37}O_2$ [M-H] 381.2799 Found 381.2796 **IR ν_{max} (cm^{-1}):** 3528.8, 2956.2, 2869.5, 1465.1, 1432.5, 1361.5, 1327.1, 1260.4, 1232.8, 1197.2, 1172.8, 1092.9, 1022.2 **^{1}H NMR** ($CDCl_3$, 400 MHz): δ 7.20 (s, 2H), 6.95 (s, 2H), 5.19 (br s, 2H), 2.87 (m, 2H), 1.44 (s, 18H), 1.19 (d, J = 10 Hz, 12H) **^{13}C NMR** ($CDCl_3$, 75 MHz): δ 149.97, 140.71, 136.68, 126.01, 125.93, 122.61, 35.01, 33.64, 29.63 24.29

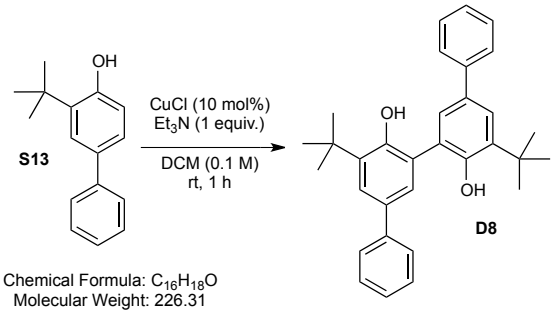

Chemical Formula: $C_{16}H_{18}O$
Molecular Weight: 226.31

Chemical Formula: $C_{32}H_{34}O_2$
Molecular Weight: 450.61

The reaction was carried out in accordance with general procedure **D** using **S13** (56.6 mg, 0.25 mmol, 1 equiv.) for 1 h to afford pure **D8** (52.9 mg, 94%).

R_f: 0.70 (silica gel, 5/1 Hexanes/EtOAc) **HR-MS (ESI$^-$, *m/z):*** Calcd for $C_{32}H_{33}O_2$ [M-H] 449.25013 Found 449.24860 **IR ν_{max} (cm^{-1}):** 3523.7, 2954.6, 1600.0, 1433.6, 1361.8, 1215.5, 1152.0. **^{1}H NMR** ($CDCl_3$, 300 MHz): δ 7.64 (d, *J* = 2.4 Hz, 2H), 7.59 (d, *J* = 7.2 Hz, 4H), 7.47-7.42 (m, 6H), 7.31 (d, *J* = 7.5 Hz, 2H), 1.52 (s, 18H) **^{13}C NMR** ($CDCl_3$, 75 MHz): δ 151.83, 140.89, 137.69, 133.78, 128.81, 127.26, 126.96, 126.86, 126.04, 122.94, 35.23, 29.63.

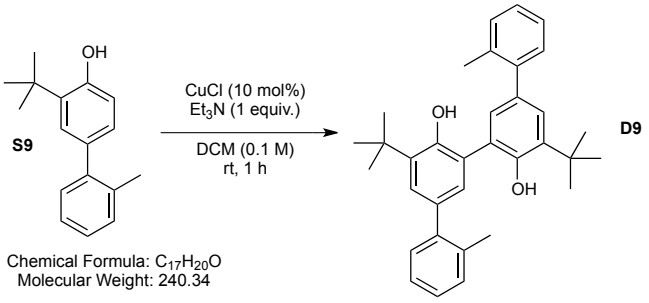

The reaction was carried out in accordance with general procedure **D** using **S9** (60.1 mg, 0.25 mmol, 1 equiv.) for 1 h. Purification by column chromatography (Silica Gel, 7/1 Hexanes/Ethyl Acetate) afforded **D9** (41.9 mg, 70%).

R_f: 0.71 (silica gel, 5/1 Hexanes/EtOAc). **HR-MS (ESI$^-$, *m/z):*** Calcd for $C_{34}H_{37}O_2$ [M-H] 477.2799 Found 477.2805 **IR ν_{max} (cm^{-1}):** 3521.9, 2953.6, 1501.0, 1458.3, 1435.9, 1390.7, 1361.3, 1262.4, 1153.6, 1094.1, 1063.6, 1029.5. **^{1}H NMR** ($CDCl_3$, 300 MHz): δ 7.35 (s, 2H), 7.29-7.22 (m, 8H), 7.14 (s, 2H), 5.46 (br s, 2H), 2.34 (s, 6H), 1.47 (s, 18H). **^{13}C NMR** ($CDCl_3$, 75 MHz): δ 151.05, 141.44, 136.84, 135.34, 134.20, 130.44, 129.94, 129.03, 128.83, 127.04, 125.84, 122.18, 35.15, 29.67, 20.76.

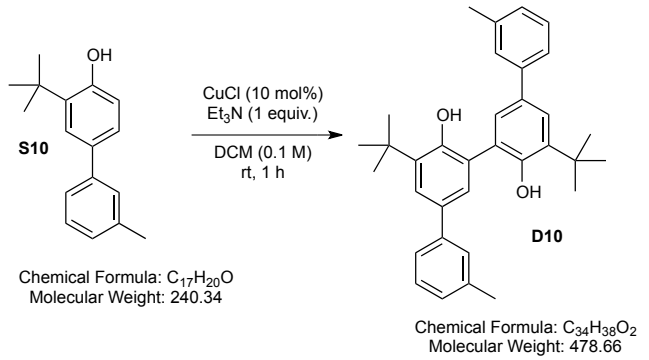

The reaction was carried out in accordance with general procedure **D** using **S10** (60.1 mg, 0.25 mmol, 1 equiv.) for 1 h. Purification by column chromatography (Silica Gel, 7/1 Hexanes/Ethyl Acetate) afforded **D10** (57.4 mg, 96%).

R_f: 0.73 (silica gel, 5/1 Hexanes/EtOAc) **HR-MS (ESI$^-$, *m/z):*** Calcd for $C_{34}H_{37}O_2$ [M-H] 477.2799 Found 477.2803. **IR ν_{max} (cm^{-1}):** 3553.2, 2955.8, 2914.1, 1436.0, 1232.1, 1163.6 **^{1}H NMR** ($CDCl_3$, 300 MHz): δ 7.62 (d, *J* = 2.1 Hz, 2H), 7.40-7.33 (m, 8H), 7.15 (d, *J* = 6.6 Hz, 2H), 5.41 (br s, 2H), 2.43 (s, 6H), 1.52 (s, 18H). **^{13}C NMR** ($CDCl_3$, 75 MHz): δ 151.75, 140.90, 138.42, 137.58, 133.88, 128.72, 127.65, 127.61, 127.29, 126.94, 123.97, 122.86, 35.22, 29.64, 21.57.

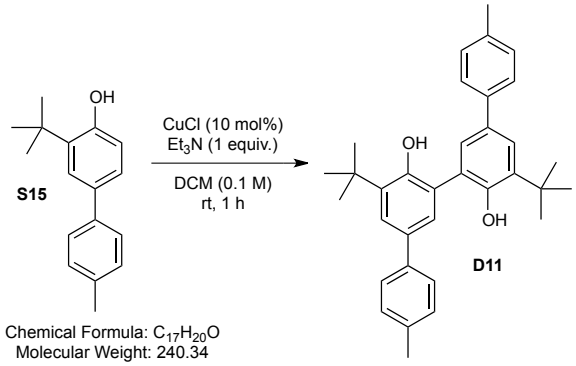

The reaction was carried out in accordance with general procedure **D** using **S15** (60.1 mg, 0.25 mmol, 1 equiv.) for 1 h to afford pure **D11** (58.0 mg, 97%).

R_f: 0.72 (silica gel, 5/1 Hexanes/EtOAc). **HR-MS (ESI$^-$, *m/z):*** Calcd for $C_{34}H_{37}O_2$ [M-H] 477.28216 Found 477.27990 **IR ν_{max} (cm^{-1}):** 3516.1, 2959.8, 2914.2, 1473.3, 1216.9. **^{1}H NMR** ($CDCl_3$, 300 MHz): δ 7.61 (d, *J* = 2.1 Hz, 2H), 7.48 (d, *J* = 8.4 Hz, 4H), 7.38 (d, *J* = 2.4 Hz, 2H), 7.24 (d, *J* = 8.4 Hz, 4H), 5.41 (br s, 2H), 2.40 (s, 6H), 1.51 (s, 18H). **^{13}C NMR** ($CDCl_3$, 75 MHz): δ 151.59, 137.58, 136.58, 133.69, 129.51, 129.43, 127.03, 126.81, 126.74, 122.91, 35.20, 29.62, 21.07.

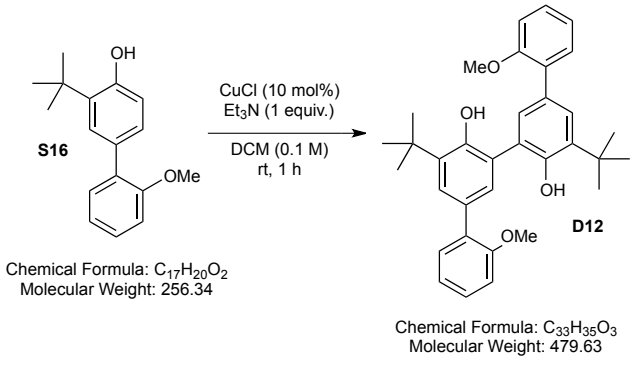

The reaction was carried out in accordance with general procedure **D** using **S16** (64.1 mg, 0.25 mmol, 1 equiv.) for 1 h. Purification by column chromatography (Silica Gel, 9/1 Hexanes/Ethyl Acetate) afforded **D12** (51.7 mg, 81%).

***R*$_f$:** 0.65 (silica gel, 5/1 Hexanes/EtOAc) **HR-MS (ESI$^-$, *m/z*)**: Calcd for $C_{34}H_{37}O_4$ [M-H] 509.2697 Found 509.2686. **IR ν_{max} (cm^{-1}):** 3518.0, 2954.4, 1596.2, 1577.1, 1494.5, 1463.2, 1427.9, 1391.2, 1361.1, 1327.5, 1236.7, 1161.8, 1121.3, 1094.1 **^{1}H NMR** ($CDCl_3$, 300 MHz): δ 7.56 (d, *J* = 3 Hz, 2H), 7.42 (d, *J* = 3 Hz, 2H), 7.35 (d, *J* = 9 Hz, 2H), 7.31 (t, *J* = 9 Hz, 2H), 7.04 (d, *J* = 6 Hz, 2H), 6.98 (d, *J* = 9 Hz, 2H), 5.64 (br s, 2H), 3.84 (s, 6H), 1.48 (s, 18H). **^{13}C NMR** ($CDCl_3$, 75 MHz): δ 156.29, 151.46, 136.77, 130.60, 130.33, 130.18, 129.34, 129.10, 128.22, 122.01, 120.88, 111.09, 55.48, 35.14, 29.63.

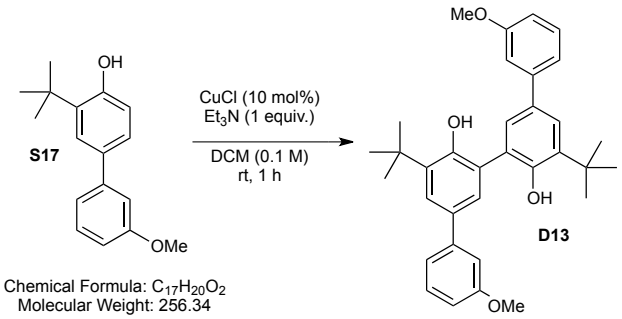

The reaction was carried out in accordance with general procedure **D** using **S17** (64.1 mg, 0.25 mmol, 1 equiv.) for 1 h. Purification by column chromatography (Silica Gel, 9/1 Hexanes/Ethyl Acetate) afforded **D13** (57.4 mg, 90%).

***R*$_f$:** 0.60 (silica gel, 5/1 Hexanes/EtOAc) **HR-MS (ESI$^-$, *m/z*)**: Calcd for $C_{34}H_{37}O_4$ [M-H] 509.2697 Found 509.2692 **IR ν_{max} (cm^{-1}):** 3523.4, 2955.7, 1598.5, 1576.3, 1464.1, 1430.6, 1390.6, 1257.2, 1233.9, 1166.2, 1090.8, 1041.7. **^{1}H NMR** ($CDCl_3$, 300 MHz): δ 7.62 (s, 2H), 7.40 (s, 2H), 7.35 (t, *J* = 9 Hz, 2H), 7.17 (d, *J* = 6 Hz, 2H), 7.11 (s, 2H), 6.87 (d, *J* = 9 Hz, 2H), 5.42 (br s, 2H), 3.86 (s, 6H), 1.50 (s, 18H). **^{13}C NMR** ($CDCl_3$, 75 MHz): δ 159.96, 151.92, 142.38, 137.66, 133.60, 129.78, 127.26, 126.99, 122.80, 119.36, 112.62, 112.18, 55.33, 35.21, 29.60.

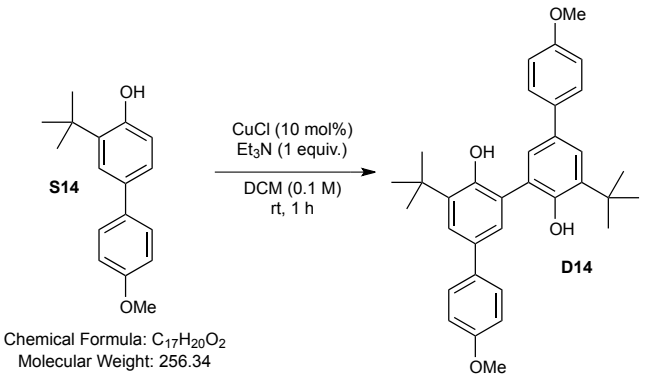

Chemical Formula: $C_{17}H_{20}O_2$
Molecular Weight: 256.34

Chemical Formula: $C_{34}H_{38}O_4$
Molecular Weight: 510.66

The reaction was carried out in accordance with general procedure **D** using **S14** (64.1 mg, 0.25 mmol, 1 equiv.) for 1 h to afford pure **D14** (60.6 mg, 95%).

R_f: 0.54 (silica gel, 5/1 Hexanes/EtOAc) **HR-MS (ESI$^-$, *m/z):*** Calcd for $C_{34}H_{37}O_4$ 509.27128 Found 509.26973 **IR ν_{max} (cm^{-1}):** 3523.6, 2955.3, 1608.8, 1513.4, 1430.6, 1284.3, 1176.8, 1030.8. **^{1}H NMR** ($CDCl_3$, 300 MHz): δ 7.57 (d, *J* = 2.1 Hz, 2H), 7.51 (d, *J* = 6.6 Hz, 4H), 7.35 (d, *J* = 2.1 Hz, 2H), 6.97 (d, *J* = 8.7 Hz, 4H), 5.31 (br s, 2H), 3.85 (s, 6H), 1.51 (s, 18H). **^{13}C NMR** ($CDCl_3$, 75 MHz): δ 158.82, 51.33, 137.58, 133.52, 133.41, 127.84, 126.81, 126.50, 122.97, 114.23, 55.37, 35.20, 29.63.

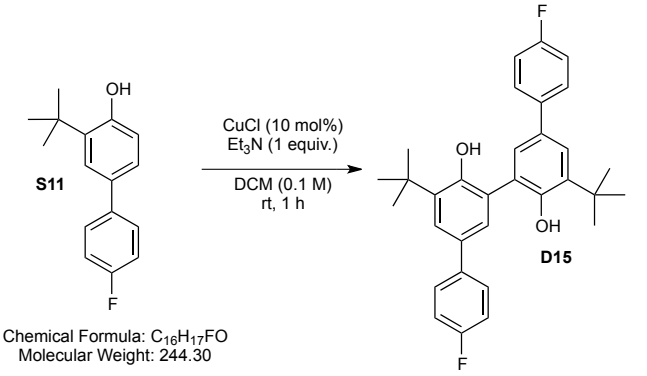

Chemical Formula: $C_{16}H_{17}FO$
Molecular Weight: 244.30

Chemical Formula: $C_{32}H_{32}F_2O_2$
Molecular Weight: 486.59

The reaction was carried out in accordance with general procedure **D** using **S11** (61.1 mg, 0.25 mmol, 1 equiv.) for 1 h to afford pure **D15** (55.9 mg, 92%).

R_f: 0.70 (silica gel, 5/1 Hexanes/EtOAc) **HR-MS (ESI$^-$, *m/z):*** Calcd for $C_{32}H_{31}O_2F_2$ [M-H] 485.23192 Found 485.22976 **IR ν_{max} (cm^{-1}):** 3526.9, 2952.7, 1598.1, 1510.8, 1435.5, 1361.4, 1217.0, 1157.5, 1094.3. **^{1}H NMR** ($CDCl_3$, 300 MHz): δ 7.55-7.50 (m, 6H), 7.33 (s, 2H), 7.11 (t, *J* = 9 Hz, 4H), 5.41 (br s, 2H), 1.45 (s, 18H). **^{13}C NMR** ($CDCl_3$, 75 MHz): δ 163.81, 160.55,

151.72, 137.80, 136.97, 136.93, 132.87, 128.37, 128.26, 127.12, 126.81, 122.91, 115.74, 115.46, 35.20, 29.58.

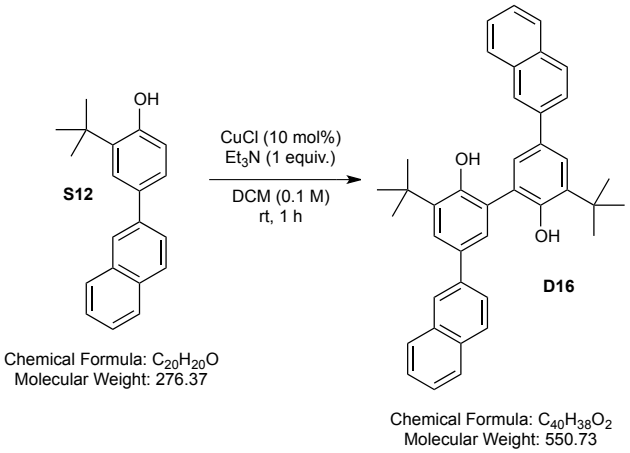

The reaction was carried out in accordance with general procedure **D** using **S12** (69.1 mg, 0.25 mmol, 1 equiv.) for 1 h to afford pure **D16** (67.5 mg, 98%).

***R*$_f$:** 0.65 (silica gel, 5/1 Hexanes/EtOAc) **HR-MS (ESI$^-$, *m/z*):** Calcd for $C_{40}H_{37}O_2$ [M-H] 549.28228 Found 549.27990 **IR ν_{max} (cm^{-1}):** 3520.6, 1953.5, 1599.7, 1431.3, 1360.7, 1234.9, 1210.5, 1198.8, 1160.5, 1092.3. **^{1}H NMR** ($CDCl_3$, 300 MHz): δ 8.06 (s, 2H), 7.95-7.89 (m, 6H), 7.81-7.76 (m, 4H), 7.60 (s, 2H), 7.52-7.46 (m, 4H), 5.30 (br s, 2H), 1.59 (s, 18H) **^{13}C NMR** ($CDCl_3$, 75 MHz): δ 151.97, 138.20, 138.87, 133.78, 133.71, 132.41, 128.50, 128.10, 127.67, 127.25, 126.35, 125.91, 125.79, 125.47, 125.21, 123.10, 35.33, 29.71.

2.6.4 Catalytic Aerobic Phenol Oxidations for Oxepinobenzofuran Syntheses

General Procedure E for Synthesis of Oxepinobenzofurans OB1-OB16 (Tables 2.8-2.9) Phenol (2.00 mmol, 1 equiv.) and cuprous chloride (19.9 mg, 0.20 mmol, 10 mol%) were added to a flame dried Radley tube equipped with a Teflon coated stir bar and capped with a rubber septum. The tube was evacuated and backfilled with Argon three times. Anhydrous EtOH (2.00 mL, 1.0 M) was added by syringe. DBED (20 μL, 17.2 mg, 0.10 mmol, 5 mol%) was added to the light yellow solution by syringe. Upon obtaining a homogeneous solution, the rubber septum was replaced with a Radley cap under high Argon pressure. The mixture was allowed to stir at room temperature under 1 bar O_2 overpressure for 15 hours. Upon completion, the mixture was concentrated *in vacuo.* The residue was dissolved in DCM and 10% $NaHSO_4$ aqueous solution.

The aqueous phase was extracted with DCM three times. The combined organic phases were dried over $MgSO_4$, filtered and concentrated *in vacuo* to afford oxepinobenzofuran.

Miscellaneous Reaction Notes

Whether dry and degassed EtOH from a purification system, or anhydrous EtOH as purchased are utilized does not impact the reaction. Pure oxepinobenzofurans can also be obtained by precipitating from the reaction mixture upon cooling at 0°C. Oxepinobenzofurans are unstable to SiO_2 and prolonged time in solution.

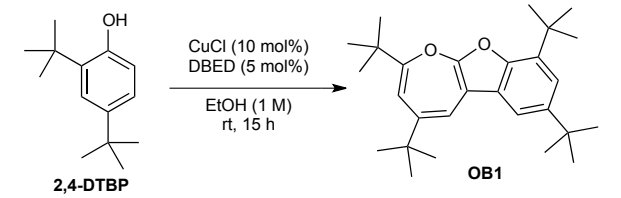

2,4-DTBP
Chemical Formula: $C_{14}H_{22}O$
Molecular Weight: 206.32

OB1
Chemical Formula: $C_{28}H_{40}O_2$
Molecular Weight: 408.62

The reaction was carried out in accordance with general procedure **E** using 2,4-DTBP (412.6 mg, 2.00 mmol, 1 equiv.) to afford **OB1** (326.9 mg, 80%). Single crystalline material was obtained by dissolving **OB1** in a methanol/dichloromethane mixture and allowing to sit overnight at 4°C.

R_f: unstable to silica gel **HR-MS (APCI$^+$, *m/z*):** Calcd for $C_{28}H_{41}O_2$ [M+H$^+$] 409.31011 Found 409.31115 **IR ν_{max} (cm^{-1}):** 2957.8, 2904.6, 2868.4, 1656.7, 1599.4 **^{1}H NMR** ($CDCl_3$, 400 MHz): δ 7.25 (d, *J*= 2Hz, 1H), 7.14, *J* = 2Hz, 1H), 6.39 (s, 1H), 5.52 (s, 1H), 1.45 (s, 9H), 1.37 (s, 9H), 1.24 (s, 9H), 1.21 (s, 9H). **^{13}C NMR** ($CDCl_3$, 75 MHz): δ 164.34, 157.10 145.81, 145.61, 133.53, 127.06, 117.37, 113.10, 112.30, 107.07, 97.83, 43.44, 37.23, 35.79, 34.94, 34.33, 31.93, 29.84, 29.22, 28.04 **Elemental Analysis:** Calcd for $C_{28}H_{40}O_2$ %C 82.30 %H 9.87 Found %C 82.22 %H 9.87

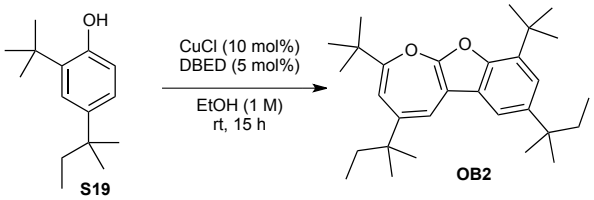

S19
Chemical Formula: $C_{15}H_{24}O$
Molecular Weight: 220.35

OB2
Chemical Formula: $C_{30}H_{44}O_2$
Molecular Weight: 436.67

The reaction was carried out in accordance with general procedure **E** using **S19** (440.4 mg, 2.00 mmol, 1 equiv.) to afford **OB2** (379.9 mg, 87%).

R_f: unstable to silica gel **HR-MS (APCI$^+$, *m/z):*** Calcd for $C_{30}H_{45}O_2$ $[M+H]^+$ 437.3414 Found 437.3418. **IR ν_{max} (cm^{-1}):** 2959.4, 2870.3, 1653.2, 1598.5, 1461.1, 1422.3, 1361.4, 1276.0, 1084.0, 1057.6, 1010.9 **^{1}H NMR** ($CDCl_3$, 300 MHz): δ 7.23 (s, 1H), 7.11 (s, 1H), 6.36 (s, 1H), 5.49 (s, 1H), 1.71 (q, *J* = 9 Hz, 2H), 1.49 (m, 11H), 1.36 (s, 6H), 1.29 (s, 9H), 1.20 (s, 6H), 0.86 (t, *J* = 6 Hz, 3H), 0.73 (t, *J* = 6 Hz, 3H). **^{13}C NMR** ($CDCl_3$, 75 MHz): δ 164.54, 154.82, 145.72, 144.05, 143.73, 133.38, 127.05, 117.88, 114.76, 113.05, 106.91, 97.84, 39.00, 38.13, 37.28, 37.19, 34.56, 34.31, 29.90, 29.01, 28.06, 27.37, 9.31, 8.98.

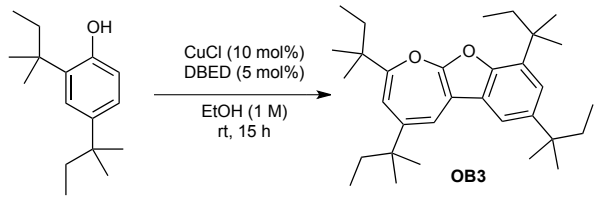

Chemical Formula: $C_{16}H_{26}O$
Molecular Weight: 234.38

Chemical Formula: $C_{32}H_{48}O_2$
Molecular Weight: 464.72

The reaction was carried out in accordance with general procedure **E** using 2,4-di-*tert*Amylphenol (468.4 mg, 2.00 mmol, 1 equiv.) to afford **OB3** (306.5 mg, 66%).

R_f: unstable to silica gel **HR-MS (APCI$^+$, *m/z):*** Calcd for $C_{32}H_{49}O_2$ $[M+H]^+$ 465.3727 Found 465.3736 **IR ν_{max} (cm^{-1}):** 2961.7, 2875.0, 1654.0, 1598.0, 1461.3, 1420.7, 1377.7, 1361.6, 1294.4, 1275.3, 1157.4, 1057.4, 1024.6, 1005.4. **^{1}H NMR** ($CDCl_3$, 300 MHz): δ 7.21 (d, *J* = 2.1 Hz, 1H), 7.03 (d, *J* = 2.1 Hz, 1H), 6.36 (s, 1H), 5.43 (s, 1H), 1.89 (q, *J* = 7.8 Hz, 2H), 1.75-1.62 (m, 4H), 1.51 (q *J* = 8 Hz, 2H), 1.43 (s, 6H), 1.35 (s, 6H), 1.21 (s, 6H), 1.20 (s, 6H), 0.75 (q, *J* = 7.5 Hz, 6H), 0.72-0.61 (m, 6H). **^{13}C NMR** ($CDCl_3$, 75 MHz): δ 162.92, 154.69, 145.67, 143.84, 143.77, 131.68, 126.94, 119.37, 114.80, 113.01, 108.89, 97.82, 40.73, 38.07, 37.89, 37.32, 34.64, 34.37, 32.15, 28.99, 27.58, 27.35, 25.95, 9.29, 9.26, 9.03, 9.00, 8.95.

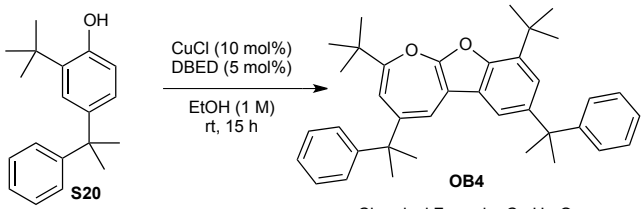

Chemical Formula: $C_{19}H_{24}O$
Molecular Weight: 268.39

Chemical Formula: $C_{38}H_{44}O_2$
Molecular Weight: 532.75

The reaction was carried out in accordance with general procedure **E** using **S20** (536.4 mg, 2.00 mmol, 1 equiv.) to afford **OB4** (388.9 mg, 73%).

R_f: unstable to silica gel **HR-MS (APCI$^+$, *m/z):*** Calcd for $C_{38}H_{45}O_2$ $[M+H]^+$ 533.3414 Found 533.3435. **IR ν_{max} (cm^{-1}):** 2963.8, 1655.5, 1598.3, 1463.8, 1418.1, 1361.8, 1278.3, 1159.3, 1059.6, 1029.7 **^{1}H NMR** ($CDCl_3$, 300 MHz): δ 7.42-7.02 (m, 12H), 6.60 (s, 1H), 5.02 (s, 1H), 1.81 (s, 9H), 1.58 (s, 9H), 1.44 (s, 6H), 1.14 (s, 6H). **^{13}C NMR** ($CDCl_3$, 75 MHz): δ 164.89, 155.05, 151.31, 148.42, 145.90, 145.35, 144.92, 133.60, 128.17, 127.95, 127.07, 126.82, 126.37, 125.91, 125.49, 119.47, 114.40, 113.89, 108.42, 97.71, 43.98, 43.27, 37.04, 34.30, 31.43, 29.85, 29.19, 27.84.

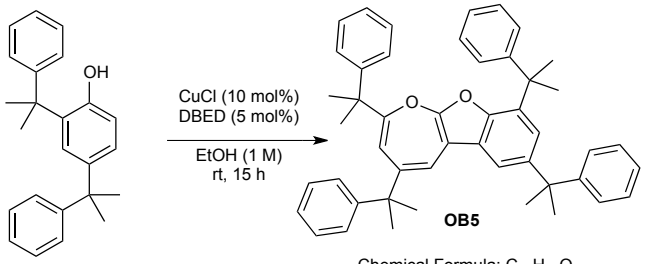

Chemical Formula: $C_{24}H_{26}O$
Molecular Weight: 330.46

Chemical Formula: $C_{48}H_{48}O_2$
Molecular Weight: 656.89

The reaction was carried out in accordance with general procedure **E** using 2,4-di-*tert*cumylphenol (660.4 mg, 2.00 mmol, 1 equiv.) to afford **OB5** (479.5 mg, 73%).

R_f: unstable to silica gel **HR-MS (APCI$^+$, *m/z):*** Calcd for $C_{48}H_{49}O_2$ $[M+H]^+$ 657.3727 Found 657.3740. **IR ν_{max} (cm^{-1}):** 2965.8, 1598.2, 1492.7, 1443.3, 1361.9, 1277.9, 1178.1, 1054.9, 1029.0 **^{1}H NMR** ($CDCl_3$, 300 MHz): δ 7.38-7.06 (m, 22H), 6.59 (s, 1H), 5.14 (s, 1H), 1.80 (s, 6H), 1.70 (s, 6H), 1.61 (s, 6H), 1.19 (s, 6H). **^{13}C NMR** ($CDCl_3$, 75 MHz): δ 163.36, 155.53, 151.30, 149.50, 148.42, 145.86, 145.59, 145.26, 144.82, 133.04, 128.26, 128.18, 127.96, 127.76, 126.91, 126.81, 126.42, 126.29, 126.12, 125.95, 125.91, 125.52, 125.43, 120.31, 114.45, 114.26, 110.83, 97.53, 44.52, 43.83, 43.27, 41.56, 31.38, 29.19, 28.97, 27.33.

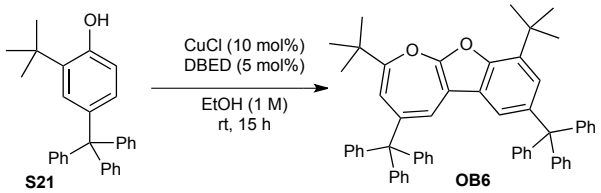

S21
Chemical Formula: $C_{29}H_{28}O$
Molecular Weight: 392.53

Chemical Formula: $C_{58}H_{52}O_2$
Molecular Weight: 781.03

The reaction was carried out in accordance with general procedure **E** using **S21** (784.4 mg, 2.00 mmol, 1 equiv.) to afford **OB6** (561.8 mg, 72%).

R_f: unstable to silica gel **HR-MS (APCI$^+$, *m/z):*** Calcd for $C_{58}H_{53}O_2$ $[M+H]^+$ 781.4040 Found 781.4071 **IR ν_{max} (cm^{-1}):** 2959.2, 1594.7, 1490.7, /442.9, 1280.2, 1165.9, 1049.2. **^{1}H NMR** ($CDCl_3$, 300 MHz): δ 7.34-7.21 (m, 29H), 6.90 (d, *J* = 12.6 Hz, 3H), 6.27 (s, 1H), 5.06 (s, 1H), 1.28 (s, 9H), 1.02 (s, 9H). **^{13}C NMR** ($CDCl_3$, 75 MHz): δ 163.39, 155.47, 147.09, 145.64, 145.03, 141.83, 141.64, 132.88, 131.23, 130.96, 127.25, 126.96, 126.96, 125.77, 125.13, 124.86, 120.86, 117.80, 111.05, 97.58, 65.31, 65.11, 36.95, 34.18, 29.77, 27.54.

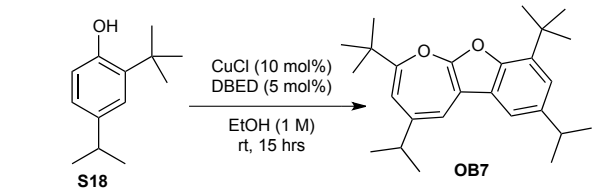

The reaction was carried out in accordance with general procedure **E** above using **S18** (384.3 mg, 2.00 mmol, 1 equiv.) to afford **OB7** (368.8 mg, 97%).

R_f: unstable to silica gel **HR-MS (APCI$^+$, *m/z):*** Calcd for $C_{26}H_{37}O_2$ $[M+H]^+$ 381.2788 Found 381.2795. **IR ν_{max} (cm^{-1}):** 2961.7, 2866.5, 1598.7, 1459.3, 1424.6, 1360.9, 1268.8, 1155.8, 1006.4 **^{1}H NMR** ($CDCl_3$, 300 MHz): δ 7.11 (s, 1H), 6.93 (s, 1H), 6.28 (s, 1H), 5.32 (s, 1H), 2.94 (m, 1H), 2.43 (m, 1H), 1.44 (s, 9H), 1.29-1.25 (m, 15H), 1.14 (d, *J* = 6 Hz, 6H). **^{13}C NMR** ($CDCl_3$, 75 MHz): δ 164.41, 154.30, 146.17, 143.66, 143.13, 134.01, 127.47, 118.75, 114.00, 113.05, 108.05, 97.90, 37.19, 35.53, 34.59, 34.22, 29.92, 28.05, 24.70, 22.34.

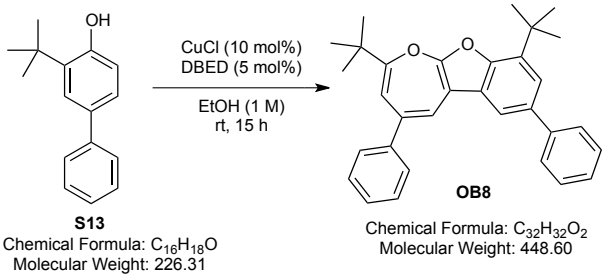

The reaction was carried out in accordance with general procedure **E** using **S13** (452.3 mg, 2.00 mmol, 1 equiv.) to afford **OB8** (224.12 mg, 50%).

R_f: unstable to silica gel **HR-MS (APCI$^+$, *m/z):*** Calcd for $C_{32}H_{33}O_2$ $[M+H^+]$ 449.24751 Found 449.24840 **IR ν_{max} (cm^{-1}):** 2957.5, 1651.5, 1597.2, 1441.2, 1415.5, 1393.8, 1362.9, 1271.8, 1171.6, 1151.5, 1056.7. **^{1}H NMR** ($CDCl_3$, 300 MHz): δ 7.63 (d, *J* = 7.8 Hz, 2H), 7.55-7.36 (m,

10H), 6.88 (s, 1H), 5.75 (s, 1H), 1.54 (s, 9H), 1.35 (s, 9H) **^{13}C NMR** ($CDCl_3$, 75 MHz): δ 165.09, 155.30, 147.47, 142.22, 141.44, 136.94, 136.28, 134.79, 128.70, 128.55, 127.84, 127.52, 127.40, 126.85, 126.02, 119.89, 117.95, 114.82, 108.84, 98.63, 37.44, 34.39, 29.87, 28.05.

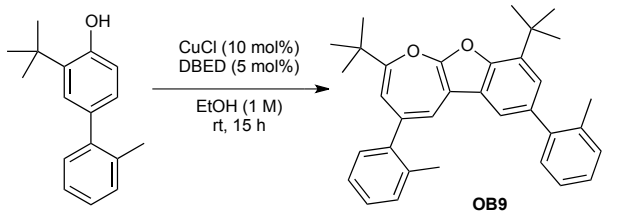

S9
Chemical Formula: $C_{17}H_{20}O$
Molecular Weight: 240.34

OB9
Chemical Formula: $C_{34}H_{36}O_2$
Molecular Weight: 476.65

The reaction was carried out in accordance with general procedure **E** using **S13** (480.7 mg, 2.00 mmol, 1 equiv.) to afford **OB9** (309.8 mg, 65%).

R_f: unstable to silica gel **HR-MS (APCI$^+$, *m/z):*** Calcd for $C_{34}H_{37}O_2$ $[M+H]^+$ 477.2788 Found 477.2800. **IR *ν_{max}* (cm^{-1}):** 2956.4, 2869.1, 1649.3, 1596.6, 1459.0, 1414.3, 1269.2, 1169.7, 1151.0, 1056.9, 1028.1. **^{1}H NMR** ($CDCl_3$, 400 MHz): δ 7.33-7.27 (m, 9H), 7.13 (s, 1H), 6.52 (s,1H), 5.49 (s, 1H), 2.45 (s, 3H), 2.34 (s, 3H), 1.55 (s, 9H), 1.35 (s, 9H). **^{13}C NMR** ($CDCl_3$, 75 MHz): δ 163.73, 154.68, 146.92, 142.68, 142.34, 137.49, 137.17, 135.77, 135.57, 134.05, 130.42, 130.28, 130.11, 128.63, 127.23, 127.07, 125.94, 125.70, 121.66, 120.07, 116.58, 116.56, 110.44, 98.35, 37.25, 34.36, 29.95, 27.96, 20.69, 20.29.

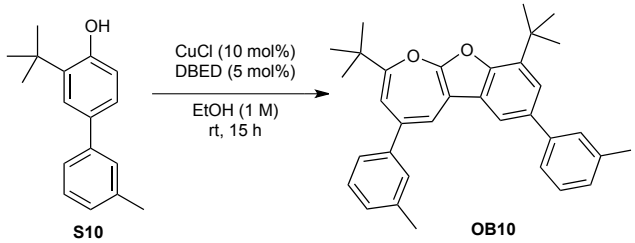

S10
Chemical Formula: $C_{17}H_{20}O$
Molecular Weight: 240.34

OB10
Chemical Formula: $C_{34}H_{36}O_2$
Molecular Weight: 476.65

The reaction was carried out in accordance with general procedure **E** using **S10** (480.7 mg, 2.00 mmol, 1 equiv.) to afford **OB10** (281.2 mg, 59%).

R_f: unstable to silica gel **HR-MS (APCI$^+$, *m/z):*** Calcd for $C_{34}H_{37}O_2$ $[M+H]^+$ 477.2788 Found 277.2804 **IR *ν_{max}* (cm^{-1}):** 2957.4, 1601.7, 1462.3, 1392.4, 1363.4, 1302.0, 1272.0, 1147.4, 1070.1, 1010.8. **^{1}H NMR** ($CDCl_3$, 300 MHz): δ 7.59 (s, 1H), 7.49-7.19 (m, 9H), 6.91 (s, 1H), 5.79 (s, 1H), 2.49 (s, 3H), 2.46 (s, 3H), 1.59 (s, 9H), 1.39 (s, 9H). **^{13}C NMR** ($CDCl_3$, 75 MHz): δ 164.92, 155.27, 147.47, 142.28, 141.52, 138.29, 138.17, 137.10, 136.42, 134.72, 128.65, 128.48,

128.33, 128.09, 127.97, 127.65, 126.77, 124.69, 123.24, 119.91, 117.89, 114.88, 109.00, 98.70, 37.46, 34.41, 30.93, 29.93, 28.10, 21.63.

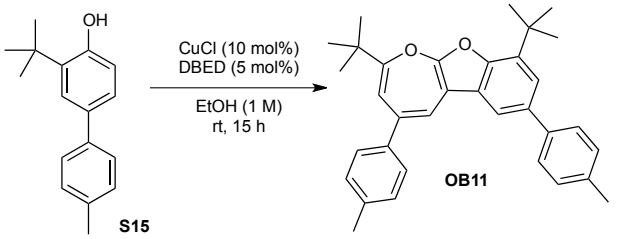

Chemical Formula: $C_{17}H_{20}O$
Molecular Weight: 240.34

Chemical Formula: $C_{34}H_{36}O_2$
Molecular Weight: 476.65

The reaction was carried out in accordance with general procedure **E** using **S15** (480.7 mg, 2.00 mmol, 1 equiv.) afforded **OB11** (262.2 mg, 55%).

R_f: unstable to silica gel **HR-MS (APCI$^+$, *m/z*):** Calcd for $C_{34}H_{37}O_2$ $[M+H]^+$ 477.2788 Found 477.2804 **IR ν_{max} (cm^{-1}):** 2957.2, 1781.7, 1660.8, 1605.2, 1462.4, 1420.7, 1392.7, 1362.6, 1231.6, 1151.6, 1078.6, 1056.7. **^{1}H NMR** ($CDCl_3$, 400 MHz): δ 7.62-7.18 (m, 10H), 6.81 (s, 1H), 5.72 (s, 1H), 2.48 (s, 3H), 2.45 (s, 3H), 1.61 (s, 9H), 1.41 (s, 9H). **^{13}C NMR** ($CDCl_3$, 75 MHz): δ 164.86, 157.90, 139.36, 138.63, 137.19, 136.80, 136.70, 136.54, 136.10, 134.67, 129.50, 129.42, 129.40, 127.33, 126.80, 125.90, 119.70, 117.25, 114.59, 110.00, 108.92, 98.62, 37.40, 34.35, 29.86, 28.04, 21.13, 21.09.

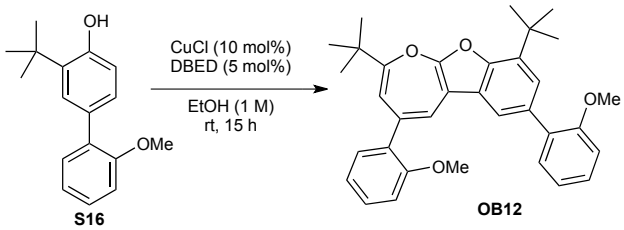

Chemical Formula: $C_{17}H_{20}O_2$
Molecular Weight: 256.34

Chemical Formula: $C_{34}H_{36}O_4$
Molecular Weight: 508.65

The reaction was carried out in accordance with general procedure **E** using **S16** (512.7 mg, 2.00 mmol, 1 equiv.) to afford **OB12** (422.2 mg, 83%).

R_f: unstable to silica gel **HR-MS (APCI$^+$, *m/z*)**: Calcd for $C_{34}H_{37}O_4$ $[M+H]^+$ 509.2686 Found 509.2708. **IR ν_{max} (cm^{-1}):** 2957.4, 1596.6, 1491.9, 1461.6, 1434.1, 1244.8, 1150.9, 1118.4, 1052.8, 1025.0 **^{1}H NMR** ($CDCl_3$, 400 MHz): δ 7.46 (s, 1H), 7.37-7.26 (m, 4H), 7.04-6.96 (m, 5H), 6.69 (s, 1H), 5.75 (s, 1H), 3.86 (s, 3H), 3.83 (s, 3H), 1.52 (s, 9H), 1.31 (s, 9H). **^{13}C NMR** ($CDCl_3$, 75 MHz): δ 163.03, 156.69, 156.51, 154.98, 147.13, 124.70, 133.88, 133.53, 131.59,

131.48, 131.26, 129.93, 128.68, 128.29, 127.32, 121.98, 120.82, 120.80, 120.65, 117.26, 111.38, 111.23, 110.16, 98.64, 55.7, 55.61, 37.21, 34.34, 29.62, 28.06.

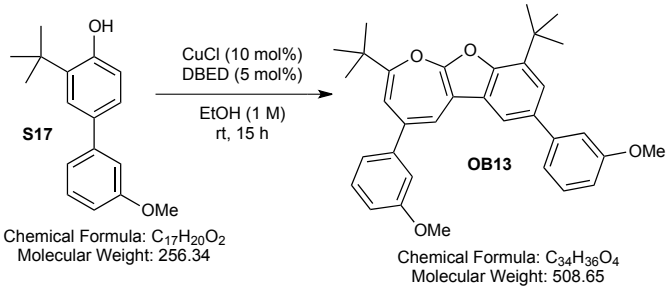

Chemical Formula: $C_{17}H_{20}O_2$
Molecular Weight: 256.34

Chemical Formula: $C_{34}H_{36}O_4$
Molecular Weight: 508.65

The reaction was carried out in accordance with general procedure **E** using **S17** (512.7 mg, 2.00 mmol, 1 equiv.) to afford **OB13** (366.2 mg, 72%).

R_f: unstable to silica gel **HR-MS (APCI$^+$, *m/z*)**: Calcd for $C_{34}H_{37}O_4$ $[M+H]^+$ 509.2686 Found 509.2708. **IR ν_{max} (cm^{-1}):** 2956.9, 1652.3, 1597.8, 1577.8, 1462.3, 1431.9, 1362.8, 1252.8, 1201.7, 1167.0, 1146.8, 1051.5, 1034.1 **^{1}H NMR** ($CDCl_3$, 300 MHz): δ 7.54 (s, 1H), 7.41-7.30 (m, 5H), 7.23-7.05 (m, 3H), 6.88 (m, 2H), 5.74 (s, 1H), 3.94 (s, 3H), 3.88 (s, 3H), 1.54 (s, 9H), 1.34 (s, 9H) **^{13}C NMR** ($CDCl_3$, 75 MHz): δ 165.03, 159.85, 159.72, 155.34, 147.52, 143.75, 142.93, 136.77, 136.10, 134.77, 129.68, 129.51, 127.77, 120.05, 119.87, 118.57, 118.11, 114.84, 113.39, 112.42, 112.14, 112.09, 108.80, 98.56, 55.4, 55.35, 37.43, 34.37, 29.86, 28.04.

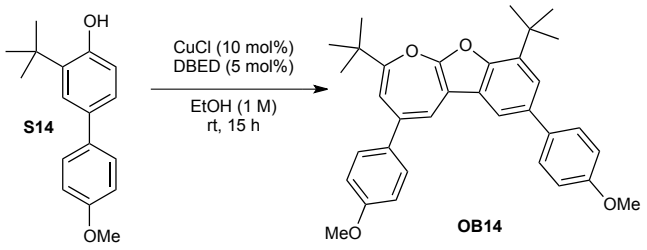

Chemical Formula: $C_{17}H_{20}O_2$
Molecular Weight: 256.34

Chemical Formula: $C_{34}H_{36}O_4$
Molecular Weight: 508.65

The reaction was carried out in accordance with general procedure **E** using **S14** (192.26 mg, 0.75 mmol, 1 equiv.) to afford **OB14** (143.1 mg, 75%).

R_f: unstable to silica gel **HR-MS (APCI$^+$, *m/z*):** Calcd for $C_{34}H_{37}O_4$ $[M+H]^+$ 509.2686 Found 509.2698. **IR ν_{max} (cm^{-1}):** 2956.3, 1596.2, 1461.3, 1434.1, 1362.4, 1242.8, 1178.1, 1117.0, 1051.7, 1024.3 **^{1}H NMR** ($CDCl_3$, 300 MHz): δ 7.46 (s, 1H), 7.40-7.26 (m, 5H), 7.07-6.93 (m, 4H), 6.69 (s, 1H), 5.75 (s, 1H), 3.86 (s, 3H), 3.82 (s, 3H), 1.52 (s, 9H), 1.31 (s, 9H). **^{13}C NMR** ($CDCl_3$, 75 MHz): δ 163.00, 156.66, 156.49, 154.95, 147.10, 134.63, 133.85, 131.56, 131.24,

129.91, 128.65, 128.25, 127.29, 121.94, 120.79, 117.22, 111.35, 111.20, 110.11, 98.60, 55.59, 55.4, 37.17, 34.30, 30.94, 28.01.

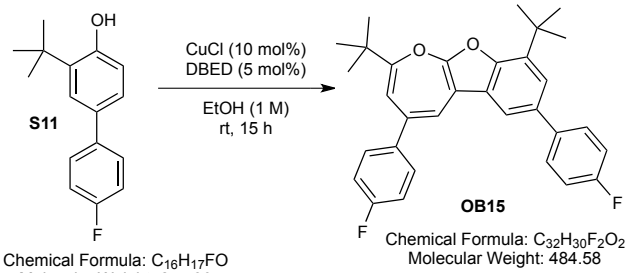

Chemical Formula: $C_{16}H_{17}FO$
Molecular Weight: 244.30

Chemical Formula: $C_{32}H_{30}F_2O_2$
Molecular Weight: 484.58

The reaction was carried out in accordance with general procedure **E** using **S11** (488.6 mg, 2.00 mmol, 1 equiv.) to afford **OB15** (256.8 mg, 53%).

R_f: unstable to silica gel **HR-MS (CI^+, *m/z):*** Calcd for $C_{32}H_{31}O_2F_2$ $[M+H]^+$ 485.2287 Found 485.2297. **IR ν_{max} (cm^{-1}):** 2957.9, 2870.2, 1600.3, 1508.0, 1464.1, 1424.2, 1394.8, 1221.8, 1151.6, 1056.0 **^{1}H NMR** ($CDCl_3$, 300 MHz): δ 7.59 (q, *J* = 1.8 Hz, 2H), 7.50-7.46 (m, 3H), 7.30 (s, 1H), 7.17-7.06 (m, 4H), 6.81 (s, 1H), 5.70 (s, 1H), 1.54 (s, 9H), 1.35 (s, 9H). **^{13}C NMR** ($CDCl_3$, 75 MHz): δ 165.29, 163.95, 163.89, 160.67, 160.64, 155.31, 147.42, 138.32, 137.55, 137.50, 136.02, 135.39, 134.92, 129.03, 127.83, 127.60, 119.76, 117.76, 115.66, 115.38, 115.23, 114.71, 108.73, 98.54, 37.46, 34.38, 29.85, 28.02.

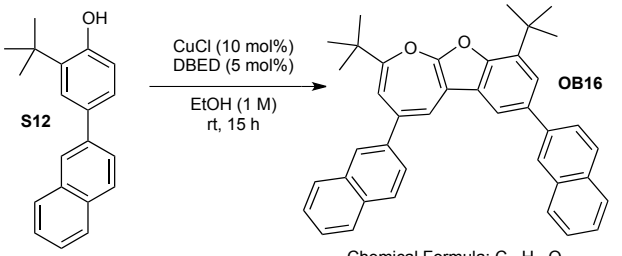

Chemical Formula: $C_{20}H_{20}O$
Molecular Weight: 276.37

Chemical Formula: $C_{40}H_{36}O_2$
Molecular Weight: 548.71

The reaction was carried out in accordance with general procedure **E** using **S12** (552.7 mg, 2.00 mmol, 1 equiv.) to afford **OB16** (543.2 mg, 99%).

R_f: unstable to silica gel **HR-MS (CI^+, *m/z):*** Calcd for $C_{40}H_{37}O_2$ $[M+H]^+$ 549.2788 Found 549.2805. **IR ν_{max} (cm^{-1}):** 2957.0, 1781.0, 1595.1, 1434.5, 1362.3, 1268.2, 1078.8, 1055.8 **^{1}H NMR** ($CDCl_3$, 300 MHz): δ 8.21 (s, 1H), 8.05-7.92 (m, 9H), 7.80 (s, 1H), 7.64 (s, 1H), 7.55 (q, *J* = 6.6 Hz, 4H), 7.17 (s, 1H), 6.02 (s, 1H), 1.72 (s, 9H), 1.51 (s, 9H). **^{13}C NMR** ($CDCl_3$, 75 MHz): δ 165.33, 155.67, 152.09, 147.71, 139.68, 138.76, 137.00, 136.25, 135.04, 133.88, 133.62, 132.86, 132.57, 128.49, 128.29, 129.25, 129.19, 127.80, 127.74, 126.47, 126.40, 126.29, 126.03, 125.88, 125.3, 124.78, 124.46, 120.28, 118.57, 115.34, 109.01, 98.94, 37.64, 34.58, 30.08, 28.25.

2.7 References and Bibliography

1. Holm, R. H.; Kennepohl, P.; Solomon, E. I. *Chem. Rev.* **1996,** *96* (7), 2239-2314.
2. Klinman, J. P. *Chem. Rev.* **1996,** *96* (7), 2541-2562.
3. Weber, M.; Weber, M.; Kleine-Boymann, M. Phenol. In *Ullmann's Encyclopedia of Industrial Chemistry*, Wiley-VCH Verlag GmbH & Co. KGaA: 2000.
4. Hock, H.; Lang, S. *Berichte der deutschen chemischen Gesellschaft (A and B Series)* **1944,** *77* (3-4), 257-264.
5. Allen, S. E.; Walvoord, R. R.; Padilla-Salinas, R.; Kozlowski, M. C. *Chem. Rev.* **2013,** *113* (8), 6234-6458.
6. Pickel, B.; Schaller, A. *Appl. Microbiol. Biotechnol.* **2013,** *97* (19), 8427-8438.
7. Hay, A. S.; Blanchard, H. S.; Endres, G. F.; Eustance, J. W. *J. Am. Chem. Soc.* **1959,** *81* (23), 6335-6336.
8. Esguerra, K. V. N. E.; Fall, Y.; Lumb, J.-P. *Submitted* **2013**.
9. Askari, M. S.; Esguerra, K. V. N. E.; Lumb, J.-P.; Ottenwaelder, X. *Manuscript in Preparation* **2013**.
10. Kushioka, K. *J.Org.Chem.* **1984,** *49*, 4456-4459.
11. Bringmann, G.; Gulder, T.; Gulder, T. A. M.; Breuning, M. *Chem. Rev.* **2010,** *111* (2), 563-639.
12. von Nussbaum, F.; Brands, M.; Hinzen, B.; Weigand, S.; Häbich, D. *Angew. Chem. Int. Ed.* **2006,** *45* (31), 5072-5129.
13. Schmidt, B.; Riemer, M.; Karras, M. *J. Org. Chem.* **2013,** *78* (17), 8680-8688.
14. .
15. Sakurai, H.; Tsukuda, T.; Hirao, T. *J. Org. Chem.* **2002,** *67* (8), 2721-2722.
16. Capparelli, M. P.; DeSchepper, R. E.; Swenton, J. S. *J. Org. Chem.* **1987,** *52* (22), 4953-4961.
17. Yakura, T.; Omoto, M.; Yamauchi, Y.; Tian, Y.; Ozono, A. *Tetrahedron* **2010,** *66* (31), 5833-5840.
18. Imahori, T.; Tokuda, T.; Taguchi, T.; Takahata, H. *Org. Lett.* **2012,** *14* (4), 1172-1175.
19. Edsall Jr, R. J.; Harris, H. A.; Manas, E. S.; Mewshaw, R. E. *Biorg. Med. Chem.* **2003,** *11* (16), 3457-3474.
20. Hajduk, P. J.; Sheppard, G.; Nettesheim, D. G.; Olejniczak, E. T.; Shuker, S. B.; Meadows, R. P.; Steinman, D. H.; Carrera, G. M.; Marcotte, P. A.; Severin, J.; Walter, K.; Smith, H.; Gubbins, E.; Simmer, R.; Holzman, T. F.; Morgan, D. W.; Davidsen, S. K.; Summers, J. B.; Fesik, S. W. *J. Am. Chem. Soc.* **1997,** *119* (25), 5818-5827.
21. Moore, G. G. I.; Kirk, A. R. *J. Org. Chem.* **1979,** *44* (6), 925-930.
22. Yamamoto, K.; Kato, S.; Tajima, K.; Mizutani, T. *Biol. & Pharm. Bull.* **1997,** *20* (5), 571-573.
23. Carter, D. S.; Hites, R. A. *J. Great Lakes Res.* **1992,** *18* (1), 125-131.
24. Kochnev, A. I.; Oleynik, I. I.; Oleynik, I. V.; Ivanchev, S. S.; Tolstikov, G. A. *Russ. Chem. Bull.* **2007,** *56* (6), 1125-1129.
25. Becker, H. D.; Gustafsson, K. *J. Org. Chem.* **1977,** *42* (18), 2966-2973.
26. Alexakis, A.; Polet, D.; Rosset, S.; March, S. *J. Org. Chem.* **2004,** *69* (17), 5660-5667.
27. Endres, G. F.; Hay, A. S.; Eustance, J. W. *J. Org. Chem.* **1963,** *28* (5), 1300-1305.
28. Becker, H.-D.; Gustafsson, K. *Tet. Lett.* **1976,** *17* (52), 4883-4886.

CHAPTER THREE

OXEPINOBENZOFURANS AS OXIDANTS

3.1 Background and Motivation

Although known for nearly sixty years, the reactivity of oxepinobenzofurans has been relatively little explored. Of particular interest is the ability of oxepinobenzofurans to act as oxidants. It is known, for *para*-diphenoquinones, that they are isomeric with the corresponding diradical, which can be obtained if the diphenoquinone possesses enough steric bulk to prevent a planar conformation[1-2]. Such singlet diradicals are especially unstable, due to the electron poor character of unpaired electrons, and will perform hydrogen abstraction rapidly. Thus, if one considers the oxepinobenzofurans to be in equilibrium with the corresponding isomeric diphenoquinone and diradical, one can expect these compounds to act as good dehydrogenation reagents.

The reduction of oxepinobenzofurans has been performed with good hydride donors, such as with LAH, which provides the biphenol or similarly by reduction with hydrogen iodide, which yields benzofuran **1.81**[3]. Only one report exists where oxepinobenzofurans are utilized as *reagents* for oxidation. In 1969, Hay and co-workers reported a patent where oxepinobenzofurans (still mistakenly assigned as benzoxets, *c.f.* Section 1.3.1) were reacted with 2,4-di-alkylated phenols at high temperatures, either solid state or at very high concentration, to produce the two corresponding biphenols (Scheme 3.1)[4].

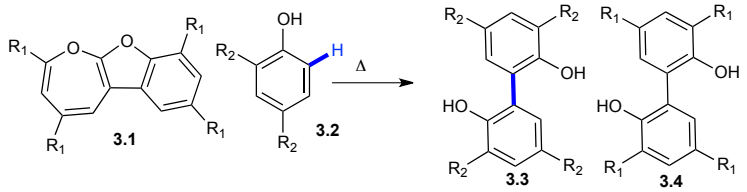

Scheme 3.1 Oxepinobenzofurans as one-electron oxidants in Hay's biphenol synthesis

We have previously developed an efficient, operationally simple synthesis of oxepinobenzofurans. Having established an efficient catalytic synthesis for oxepinobenzofurans,

we set out to explore their reactivity as oxidants, and the possible mechanism by which they effect dehydrogenation.

3.2 Oxepinobenzofuran Dehydrogenations – Optimization and Scope

3.2.1 Optimization of reaction conditions

Optimization of oxepinobenzofuran mediated dehydrogenations started with the oxidation of dihydroanthracene to anthracene. Dihydroanthracene is a good hydrogen atom donor, and in the presence of 1.25 equivalents of oxepinobenzofuran undergoes dehydrogenation to anthracene in 100 % NMR yield along with quantitative recovery of the biphenol when the components are heated to 100 ^{o}C in PhMe (Table 3.1, Entry 1).

Since PhMe is a potential H-atom donor, we investigated C_6H_6 as solvent. At 80 ^{o}C, redox is slower, and returns incomplete conversion after 2 hours (Table 3.1, Entry 2). We were pleased to see better results when the reaction was run at 100 ^{o}C in a sealed vessel (Table 3.1, Entry 3).

Table 3.1 Reaction optimization of oxepinobenzofuran-mediated dehydrogenation of dihydroanthracene[(a)]

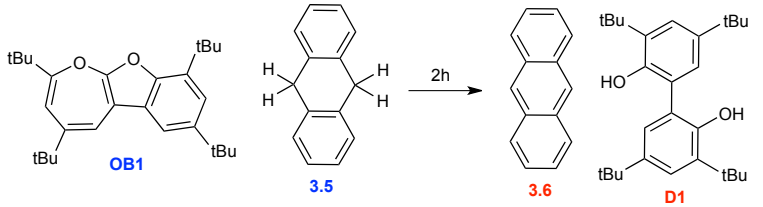

Entry	OB1 (Eq.)	**3.5** (Eq.)	Solvent (M)	T (^{o}C)	OB1/D1[(b)] (%)	3.5/3.6[(b)] (%)
(1)	1.25	1.0	PhMe (2.5)	100	0 / > 95	0 / > 95
(2)	1.25	1.0	PhH (2.5)	80	65 / 25	63 / 30
(3)	1.25	1.0	PhH (2.5)	100	0 / > 95	0 / > 95
(4)	1.50	1.0	PhH (2.5)	100	0 / > 95	0 / > 95
(5)	1.25	1.0	EtOH (2.5)	100	0 / > 95	0 / > 95

(a) Reactions were performed on 0.25 mmol of dihydroanthracene (b) Yields determined by ^{1}H NMR spectroscopy using hexamethylbenzene as an internal standard

It is important to note that the oxepinobenzofuran is utilized in 0.25 molar equivalents excess than dihydroanthracene. At the end of the reaction, however, only the reduced form of the oxepinobenzofuran, the biphenol, is observed, even when the reaction is run in a benign solvent

such as benzene. Using even higher loadings of the oxidant relative to dihydroanthracene furnishes similar results (Table 3.1, Entry 4). The source of reductant following complete consumption of dihydroanthracene remains unclear. We suspect that the open form of the oxepinobenzofuran may exist as a kinetic trap, which cannot isomerize to the oxepinobenzofuran upon cooling. Reduction of this species may then occur upon addition of the hexamethylbenzene NMR standard which is added for direct analysis of the reaction mixture by ^{1}H NMR.

It is known that protic solvents favor isomerization of diphenoquinones to the oxepinobenzofuran. Yet performing the reaction in ethanol works very well, with quantitative conversion and yields (Table 3.1, Entry 5).

Overall, the reaction seems to require temperatures of at least 100^{o}C, but works well in various solvents at very high concentration in just 2 hours. We have succeeded in extending the utility of oxepinobenzofuran as oxidants to C-H donors as well as O-H donors.

3.2.2 Scope of reductant

We next investigated the scope of the reductant (Table 3.2). The reaction works well with 2,4-di-cumyl phenol and 2,4-DTBP[4], providing the corresponding biphenols, however conversion and yield drop when experimenting with substrates harder to oxidize. Dihydronaphthalene shows only 50% conversion (Table 3.2, Entry 2), and neither tetrahydroquinoline nor tetrahydro-isoquinoline show any dehydrogenated product upon reaction with oxepinobenzofuran (Table 3.2, Entries 3-4).

Cyclohexadiene is a good substrate for this reaction, however its low boiling point renders it operationally difficult. In order to observe the reaction products easily by ^{1}H NMR, the reaction was run neat in a sealed vessel. Importantly, the reaction works (as 5% of benzene is observed), but cyclohexadiene is not fully converted. Loss of mass balance can be attributed to evaporation of product.

Dehydrogenation of cyclohexadienone with easily accessible oxepinobenzofurans could provide a good route towards phenols. The reaction of 2,4-di-phenyl-cyclohexadienone with oxepinobenzofuran showed no conversion (Table 3.2, Entry 6).

Table 3.2 Reductant Scope of oxepinobenzofuran-mediated dehydrogenation of dihydroanthracene[a]

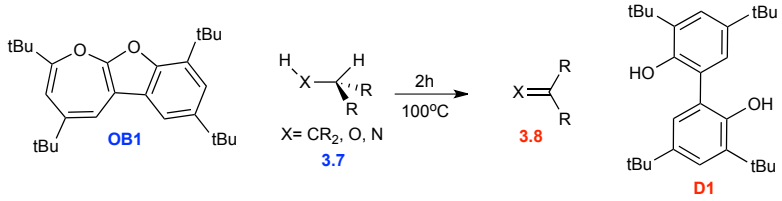

Entry	OB1 (Eq.)	Reductant	Solvent (M)	OB1/D1 (%)	3.7/3.8 (%)
(1)	1.25	2,4-di-cumyl phenol	EtOH (2.5)	0 / > 95	0 / 87
(2)	0.5	Dihydronaphthalene	PhH (2.5)	0 / > 95	50 / 50
(3)	2.0	tetrahydroquinoline	PhH (2.5)	0 / 90	0 / 0
(4)	2.0	tetrahydroisoquinoline	PhH (2.5)	0 / > 95	60 / 0
(5)	1.25	cyclohexadiene	Neat	5 / 75	37.5 / 5
(6)	1.25	3,5-di-phenyl-cyclohexadienone	PhH (2.5)	0 / 50	> 95 / 0

(a) Yields determined by ^{1}H NMR spectroscopy using hexamethylbenzene as internal standard

3.2.3 Scope of oxidant

Several differentially substituted oxepinobenzofurans were evaluated in order to investigate substituent effects on the redox process (Table 3.3). Almost all oxepinobenzofurans work very well to dehydrogenate dihydroanthracene, and no major electronic effect is observed when changing substituents. We attribute the low levels of conversion of *para*-trityl-substituted oxepinobenzofuran to decreased solubility in ethanol at such a high concentration (2.5 M).

Table 3.3 Oxidant Scope of oxepinobenzofuran-mediated dehydrogenation of dihydroanthracene[a]

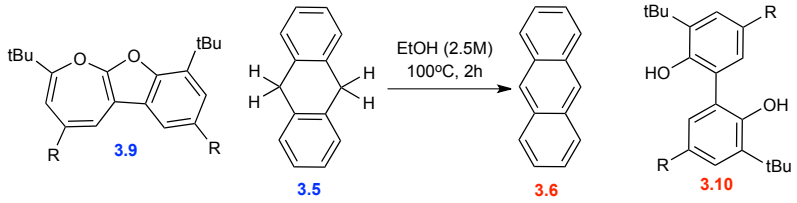

Entry	R	3.9/3.10[b] (%)	3.5/3.6[b] (%)
(1)	trityl	0 / > 95	41 / 35
(2)	phenyl	0 / > 95	6 / 80
(3)	p-F-phenyl	0 / > 95	5 / 90
(4)	p-OMe-phenyl	0 / > 95	10 / 75

(a) Reactions were performed on 0.25 mmol of dihydroanthracene (b) Yields determined by ^{1}H NMR spectroscopy using hexamethylbenzene as an internal standard

Although most reactions worked well, an unexplained loss of mass balance of dihydroanthracene is observed. It is possible that the dihydroanthracene radicals polymerize, as a completely insoluble solid was recovered from the reaction mixture.

3.2.4 Progress towards aerobic catalytic dehydrogenation reactions

Since oxidation of dihydroanthracene produces the biphenol, a catalytic amount of oxepinobenzofuran could be used if a suitable reoxidation of the biphenol could be developed (Scheme 3.2). This would provide an attractive means of running dehydrogenation reactions using O_2 as the terminal oxidant, which represents a more efficient alternative to traditional approaches[5]. We have already developed dehydrogenation conditions using oxepinobenzofurans. To complete the catalytic cycle, it is necessary to optimize the oxidation of the biphenol **3.10** to the oxepinobenzofuran **3.9.**

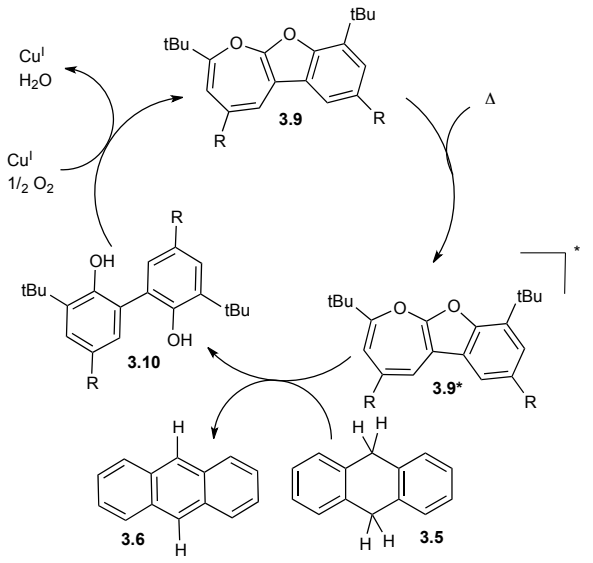

Scheme 3.2 Copper catalytic aerobic dehydrogenation reactions

Optimization of conditions for the oxidation of biphenol **D1** to oxepinobenzofuran **OB1** started from our optimized conditions for the oxidation of phenol to oxepinobenzofuran, which return incomplete conversion of **D1** into **OB1** after 4 hours (Table 3.4, Entry 1). Increasing the catalyst loading to 20 mol% of CuCl and 10mol% of DBED improved the reaction efficiency and provided the product oxepinobenzofuran in 100% NMR yield (Table 3.4, Entry 3). Good conversion is maintained at decreased reaction times.

Table 3.4 Optimization of copper-catalyzed aerobic biphenol oxidation[a]

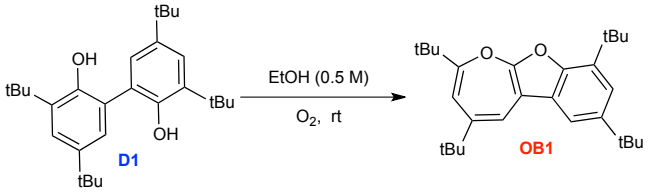

Entry	CuCl (mol%)	DBED (mol %)	Time (h)	D1:OB1[b]
(1)	10	5	4	20:80
(2)	20	40	13	9:91
(3)	20	10	13	0:100
(4)	20	10	8	0:100
(5)	20	10	4	5:95

(a) Reactions were performed on 0.25 mmol of biphenol (b) Ratios determined by ^{1}H NMR spectroscopy

Next, the scope of the oxidation was investigated, using a series of biphenols (Table 3.5). The reaction works very well with neutral and electron withdrawing substituents, but is slowed by electron-donating groups (Table 3.5, Entry 5). We attribute these decreases in conversion to an increased pKa value of the biphenol, which disfavors deprotonation of the biphenol by the amine ligand, and thus binding to to the Cu-catalyst. We attribute the low conversion of *para*-trityl-substituted biphenol **3.10** to poor solubility in EtOH at room temperature. Higher reaction times and temperatures could be a strategy for increasing product yield and conversions for the substrates that are less reactive.

Table 3.5 Scope of copper-catalyzed aerobic biphenol oxidation[a]

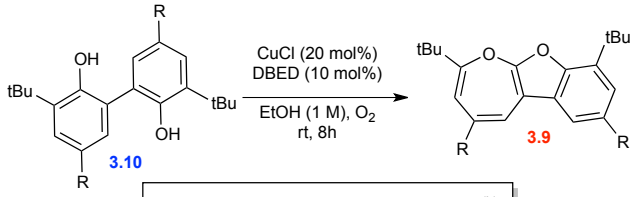

Entry	R	3.10 / 3.9[b]
(1)	*t*Bu	0:100
(2)	trityl	83:17
(3)	phenyl	0:100
(4)	p-F-phenyl	0:100
(5)	p-OMe-phenyl	28:71

(a) Reactions were performed on 0.25 mmol biphenol (b) Ratios determined by ^{1}H NMR spectroscopy

Overall, a catalytic aerobic method to oxidize biphenols to oxepinobenzofurans was devised and applied. This evidences the potential for the development of a catalytic aerobic dehydrogenation reaction, allowed through the redox transfer of oxepinobenzofurans and biphenols. There remains only to optimize the overall catalytic reaction, for which both temperature and reaction concentration will have to be looked at carefully as those two parameters differ in the separate biphenol oxidation and dehydrogenation reactions.

3.3 Studies of the Mechanism of Oxepinobenzofuran-Mediated Dehydrogenations

Oxepinobenzofurans act as dehydrogenation agents, yet cursory inspection of the compound does not readily reveal the mechanism of this transformation. One possibility is that oxepinobenzofurans are in equilibrium with their corresponding diradical isomers (Scheme 3.3).

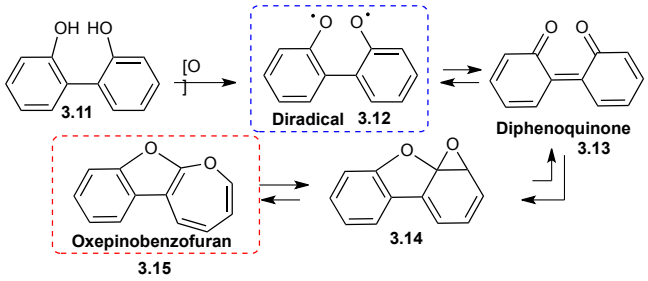

Scheme 3.3 Oxepinobenzofuran isomerism with diphenoquinone and singlet diradical

The identification of the above equilibrium with the diradical species would provide mechanistic insights into oxepinobenzofuran-mediated oxidations, and thus aid in reaction optimization efforts and potentially provide additional avenues of reactivity. Additionally, equilibrium with a diradical species would suggest that oxepinobenzofurans have the potential to show very different physical properties, depending on the surrounding environment. The oxepinobenzofuran does not have magnetic susceptibility, however if the equilibrium is shifted to the corresponding diradical, by modifying environmental variables, it becomes paramagnetic. This could be very valuable in the field of electronics. The oxepinobenzofurans could also find applications in materials, where, if integrated within a conducting polymeric framework, the polymer conjugation (and conduction properties) could be effectively turned on and off by opening and closing the oxepinobenzofuran.

We started our investigation for the oxepinobenzofuran mechanism of oxidation by verifying whether a radical signal could be observed when varying environmental parameters (temperature, solvent, concentration, oxygen presence). An important tool to study radical species is Electron Paramagnetic Resonance (EPR).

3.3.1 Electron Paramagnetic Resonance (EPR) Overview

Electron Paramagnetic Resonance is analogous to Nuclear Magnetic Resonance (NMR), with the studied species being the electron instead of the atom. Electrons possess two possible spin values, $m_s = \pm ½$[6]. In the absence of an external magnetic field, the energy difference between these two states is 0, however upon application of a magnetic field the states split into two distinct energy levels (Figure 3.1)[7]. This is termed the Zeeman effect and is due to the electron magnetic moment being aligned with or against the applied magnetic field[7].

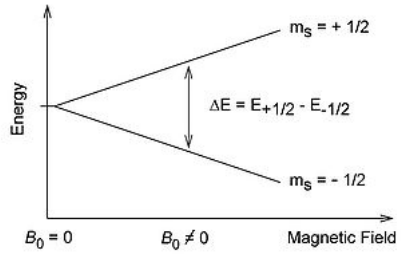

Figure 3.1 Magnetic field induced differentiation of electron spin energies

If an unpaired electron is present in the studied sample, it will have the ability to move between the different energy levels. Applying the right energy will allow an electron to move to an excited state. EPR measures the energy of absorption by electrons, which is characteristic of the radical studied and its surrounding environment[7]. Considering the energy gap between the two electron spin levels is quite large, microwaves are typically used in EPR experiments to excite unpaired electrons to higher energy levels[7].

Equation (**1**) describes the energy of absorption of a given unpaired electron:

$$\Delta E = h\nu = g\mu_B B_0 \quad \textbf{(1)}$$

where h is Planck's constant, ν is the energy wavelength, μ_B is the Bohr magneton constant, B_0 is the strength of the applied magnetic field, and g is the g-factor. The g-factor is analogous to an atom's chemical shift in NMR spectroscopy, integrating the influence of attached and neighboring nuclei in the value of energy absorption by the electron. The g-value is calculated as

the energy at the middle of any observed signal. A free electron shows a g-factor of $g = 2.0023$[8] and most organic radicals have g-factors around g = 2.00.

Importantly, electron spins are also split by the interaction of spins of attached neighboring nuclei[7]. The resulting 'splitting' of lines in an EPR spectrum is called hyperfine splitting. For nuclei having non-null spins ($I \neq 0$), the total number of possible electron spin energies will be given by equation **(2)**:

$$\# = 2NI+1 \qquad \textbf{(2)}$$

where N is the number of equivalent nuclei the electron can couple to[7]. Thus EPR spectroscopy can also provide information about the atoms attached to the studied electron, The intensity of the lines is given by Pascal's triangle[7], if the spin of the neighboring nuclei is I= ½ .

Overall, EPR spectroscopy can give information about whether an unpaired electron is present, but also indicate the type of radical it is and the structural environment it is occupying.

3.3.2 Calibration of the EPR Instrument for Diradical Qualitative Simulation

Although EPR provides a lot of information about a given unpaired electron, a thorough method for identification of a radical's structure is that of simulating the EPR spectrum and subsequently comparing those results against experimental data. In order to verify whether an observed EPR signal could be the proposed diradical structure, collaboration was set up with Prof. Andrews.

Before the proposed diradical can be simulated, the model elaborated by Prof. Andrews for spectra simulation of diradicals must be calibrated against a known species, as well as the particular EPR instrument utilized. Yang's biradical was chosen as the standard to verify the model (Scheme 3.4), as its spectrum had been reported numerous times[9-15]. Synthesis of Yang's biradical was carried out by two different methods, both equally efficient. The first[16] involved *para*-bromination of 2,6-di-*tert*-butyl phenol, followed by silyl protection of the phenol. Addition of three equivalents of this species, after lithium-halogen exchange, afforded a tri-silyl-ether carbinol. Immediate deprotection in acidic media gave the *para*-quinone methide which, upon oxidation with basic potassium ferricyanide, provided Yang's biradical.

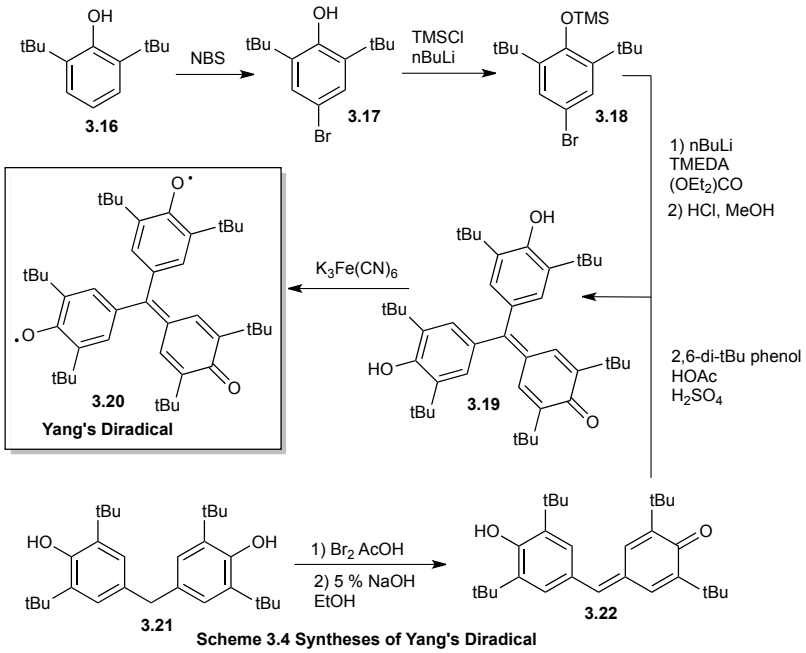

Scheme 3.4 Syntheses of Yang's Diradical

The second method[17] involved benzylic bromination of a methylene-bridged biphenol, followed by elimination with base to yield a *para*-quinone methide. The quinone methide undergoes addition to a molar equivalent of 2,6-di-*tert*-butyl phenol in acidic media, to provide the biphenolic precursor to Yang's biradical. Again, basic potassium ferricyanide oxidation of this species provides the desired diradical.

EPR spectroscopy of Yang's biradical furnished a seven peak spectrum, as reported in the literature (Figure 3.2)[12]. Obtaining a well-resolved spectrum necessitated optimization of the conditions of recording. Thus, it was found that oxygen was deleterious to observation of hyperfine splitting, and needed to be excluded from EPR samples by freeze-pump-thawing. Furthermore, splitting was only observed at lower concentrations (10^{-4} M).

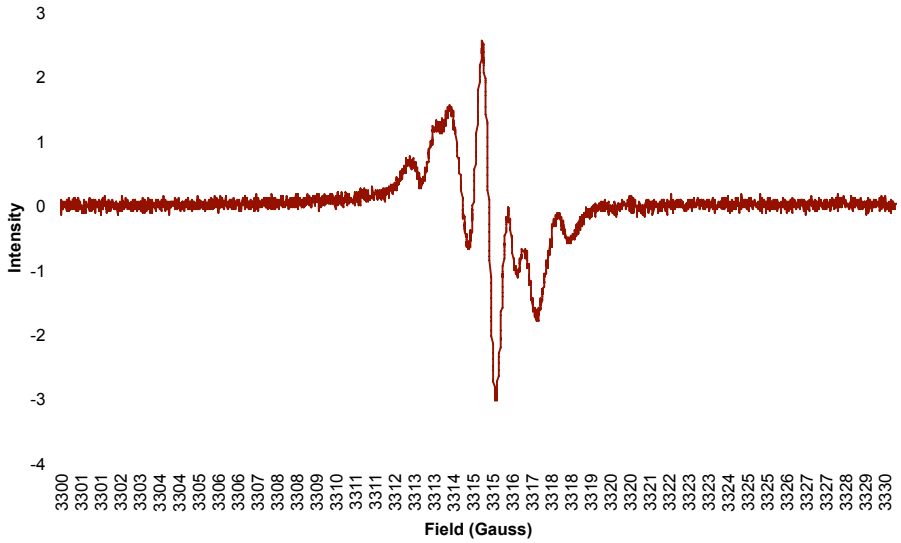

Figure 3.2 EPR spectrum of Yang's Diradical (in anaerobic Benzene 2x10-4M, RT, 55dB power, 0.1 G modulation, 30 dB receiver gain).

3.3.3 EPR Measurements of 2,5,7,9-tetra-*tert*-butyl oxepinobenzofuran

After verification that a previously reported diradical spectra could be reproduced successfully, we started our investigation of the potential oxepinobenzofuran equilibrium with a diradical by studying 2,5,7,9-tetra-*tert*-butyl oxepinobenzofuran by EPR. Thus, the oxepinobenzofuran was studied at increasingly high temperatures, since oxepinobenzofurans as oxidants had shown better reactivity at 100°C than 80°C (*c.f.* Section 3.2). EPR measurements were recorded for a solid-state sample, or dissolved in benzene, bromobenzene or biphenyl (Figure 3.3-3.4).

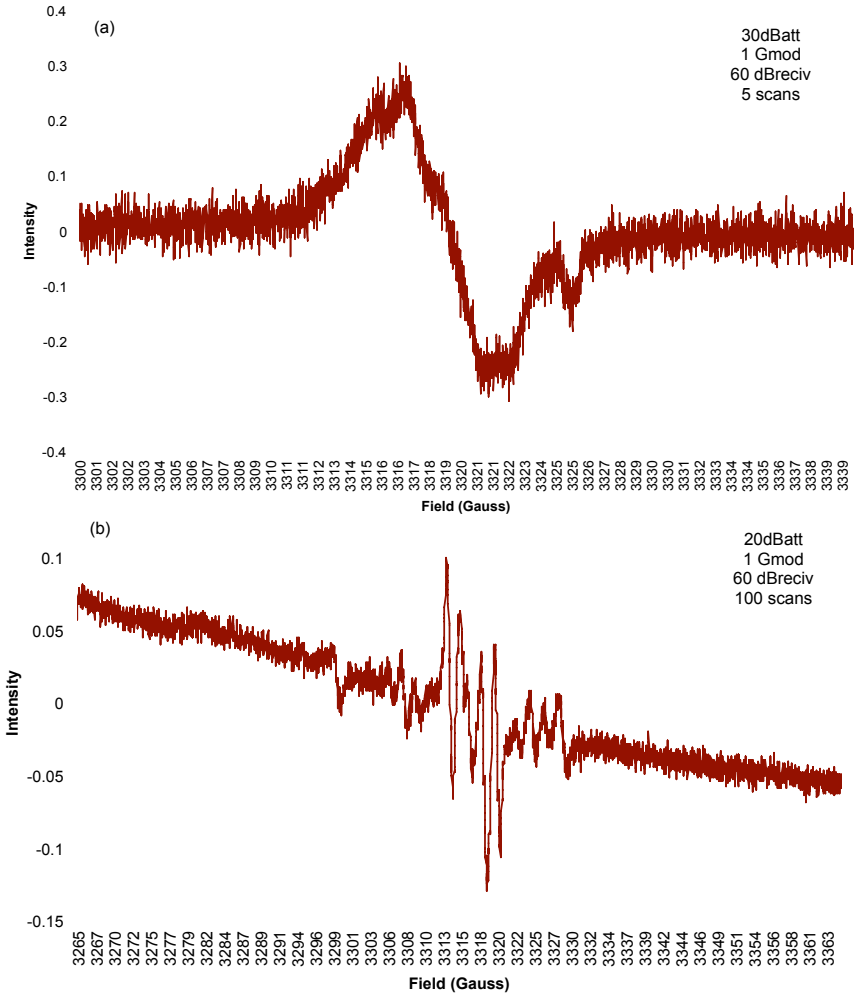

Figure 3.3 EPR spectra of 2,4,7,9-tetra-*tert*-butyl oxepinobenzofuran (a) solid state (120°C) (b) Benzene (10^{-3}M, 80°C)

As expected, a signal was observed above 100°C, and whereas at the boiling point of benzene (80 °C) only a very small signal is observed. All four samples show very similar g-values (Table 3.6), which are indicative of the presence of an organic radical. These four measurements show that as temperature is increased, a radical grows where it was not previously present, starting at a very specific temperature (between 100-120°C) (see Supporting Information and Figure 3.7). This information leads to the conclusion that a threshold temperature must be reached for the opening of the oxepinobenzofuran to the diradical. It should be considered, however, that singlet diradicals are not EPR detectable, and only triplets can be seen[7]. Thus, there is an additional equilibrium to be considered, between the 'opened oxepinobenzofuran' (the singlet diradical) and the triplet diradical. This spin intersystem crossing might also necessitate energy, if the triplet state is energetically higher than the singlet state, and thus might be causing the 'threshold' temperature effect observed by EPR.

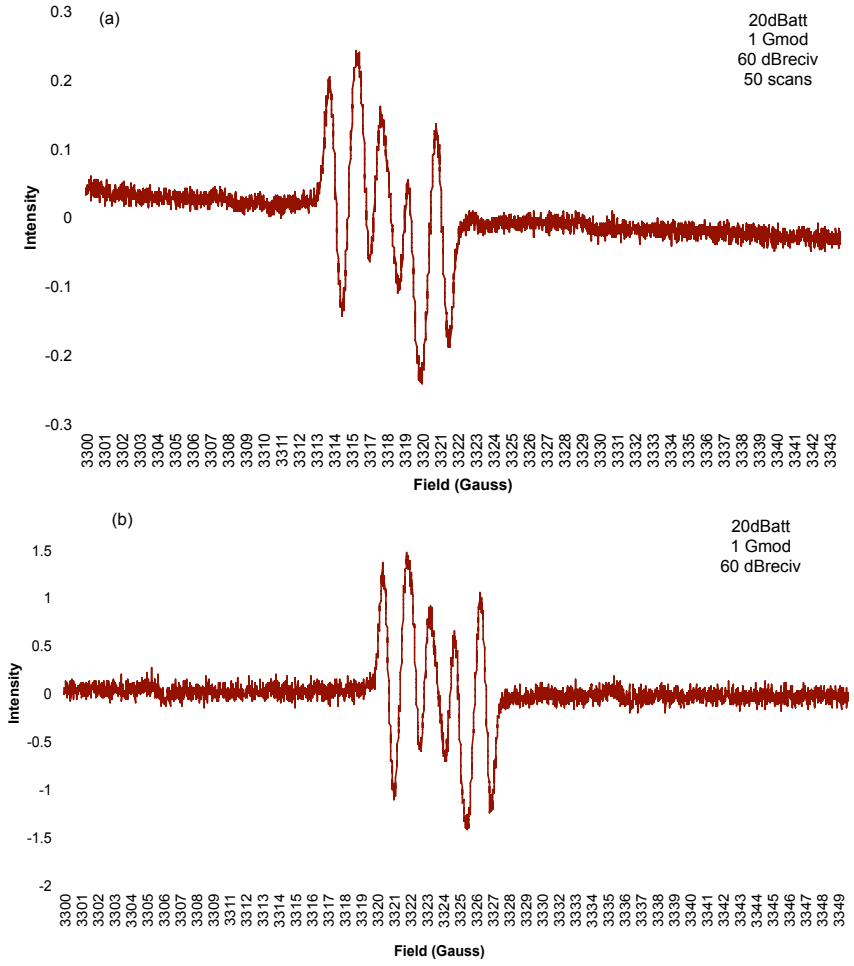

Figure 3.4 EPR spectra of 2,4,7,9-tetra-*tert*-butyl oxepinobenzofuran (a) in biphenyl (10^{-3}M, 120°C) (b) in bromobenzene (10^{-2}M, 120°C)

The solid-state sample provides very little hyperfine resolution. This is due to anisotropy of the sample, as well as increased spin-spin interactions of the unpaired radicals, both causing line broadening. A five-line spectrum is observed when a high enough radical concentration is reached and hyperfine splitting is clear (Figure 3.4a-b). A five-line spectrum could be the result of splitting by four hydrogens, as per Equation **(2)** (Section 3.3.1). Thus, the observed spectra do not discount the possibility of the proposed diradical.

Table 3.6 Measured g-values for observed radical signal from oxepinobenzofuran

Entry	State	g-value
(1)	Solid	2.00477
(2)	Benzene	2.00472
(3)	Biphenyl	2.00475
(4)	Bromobenzene	2.00472

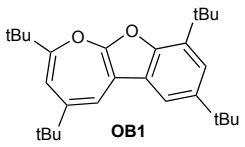

OB1

Interestingly, as the solid-state sample is cooled down to room temperature after measurement, the radical signal remains (Figure 3.5a). This is not the case with the samples measured in benzene or biphenyl, which show no signal after cooling. A possible reason for this peculiar effect could be that energy is required to revert back from a diradical species to the oxepinobenzofuran. In dissolved samples, the solvent takes a longer time to cool, liberating enough energy to allow the diradical to close to the oxepinobenzofuran. This is impossible in the solid state. Additionally, only the singlet diradical will be able to revert to the oxepinobenzofuran. Thus, a spin crossover event needs to occur before refurnishing the starting material. Triplet-singlet crossover is known to occur as two triplets collide (triplet annihilation)[18]. Collisions are greatly facilitated when samples are dissolved, yet in solid-state are difficult unless significant energy (heat) is applied.

When the oxepinobenzofuran is dissolved in bromobenzene, however, the EPR signal also remains after cooling back to room-temperature, and even after freezing at – 78^{o}C (Figure 3.5b). This is difficult to explain, although the fact that bromine atoms are known to facilitate singlet-triplet intersystem crossing through a large spin-orbit coupling could be involved[19].

Proton NMR measurements of samples used in EPR experiments show only oxepinobenzofuran. Control experiments where oxepinobenzofuran is heated for several hours have revealed that no conversion is occurring at 80^{o}C in PhH, either after two hours or overnight. At 100^{o}C however, biphenol is observed after two hours in either PhH or PhMe.

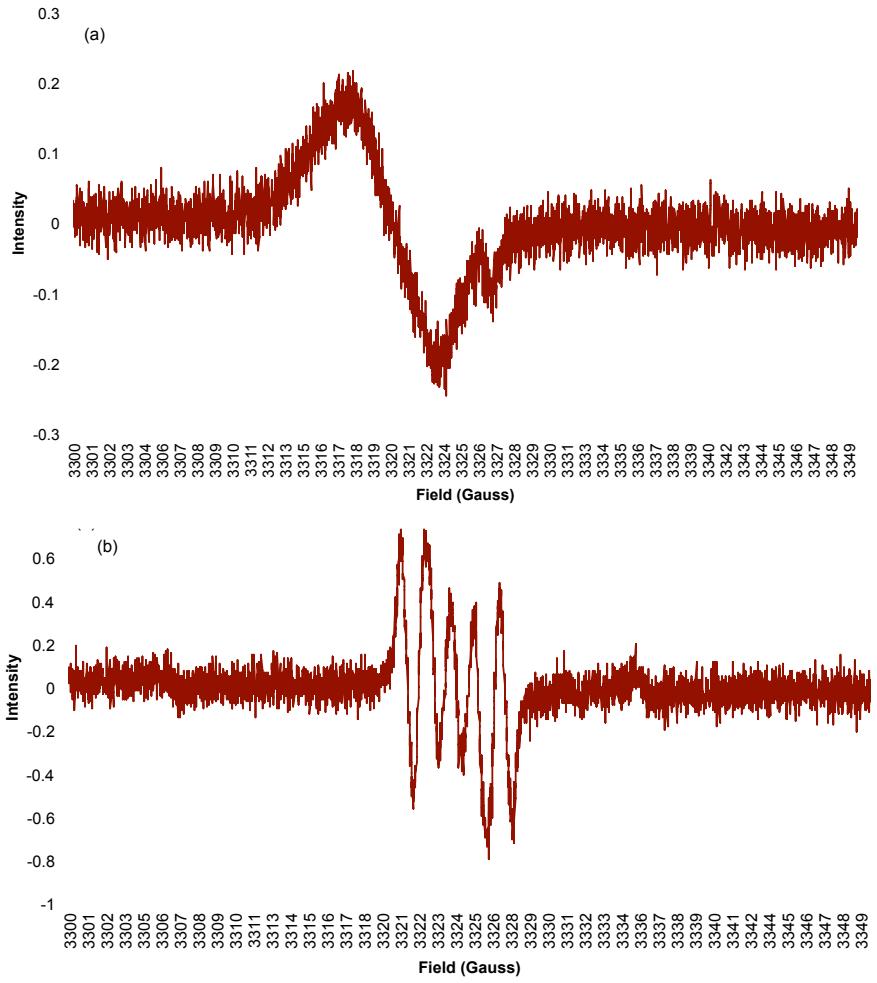

Figure 3.5 EPR spectra at RT after experiment of 2,4,7,9-tetra-*tert*-butyl oxepinobenzofuran (a) solid state (b) bromobenzene (10-2M) at 30dB power, 1G modulation, 30dB receiver gain and 20dB power, 1G modulation, 60dB receiver gain respectively

Incremental temperature EPR measurements of two other oxepinobenzofurans were effected in bromobenzene, mainly with 2,9-di-*tert*-butyl-4,7-di-phenyl oxepinobenzofuran (OB8) and 2,9-di-*tert*-butyl-4,7-di-(4'-fluorophenyl) oxepinobenzofuran (OB15) (Figure 3.6). For both compounds, a higher temperature of 155 ^{o}C was required for observation of a radical signal. This is consistent with the electron-poor nature of the two oxepinobenzofurans, relative to 2,5,7,9-tetra-*tert*-butyl oxepinobenzofuran, that will provide less stabilized radicals. As expected, more detailed hyperfine splitting is observed for both species. In effect, the radical will be split by more hydrogens, and in the case of the fluorinated analogue will also be split by fluorine atoms.

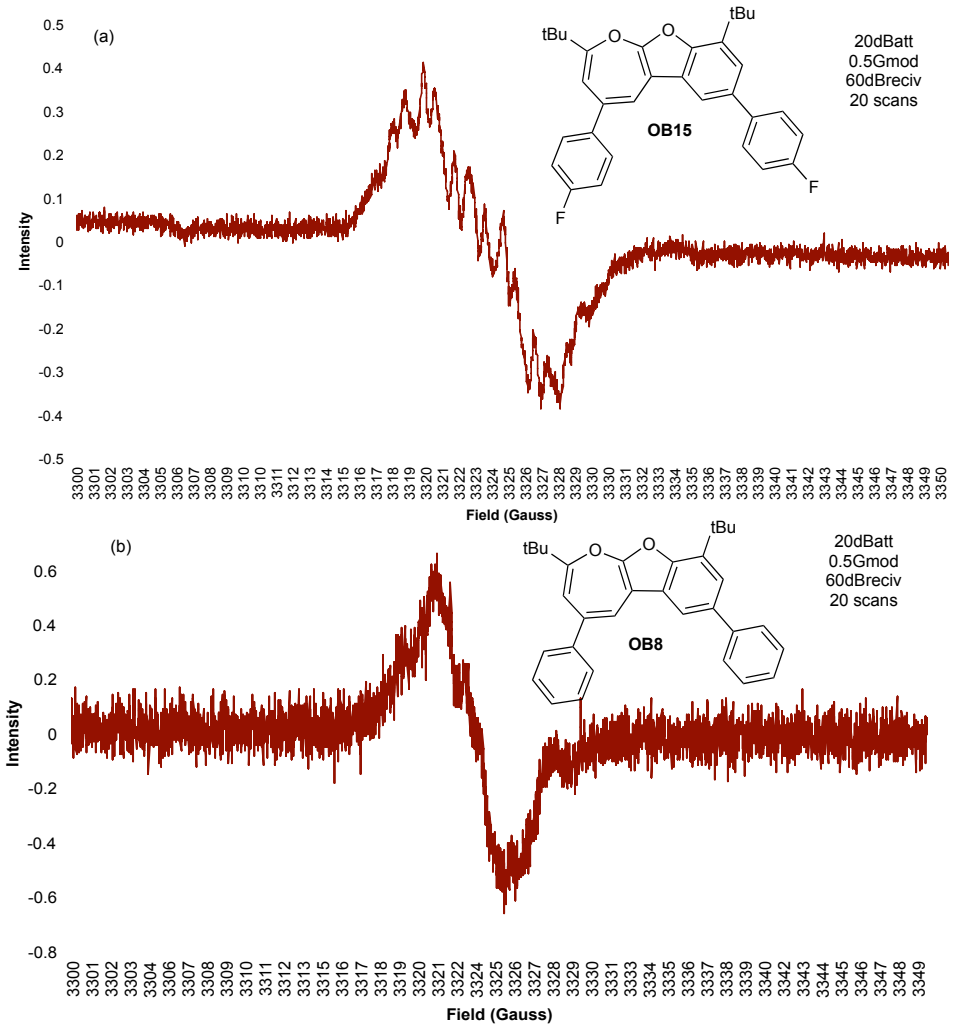

Figure 3.6 EPR spectra at 155oC in bromobenzene (10-2M) of (a) 2,9-di-*tert*-butyl-4,7-di-(4'-fluorophenyl) oxepinobenzofuran (b) 2,9-di-*tert*-butyl-4,7-di-phenyl oxepinobenzofuran at 20dB power, 0.5G modulation, 60dB receiver gain (20 averaged scans)

Overall, it was found that oxepinobenzofurans are able to furnish radical species upon heating. Spectra of this radical do not rule out the proposed diradical structure, and evidence a subtle interplay between the species and its environment (solvent, temperature) that needs to be further investigated.

3.3.4 Radical Quantification – Calibration and Calculations

Quantification of the amount of unpaired electrons in a sample at a given temperature and time will allow a better understanding of the equilibrium between the oxepinobenzofuran and the observed radical species. In order to quantify the unpaired spins, calibration curves were built using TEMPO as an external standard. Analytically pure TEMPO possesses a spin concentration of 100%, thus the TEMPO concentration measured is identical to the radical concentration, and will be easily compared to the oxepinobenzofuran unpaired electron concentration.

To be able to make a comparison between integrals of standard measurements and that of the unknown radical, it is important that the spectra be recorded under precisely the same conditions[7]. Thus, TEMPO calibration curves were obtained at all relevant temperatures, with constant recording and processing EPR parameters and identical sample preparation techniques as those for the oxepinobenzofuran measurements. It was necessary to use a lower receiver gain value for TEMPO measurements than for the oxepinobenzofurans, due to the much larger concentration of radicals present in the standard sample. Thus, obtained integral values for the standard and for the oxepinobenzofuran need to be normalized to account for this difference. The EPR signal areas are known to scale linearly with gain[7], thus the following formula (Equation 3) will provide gain normalized integrals:

$$I_n = \frac{I_0}{gain} \qquad \textbf{(3)}$$

Where I_n is the normalized integral value, I_0 is the absolute integral area, and gain is the utilized gain setting.

When comparing standard and analyte, it is also wise to consider differences in spin values[7]. Both TEMPO and the proposed diradical are oxygen based, however TEMPO should show a spin of S=1/2 whereas the proposed diradical, being observed by EPR is a triplet, and should possess a spin of S=1. Thus, both TEMPO and oxepinobenzofurans' absolute integral values are normalized to account for the spin and gain differences according to Equation 4,[7] where S is the considered sample's spin.:

$$I_n = \frac{I_0}{gain\,[S(S+1)]} \qquad \textbf{(4)}$$

Finally, calibration curves for TEMPO were obtained at all relevant temperatures, and all possess $R^2 > 0.99$ (*c.f.* Supporting Information). Similarly, the normalized intensity for all three studied oxepinobenzofurans was calculated and plotted against temperature (Figure 3.6). The plots show a clear increase in intensity with higher temperatures, as expected. Negative integral values are due to intensive noise if a spectrum with no signal is integrated.

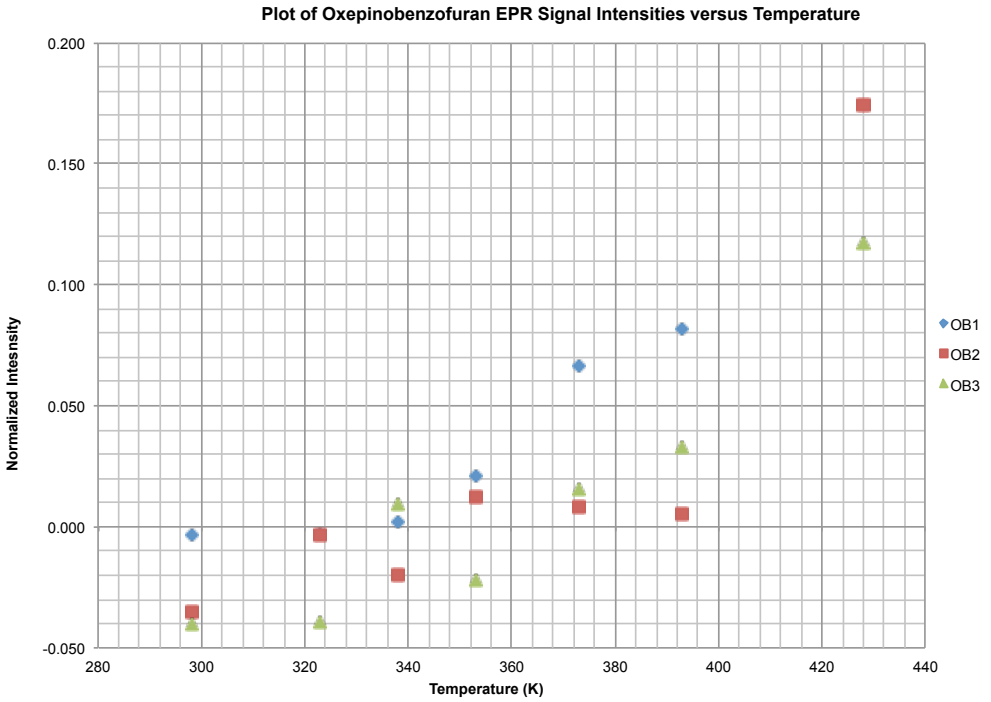

Figure 3.7 Plot of normalized EPR signal intensity relative to temperature for OB1 (2,5,7,9-tetra-*tert*-butyl oxepinobenzofuran), OB2 (2,9-di-*tert*-butyl-4,7-di-phenyl oxepinobenzofuran) and OB3 (2,9-di-*tert*-butyl-4,7-di-(4'-fluorophenyl) oxepinobenzofuran)

The radical concentrations for all three oxepinobenzofuran samples were calculated using the following equation (5):

$$C_B = \frac{I_{n(B)} - b}{m} \qquad \textbf{(5)}$$

Where C_B is the oxepinobenzofuran unpaired electron concentration, $I_{n(B)}$ is the normalized integral value of the measured oxepinobenzofuran signal, m and b are the slope and constant of the calibration curve at the studied temperature, respectively (calibration curves are linear and expressed as I=mC+b). Calculated spin concentrations relative to temperature for the three studied oxepinobenzofurans, OB1, OB8 and OB15, are shown in Table 3.7.

Table 3.7 Calculated concentrations of diradical for three oxepinobenzofurans

T (K) \ S.M.	OB1	OB8	OB15
298	-1.101×10^{-7} M	-1.039×10^{-7} M	-1.190×10^{-6} M
323	-9.423×10^{-8} M	-1.109×10^{-7} M	-1.259×10^{-6} M
338	6.979×10^{-8} M	-8.198×10^{-7} M	3.878×10^{-7} M
353	1.092×10^{-6} M	6.280×10^{-7} M	-1.150×10^{-6} M
373	3.505×10^{-6} M	4.324×10^{-7} M	8.246×10^{-7} M
393	6.292×10^{-6} M	4.381×10^{-7} M	2.558×10^{-6} M
428	-	1.439×10^{-5} M	9.670×10^{-6} M

S.M. = Starting Material

For all three studied oxepinobenzofurans, an increase in spin concentration is observed with higher temperatures. At 393 K, a higher radical concentration is determined for OB1 than for OB8 or OB15. At 428 K, OB8 has a more significant spin content than OB15. These results coincide with the substrates electronic characteristics: an oxepinobenzofuran bearing more electron rich substituents will offer better radical stabilization and thus lower the energy requirement for isomerization to an EPR active species. The oxepinobenzofuran concentration of all studied samples was kept at 10^{-2}M. We can thus calculate the percent amount of EPR active diradical relative to oxepinobenzofuran content at different temperatures (Table 3.8).

Table 3.8 Calculated percent diradical at relevant temperatures

T (K) \ S.M.	OB1	OB8	OB15
298	-0.001 %	-0.010 %	-0.012 %
323	-0.001 %	-0.001 %	-0.013 %
338	0.001 %	-0.008 %	0.004 %
353	0.011 %	0.006 %	-0.012 %
373	0.035 %	0.004 %	0.008 %
393	0.063 %	0.004 %	0.026 %
428	-	0.144 %	0.097 %

S.M. = Starting Material

The calculated spin concentrations for the studied oxepinobenzofurans are small. In theory, the two spin energy levels of unpaired electrons have a very small energy difference, and are almost equally populated, with a slight excess of the S= -1/2 level. The population of each state is a function of the Boltzmann distribution, and is dependent on temperature such that a lower temperature will induce a higher population difference between the two states, thus creating a higher EPR signal. Thus, as the temperature increases, the spin states are equally

populated, decreasing the EPR signal[7]. The derived TEMPO and oxepinobenzofuran signal intensities can thus be misleading with regards to the actual unpaired eletron content, in that it indicates a lower amount than is actually present.

To reinforce obtained results, it is feasible to perform a radical titration within the EPR tube once the signal has formed and stabilized to a maximum intensity. Thus, known amounts of a more stable radical (such as DPPH) could be added to the sample until the initial EPR signal has disappeared and is replaced by the sole DPPH spectrum.

UV/Vis spectroscopy could also be utilized for quantitation. The oxepinobenzofuran and observed triplet diradical should show very different UV/Vis spectra, and thus the oxepinobenzofuran depletion can be monitored as the radical growth is observed, providing with a relative ratio of starting material to radical at given temperatures and times.

Overall, quantitative measurements of oxepinobenzofuran derived radical species show that only a very small amount of starting material is converted to an EPR active compound. Even at such low radical concentrations however, the effect of substituents and added electron-withdrawing capabilities are observed.

3.4 Conclusions

Oxepinobenzofurans were shown to act as dehydrogenation agents, although with limited oxidant power. Their readily available nature, however, coming directly from phenols through a Cu-catalyzed aerobic oxidation, allows for potential modification and optimization of the oxidant. Furthermore, their reduced form is also easily re-oxidized to the oxepinobenzofuran using catalytic aerobic conditions. Future research in this area could include the development of a catalytic aerobic dehydrogenation method, with oxepinobenzofurans as redox-transfer agents and water as sole byproduct, as well as the assessment of oxidizing power based on electronic and steric properties of the oxepinobenzofurans. Overall, the oxepinobenzofurans show promise as readily available, labile and green dehydrogenation agents.

Although the identity of the active species effecting dehydrogenation is not completely revealed, a very interesting thermal equilibrium between oxepinobenzofurans and a radical species was uncovered. Evidence points towards a diradical species and confirmation of the structure will be given with the simulation of its triplet EPR spectrum and comparison with

experimental data. Finally, primary attempts for quantification of the radical showed that the extent of the equilibrium between the oxepinobenzofuran and the diradical species is very limited, and that it can be influenced by the system's electronics.

3.5 Supporting Information

3.5.1 General Experimental

Chemicals and solvents were purchased from Sigma Aldrich, Alfa Aesar, Strem Chemicals or TCI. Dihydroanthracene was purified by recrystallization prior to use. Solvents were dried and purified using a PureSolv MD 7 (from Innovative Technology) or MB SPS 800 (from MBraun). Unless otherwise noted, reactions were performed in flame-dried glassware under a positive pressure of nitrogen using standard synthetic organic, inert atmosphere techniques.

Proton nuclear magnetic resonance (^{1}H NMR) spectra were acquired using Varian Inova 400 MHz and Varian Mercury 300 MHz spectrometers. Chemical shifts (δ) are reported in parts per million (ppm) and are calibrated to the residual solvent peak. Coupling constants (*J*) are reported in Hz. Multiplicities are reported using the following abbreviations: *s* = singlet; *d* = doublet; *t* = triplet; *q* = quartet; *m* = multiplet (range of multiplet is given).

All oxepinobenzofurans and biphenols utilized for dehydrogenations and EPR experiments were synthesized from the corresponding phenols by catalytic-aerobic oxidations according to the respective procedures outlined in Chapter Two, Supporting Information.

Yang's biradical was synthesized according to the procedures of Yang[17] or Harrer[16].

3.5.2 Oxepinobenzofuran-mediated dehydrogenation reactions

General Procedure: Oxepinobenzofuran (1.25 or 2.0 equiv.) and reducing agent (1.0 equiv.) were added to a flame-dried conical microwave vial equipped with a Teflon coated stir bar. Solvent (2.5 M) was added by syringe to afford a heterogeneous solution. The vial was sealed with a microwave vial cap, and freeze-pump-thawed three times. The mixture was allowed to heat at 100^{o}C for two hours with stirring. Upon completion, the mixture was cooled to room-temperature. The solvent was removed *in vacuo* to afford an oily mixture, to which

hexamethylbenzene (0.15 equiv.) was added. The resulting mixture was analyzed directly by ^{1}H NMR.

3.5.3 Catalytic-aerobic biphenol oxidations

General Procedure: Biphenol (0.25 mmol, 1 equiv.) and cuprous chloride (4.95 mg, 0.05 mmol, 20 mol%) were added to a flame-dried Radley tube equipped with a Teflon coated stir-bar. The tube was sealed with a rubber septum and evacuated and backfilled with Argon three times. Under Argon, EtOH (0.25 mL, 1 M) was added by syringe. The resulting mixture was allowed to homogenize and DBED (5 μL, 4.31 mg, 0.025 mmol, 10 mol%) was added by syringe. Under strong Argon pressure, the septum was replaced with a Radley cap and the reaction was pressurized with O_2 (1 bar overpressure). The mixture was allowed to stir at room temperature under oxygen for 8 hours. Upon completion, EtOH was removed *in vacuo*. The resulting residue was dissolved in DCM and 10 % aqueous $NaHSO_4$. The biphasic mixture was extracted three times with DCM. The combined organic phases were dried over $MgSO_4$, filtered and concentrated *in vacuo* to afford the crude reaction mixture, which was analyzed directly by ^{1}H NMR.

3.5.4 EPR Sampling and Measurements

Sample Preparation

Wilmad 4mm precision thin-wall Quartz or 2mm thin wall Quartz EPR tubes were used for the EPR samples. Compound stock solutions at known concentrations were made prior to sample preparation. A known amount of solution was inserted into EPR tubes, which was subsequently capped with a rubber septum. All EPR samples were degassed by freeze-pump-thawing three times. EPR measurements were performed immediately after sample preparation.

For all quantitation experiments, samples were prepared at a known concentration in bromobenzene. Only 2mm Thin Wall Wilmad Quartz EPR tubes were used for quantitation measurements.

EPR Measurements

The spectra were measured using a Bruker Elexsys E500 Spectrometer equipped with a super-high Q cavity. The instrumental conditions were: microwave power, P = 20-30 dB, microwave frequency, ν = 9.34 GHz, modulation frequency, 1.0×10^5 Hz, modulation amplitude, $A_m = 5 \times 10^{-5}$ T, receiver gain, 30-60, sweep time, 0.00512 s, time constant, $\tau = 0.00128$ s, number of points, NP = 4096, and number of scans, NS=1-100 (per spectrum). Accurate g-values were obtained using the built-in microwave frequency counter and a DPPH (2,2-diphenyl-1-picrylhydrazyl) powder standard (g = 2.0037).

For all quantitation measurements, instrumental settings were: microwave power, P = 20 dB, microwave frequency, ν = 9.34 GHz, modulation frequency, 1.0×10^5 Hz, modulation amplitude, $A_m = 1 \times 10^{-4}$ T, receiver gain, 30 dB or 60 dB, sweep time, 0.00512 s, time constant, $\tau = 0.00128$ s, number of points, NP = 4096, and number of scans, NS=1 (per spectrum).

Preparation of TEMPO Calibration Curves

Absolute integration values for TEMPO at 10^{-5} M, 10^{-4} M, 10^{-3} M and 10^{-2} M concentrations and 298 K, 323 K, 353 K, 373 K, 393 K, 428 K temperatures were obtained after double integration of the corresponding EPR spectra using the Xepr Bruker software (Table S1). Raw integral values were normalized according to Equation (4). Resulting normalized integral values (Table S2) for TEMPO were plotted as a function of concentration and a linear trendline model was applied to each temperature data-set to obtain the calibration curve equations (Figure S1).

Table S1 Absolute Integral values of TEMPO

Conc. (M) \ T (K)	298	323	338	353	373	393	428
0.00001	23.34	21.86	18.27	14.08	11.79	16.22	6.93
0.0001	120.35	85.44	45.67	29.72	48.40	27.59	12.26
0.001	857.37	612.52	848.37	326.96	400.36	157.59	318.86
0.01	7590.91	7032.20	5408.71	4337.80	4283.30	2927.86	2725.38

Table S2 Normalized Integral values of TEMPO

Conc. (M) \ T (K)	298	323	338	353	373	393	428
0.00001	1.04	0.97	0.81	0.63	0.52	0.72	0.31
0.0001	5.35	3.80	2.03	1.32	2.15	1.23	0.54
0.001	38.11	27.22	37.71	14.53	17.79	7.00	14.17
0.01	337.37	312.54	240.39	192.79	190.37	130.13	121.13

Calculation of Radical Concentrations

Absolute integration values for oxepinobenzofurans OB1 (2,5,7,9-tetra-*tert*-butyl oxepinobenzofuran), OB8 (2,9-di-*tert*-butyl-4,7-di-phenyl oxepinobenzofuran) and OB15 (2,9-di-*tert*-butyl-4,7-di-(4'-fluorophenyl) oxepinobenzofuran) at different temperatures were obtained after double integration of the EPR spectra using Xepr Bruker software (Table S3). Raw integral values were normalized according to Equation (4). Resulting normalized integral values (Table S3) were utilized in Equation (5) (Section 3.3.4) to afford radical concentrations at each temperature (Table 3.7).

Table S3 Oxepinobenzofuran integral values

	Absolute			Normalized		
T (K)	OB1	OB8	OB15	OB1	OB8	OB15
298	-0.45	-2.11	-4.83	-0.00372	-0.0351	-0.0402
323	-0.35	-0.42	-4.72	-0.00294	-0.00346	-0.0393
338	0.20	-2.38	1.12	0.00169	-0.0198	0.0094
353	2.52	1.45	-2.65	0.0210	0.0121	-0.0221
373	8.00	0.99	1.88	0.0667	0.00823	0.0157
393	9.78	0.68	3.98	0.0815	0.00567	0.0331
428	-	20.95	14.08	-	0.1746	0.1173

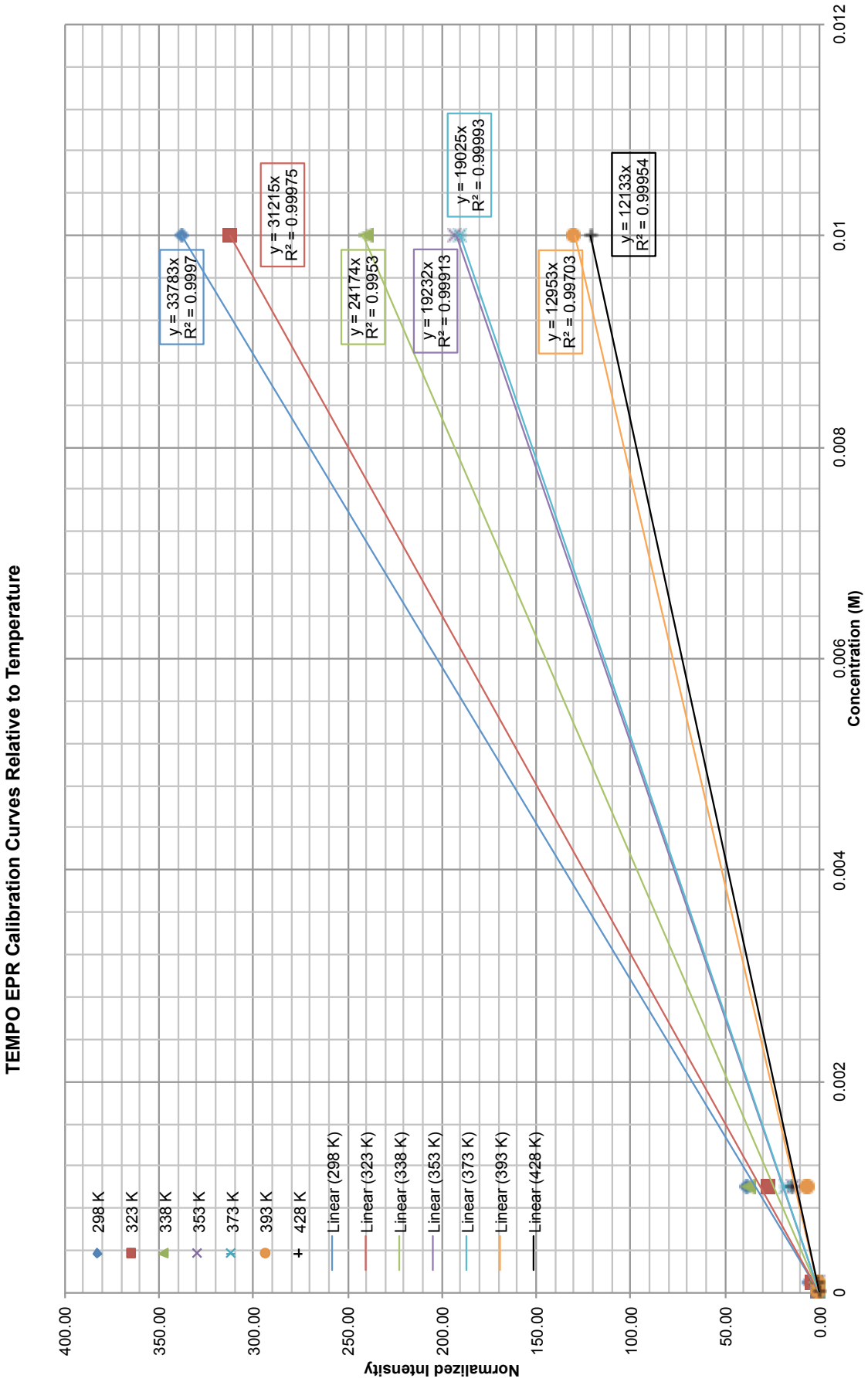

Figure S1: TEMPO Calibration Curves and associated R² values at relevant temperatures

3.6 References and Bibliography

1. Barbiero, G.; Kim, W.-G.; Hay, A. S. *Tet. Lett.* **1994,** *35* (34), 6199-6202.
2. Barbiero, G.; Kim, W.-G.; Hay, A. S. *Tet. Lett.* **1994,** *35* (32), 5833-5836.
3. Müller, E.; Mayer, R.; Narr, B.; Rieker, A.; Scheffler, K. *Just. Lieb. Ann. Chem.* **1961,** *645* (1), 25-35.
4. Hay, A. S.; Becker, H. D. Biphenols and spiroquinol ethers. DE1900680A, 1969.
5. Stahl, S. S. *Angew. Chem. Int. Ed.* **2004,** *43* (26), 3400-3420.
6. Gerlach, W.; Stern, O. *Zeit. fur Phys.* **1922,** *9* (1), 353-355.
7. Eaton, G. R.; Eaton, S. S.; D.P., B.; Weber, R. T. *Quantitative EPR*. Springer: New York, 2010.
8. Odom, B.; Hanneke, D.; D'Urso, B.; Gabrielse, G. *Phys. Rev. Lett.* **2006,** *97* (3), 030801.
9. van Willigen, H.; Plato, M.; Möbius, K.; Dinse, K.-P.; Kurreck, H.; Reusch, J. *Mol. Phys.* **1975,** *30* (5), 1359-1366.
10. Mukai, K.; Sogabe, A. *J. Chem. Phys.* **1980,** *72* (1), 598-601.
11. Mukai, K. *Bull. Chem. Soc. Jpn.* **1978,** *51* (1), 313-314.
12. Mukai, K.; Mishina, T.; Ishizu, K. *J. Chem. Phys.* **1977,** *66* (4), 1680-1684.
13. Kreilick, R. *J. Chem. Phys.* **1965,** *43* (1), 308-309.
14. Kirste, B.; Kurreck, H.; Sordo, M. *Chem. Ber.* **1985,** *118* (5), 1782-1797.
15. Bock, H.; John, A.; Havlas, Z.; Bats, J. W. *Angew. Chem. Int. Ed. in English* **1993,** *32* (3), 416-418.
16. Harrer, W.; Kurreck, H.; Reusch, J.; Gierke, W. *Tetrahedron* **1975,** *31* (6), 625-632.
17. Yang, N. C.; Castro, A. J. *J. Am. Chem. Soc.* **1960,** *82* (23), 6208-6208.
18. Shao, M.; Yan, L.; Li, M.; Ilia, I.; Hu, B. *J. Mat. Chem. C.* **2013,** *1* (7), 1330-1336.
19. Condon, E. U.; Shortley, G. H. *The Theory of Atomic Spectra*. Cambridge University Press: 1935.

CONCLUSIONS

Copper catalyzed aerobic phenol oxidations represent important synthetic methodologies, having the potential of providing numerous structurally different classes of products from one given readily available and cheap starting material. This approach is efficient and versatile, but is also greener than many alternatives, eliminating the need for pre-functionalization, protecting groups or stoichiometric amounts of toxic oxidants and byproducts.

The versatility of these methods is well evidenced through the successful developments of catalytic aerobic syntheses of oxepinobenzofurans and biphenols from phenols. Screening of the two reactions for a range of phenols demonstrated the robustness of the reaction conditions, which remain selective and efficient independently of substrate steric and electronic variations.

With an efficient oxepinobenzofuran synthesis in hand, their reactivity was explored. Oxepinobenzofurans showed promise as dehydrogenation agents, likely due to a reversible opening of the oxepinobenzofuran ring to a diradical system at high temperature. The reduced form of the oxepinobenzofurans is the biphenol, which was efficiently re-oxidized to the oxepinobenzofuran *via* a catalytic aerobic reaction, demonstrating the possibility of catalytic dehydrogenation reactions using dioxygen as the terminal oxidant and generating water as only by-product.

In conclusion, advancements were made in the identification of the factors governing selectivity in copper-aerobic phenolic oxidations, and two new synthetic methods were provided. The relatively little explored oxepinobenzofurans were identified as dehydrogenation agents. The confirmation of the reactive intermediate effecting hydrogen abstraction remains to be accomplished, as does the development of a catalytic aerobic dehydrogenation method, and both could constitute future research areas.